Geological Field Trips and Maps

Società Geologica Italiana

ISPRA
Dipartimento per il
SERVIZIO GEOLOGICO D'ITALIA
Organo Cartografico dello Stato (legge n°68 del 2-2-1960)

Sistema Nazionale per la Protezione dell'Ambiente

2018
Vol. 10 (1.1)

INDEXED IN EMERGING SOURCES CITATION INDEX THOMSON REUTERS

ISSN: 2611-6189

Past to present deformation of the central-eastern Southern Alps: from the foreland to the Giudicarie belt

2017 Annual Meeting of the Structural Geology Italian Group (GIGS) of the Italian Geological Society

DOI: 10.3301/GFT.2018.01

GFT&M - *Geological Field Trips and Maps*

Periodico semestrale del Servizio Geologico d'Italia - ISPRA e della Società Geologica Italiana
Geol. F. Trips Maps, Vol.**10** No.1.1 (2018), 78 pp., 71 Figs. (DOI 10.3301/GFT.2018.01)

Past to present deformation of the central-eastern Southern Alps: from the foreland to the Giudicarie belt

2017 Annual Meeting of the Structural Geology Italian Group (GIGS) of the Italian Geological Society

Alfio Viganò[1], Dario Zampieri[2], Sandro Rossato[2], Silvana Martin[2], Luigi Selli[3], Giacomo Prosser[4], Susan Ivy-Ochs[5], Paolo Campedel[1], Fabio Fedrizzi[1], Marco Franceschi[2], Manuel Rigo[2]

[1] Servizio Geologico, Provincia Autonoma di Trento, Via Zambra 42, 38121 Trento
[2] Dipartimento di Geoscienze, Università degli Studi di Padova, Via Gradenigo 6, 35131 Padova
[3] Dipartimento di Scienze Biologiche, Geologiche e Ambientali, Università degli Studi di Bologna, Piazza di Porta San Donato 1, 40136 Bologna
[4] Dipartimento di Scienze, Università degli Studi della Basilicata, Viale dell'Ateneo Lucano 10, 85100 Potenza
[5] Department of Earth Sciences, ETH Zürich, Sonneggstrasse 5, 8092 Zürich

Corresponding Author e-mail address: alfio.vigano@provincia.tn.it

ISSN: 2611-6189

http://gftm.socgeol.it/

DOI: 10.3301/GFT.2018.01

INDEX

Information

Excursion notes

Itinerary

DOI: 10.3301/GFT.2018.01

Abstract

A field trip across the central-eastern sector of the Southern Alps, from the foreland to the Giudicarie fold-and-thrust belt, is here described. The field trip, which was held on 12-13 July 2017, followed the Annual Meeting of the Gruppo Italiano di Geologia Strutturale (GIGS) of the Italian Geological Society. It was organized by the Geoscience Department of the University of Padova as a 2-day itinerary in Veneto and Trentino. This guide provides a geological overview of the main structural domains of the central-eastern Southern Alps (the Giudicarie and Schio-Vicenza domains) and focuses on evidence of past and present brittle deformation, principally within carbonate rocks of Late Triassic to Early Cretaceous age. The itinerary and Stop descriptions are particularly devoted to observation and discussion of exhumed faults, present and past seismicity, large landslides/rock avalanches of Holocene to historic age, and their interactions. The observation of specific outcrops is also combined with spectacular panoramas illustrating the regional tectonic setting of the Southern Alps and of the nearby Austroalpine units.

Key words: *Structural geology, faults, rock-avalanches, historical seismicity, seismic faulting, Southern Alps, Veneto, Trentino.*

Program summary

During the first day of the field trip, the geological evidence of brittle tectonics and active deformation (exposed faults; large landslides/rock avalanches, with structural control and in some cases triggered by earthquakes) in the central-eastern Southern Alps is shown and discussed. The second day focuses on the geology of the central Brenta Massif and related tectonics.
Here below a brief description of the field trip and related stop points (see Fig. 1 for the first day and Fig. 2 for the second day).

DAY 1 – "Geology and tectonics of the Astico Valley and southern Trentino: faults, rock-avalanches and seismicity"
The field trip starts at Piovene Rocchette north of Vicenza (STOP 1.1), approaching the Southern Alps front nearly where the Bassano thrust (one of the seismogenic sources of the ENE-WSW active front of the eastern Southern Alps; DISS Working Group, 2018) reaches the surface. Here we can observe the Last Glacial Maximum

DOI: 10.3301/GFT.2018.01

(LGM) alluvial fans of the Astico river and, continuing to the north along the Astico Valley, the present river incision in the Mesozoic bedrock (hanging-wall of the Bassano thrust).
The middle Astico Valley is today partly infilled with a large landslide deposit (La Marogna, STOP 1.2), which is being actively quarried. The La Marogna principal slip surface of failure is a fault plane (thrust with 35° dip towards the valley), which can be also observed at the base of the main scarp (Zampieri and Adami, 2013). The deposit is historical in age (^{14}C dating, Barbieri and Grandesso, 2007) and correlates with other earthquake-triggered landslides of similar age in the Adige Valley (Ivy-Ochs et al., 2017a; 2017b; see STOP 1.6 and STOP 1.7).
Along the upper Astico Valley near Lastebasse (STOP 1.3), N-S-trending Jurassic synsedimentary faults are visible (Lavarone plateau) (Zampieri and Massironi, 2007).
STOP 1.4 and STOP 1.5 are both related to the Cornetto di Folgaria-Becco di Filadonna pop-up, which is due to the transpressional reactivation of a western lateral ramp (Calisio fault) of the Valsugana fault and the (possibly Jurassic) Centa fault (Zampieri et al., 2003). All these faults, which are also seismotectonically active in depth (Viganò et al., 2015), have produced a prominent morphology and local slope instabilities. At the Fricca Pass (STOP 1.5) we can also directly observe the damage zone of the Centa fault, with several discrete slip planes with associated gouge.
After the descent in the Adige Valley, we can observe the Castelpietra landslide (Stop 1.6.1) and the Lavini di Marco rock avalanche (Stop 1.6.2). Both are described and discussed, in terms of geology (lithologies, structures), geomorphology (deposit shape, volume and characters) and age (Martin et al., 2014; Ivy-Ochs et al., 2017a). Particular attention is deserved on the triggering mechanisms, also in relation with historical and present seismicity (Ivy-Ochs et al., 2017a; 2017b).
The itinerary then moves to the west, in the lower Sarca Valley, entering the Giudicarie fault system (Jurassic to Cenozoic geological formations, with volcanics of the Venetian Paleogene magmatism). In this area, NW-SE oriented nearly vertical strike-slip faults, belonging to the Schio-Vicenza system, cut across the Giudicarie faults dislocating originally adjacent structural blocks. North of Dro we observe the Marocche di Dro rock avalanches, some of the most famous and most beautiful of Alpine rock avalanche deposits (STOP 1.7). These deposits are subdivided in two main rock avalanche bodies: the Marocca Principale to the north (1000 X 10^6 m^3 volume) and the Kas to the south (300 X 10^6 m^3 volume) (Ivy-Ochs et al., 2017b). The age of Marocca Principale (5300 ± 860 yr ago) suggests occurrence during a known period of enhanced slope instability in the Alps, possibly related to the shift to wetter, colder climate conditions at the transition from the middle to the late Holocene. Conversely, the age of Kas (1080 ± 160 yr ago) implies an earthquake as trigger, and specifically the "Middle

DOI: 10.3301/GFT.2018.01

Adige Valley" 1046 AD earthquake (^{36}Cl exposure dating by Ivy-Ochs et al., 2017b).
After this last stop for the day, we go across the Giudicarie Valley to Tione di Trento and Madonna di Campiglio in the Rendena Valley. During this trip we can observe the Southalpine basement (Rendena schists) intruded by Permian granitoids (Caderzone and Doss del Sabion granodiorites), and the Cenozoic Adamello tonalite. Along the road between Carisolo and Sant'Antonio di Mavignola, the strongly foliated Central Presanella tonalite is clearly crosscut by the South Giudicarie fault.

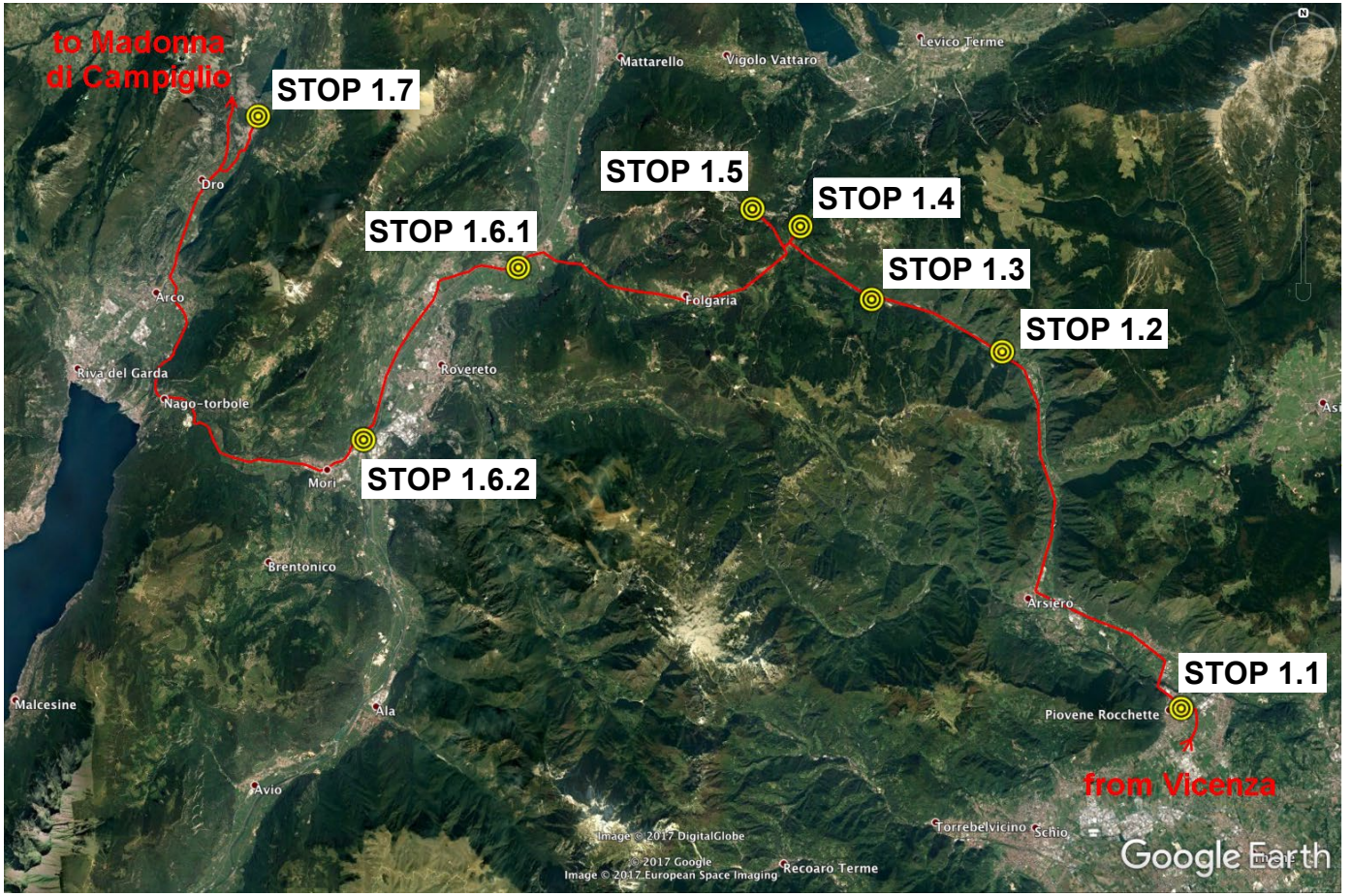

Fig. 1 - Itinerary of the field trip first day (base map from Google Earth).

DAY 2 - "Geology and structures of the central Brenta Dolomites"
During the second day of the field trip three stops are planned in the Brenta Massif (Grostè, Pietra Grande and Monte Spinale). The first one is at the Grostè Pass (Stop 2.1.1), reached by the cableway, with the geological introduction of the area. After a one-hour walk ("Vidi" protected climbing path) the Pietra Grande thrust is reached (Stop 2.1.2). Soon after, a grassy terrace allows for a panoramic view of the surrounding mountains belonging to the Adamello-Presanella and Cevedale massifs (STOP 2.2).
At Monte Spinale (STOP 2.3) the limestones of the Calcare di Zu override the carbonates of the Calcari Grigi Group (Monte Spinale klippe), as similarly observed for the Pietra Grande klippe and the Cima di Val Scura klippe (to the NE). The Monte Spinale thrust shows successive west-vergent reactivations, which deform also

DOI: 10.3301/GFT.2018.01

the Monte Spinale breccias. Even if their interpretation is still debated, they most probably represent fine-matrix rich stratified gravitational fluxes emplaced from the east (Grostè area).

Safety

The field trip goes through rough mountain terrains and reaches heights of about 2600 meters. Therefore, adequate technical personal equipment is required, especially for the "Vidi" protected climbing path (Stops 2.1.2 and 2.2). The best seasons for the visit are summer and autumn, with absence of snow cover. Avoid scheduling the visit after days of heavy rain.

Useful phone numbers:
Fire Fighters – 115 – Vigili del Fuoco
Police – 113 – Polizia

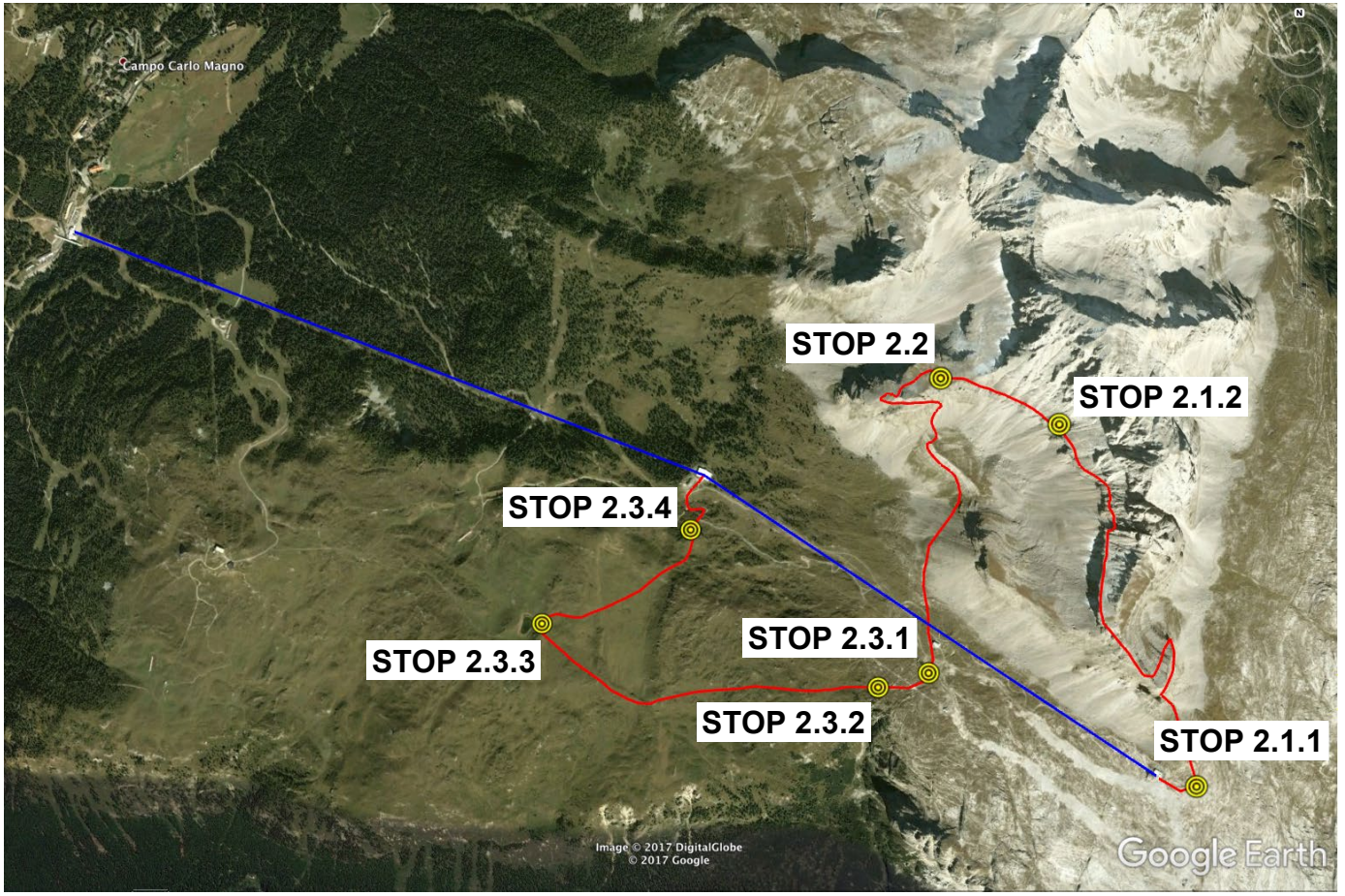

Fig. 2 - Itinerary of the field trip second day (base map from Google Earth).

Hospitals

Santorso (Vicenza) – Ospedale Alto Vicentino, Via Garziere 42, 36014 Santorso - Tel. 0445 571111
Trento – Ospedale Santa Chiara, Largo Medaglie d'Oro 9, 38122 Trento - Tel. 0461 903111
Rovereto – Ospedale S. Maria del Carmine, Corso Verona 4, 38068 Rovereto - Tel. 0464 403111

DOI: 10.3301/GFT.2018.01

Arco – Ospedale Civico, Via dei Capitelli 48, 38062 Arco - Tel. 0464 582222
Tione di Trento – Ospedale, Via Ospedale 11, 38079 Tione di Trento - Tel. 0465 331111

Other phone numbers:
Emergency – 112 – Emergenza (the only one emergency number in Trentino)
Ambulance – 118 – Ambulanza

Accommodation

Azienda per il turismo Trento, Monte Bondone, Valle dei Laghi, http://www.discovertrento.it
Trentino Marketing, https://www.visittrentino.info/it

Other phone numbers:
Servizio Geologico, Protezione Civile della Provincia Autonoma di Trento, www.protezionecivile.tn.it, Tel. 0461 495200
Parco Naturale Adamello-Brenta, www.pnab.it, Tel. 0465 806666
MuSE – Museo delle Scienze, www.muse.it, Tel. 0461 270311
SAT – Società degli Alpinisti Tridentini, www.sat.tn.it, Tel. 0461 981871

DOI: 10.3301/GFT.2018.01

The following introductory instruction notes are organized in two different sections. The first section is a general overview on geology and seismotectonics of the central-eastern sector of the Southern Alps. The second section is a specific focus on the geology of the Brenta Dolomites, a relatively small area within the central-eastern Southern Alps, and it represents the specific introduction of the second-day field trip.

1. Geology and seismotectonics of the central-eastern Southern Alps

The central-eastern Southern Alps are one of the most active areas of the Alpine belt where seismicity is related to deformation along the western margin of the Adriatic indenter (Slejko et al., 1989; Viganò et al., 2008; 2015). Deep seismic soundings show a complex structure of the Adriatic crust with local fragmentation and lower crust wedges, as similarly observed for upper crustal strong heterogeneities by local earthquake tomography (Viganò et al., 2013a). At the lithospheric scale, seismic tomography suggests an abrupt change of polarity of subduction along the Giudicarie realm (Europe subduction in the Western Alps vs. Adria subduction in the Eastern Alps; Kissling et al., 2006 and references therein).
Stratigraphy extends from pre-Permian metamorphic basements of the Austroalpine and Southalpine domains to Pliocene-Quaternary rocks in the Po and Venetian plains. Sedimentary covers of mainly carbonate sequences of Middle Triassic-Jurassic age extensively outcrop south of the Insubric Line, with variable lateral thicknesses between the so-called reduced Trento platform and the Lombardian Basin to the west and the Belluno Basin to the east (Doglioni and Bosellini, 1987; Picotti et al., 1995; Castellarin et al., 2006). Large magmatic bodies of Permian, Triassic, and Cenozoic age intrude the upper crust (Fig. 3).
The intricate fault pattern of the Southern Alps is the result of a polyphase deformation history since the Late Permian (Doglioni and Bosellini, 1987; Castellarin et al., 2006; Pola et al., 2014; Franceschi et al., 2014a) resulting in four main tectonic systems: the N-S Early Jurassic extensional fragmentation of the Trento platform, the ENE-WSW compressive Valsugana, the NNE-SSW transpressive Giudicarie, and the NW-SE strike-slip Schio-Vicenza fault systems (Fig. 3). In particular, two main compressive tectonic events accommodated deformation during the Neogene, by contraction and oblique inversion of the Mesozoic passive margin of the Adria plate: (i) along the Giudicarie fold-and-thrust belt and the Valsugana system (Middle-Late Miocene event), and (ii) along the Bassano del Grappa-Montello thrusts (Late Miocene-Pliocene event; Castellarin et al., 2006).
The eastern Southern Alps are a SSE-vergent mountain belt arranged in an imbricate fan of ca. ENE-WSW thrust sheets involving the crystalline basement (Fig. 3). In plan view, the thrusts show several undulations controlled

DOI: 10.3301/GFT.2018.01

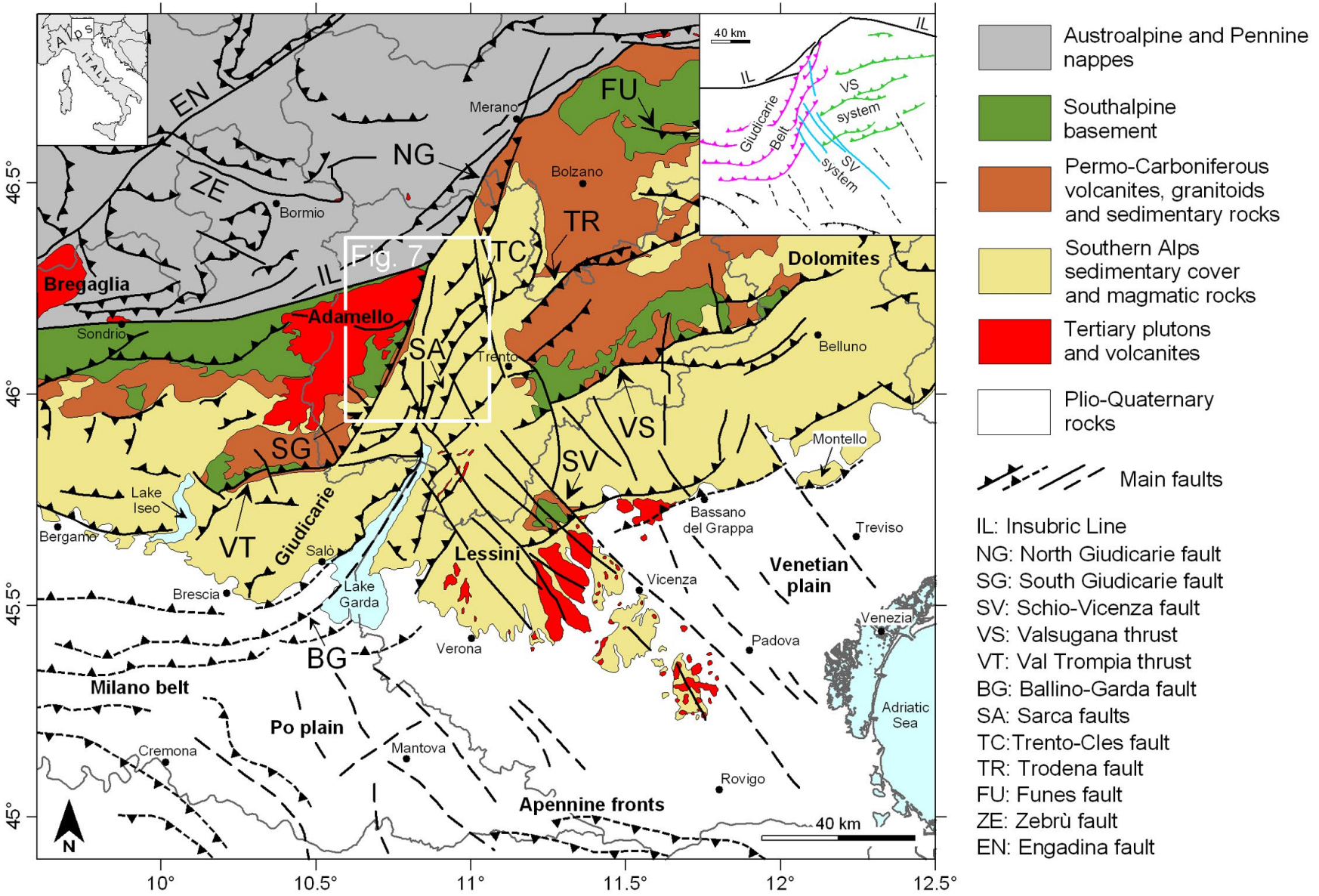

Fig. 3 - Geological map of the central-eastern Alps. In the sketch, the complex structural patterns at the junction of the three regional fault systems (Valsugana, Giudicarie and Schio-Vicenza). (Reprinted from Tectonophysics, 661, Viganò et al., *Earthquake relocations, crustal rheology, and active deformation in the central-eastern Alps (N Italy)*, 81-98, Copyright (2015), with permission of Elsevier).

DOI: 10.3301/GFT.2018.01

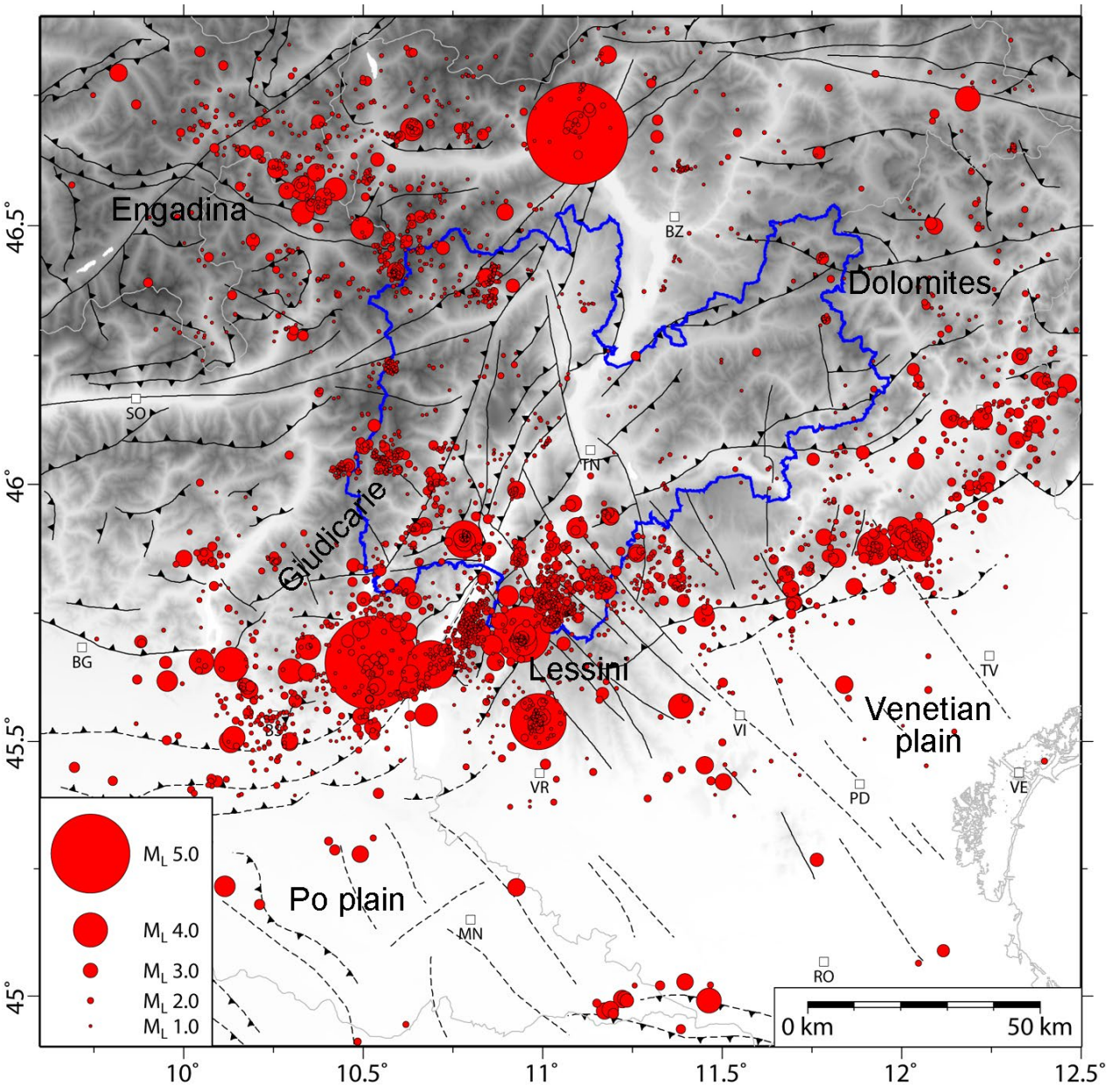

Fig. 4 - Instrumental seismicity distribution in the period 1994-2015, classified by local magnitude (courtesy of the Trentino seismic network of the Autonomous Province of Trento).

by inherited features, such as N-S to NNE-SSW Norian-Early Cretaceous normal faults and, in the western Veneto Region, NNW-SSE Paleogene normal faults. Crossing the Prealps from the southern foreland towards the north, west of the Adige Valley the Neogene structures trend NNE-SSW (Giudicarie belt), due to the sinistral transpression of the tectonically controlled western margin of the Trento carbonate platform (Fig. 3). In particular, the Giudicarie belt is a first-order deformation fault zone where Mesozoic extensional faults were inverted into compression systems, mostly during the Neogene, with important structural interactions with the Valsugana and the Schio-Vicenza faults (Castellarin et al., 2006).

The whole area shows relevant historical and instrumental seismicity; the proposed present-day seismotectonic model is based on earthquake distributions, focal mechanisms, and other geological constraints (Figs. 4 and 5) (Viganò et al., 2015). This seismotectonic model shows (dominant) compression along the Giudicarie and Belluno-Bassano-Montello fronts, with strain partitioning along dominant right-lateral strike-slip faults in the middle zone (Fig. 5). The present-

DOI: 10.3301/GFT.2018.01

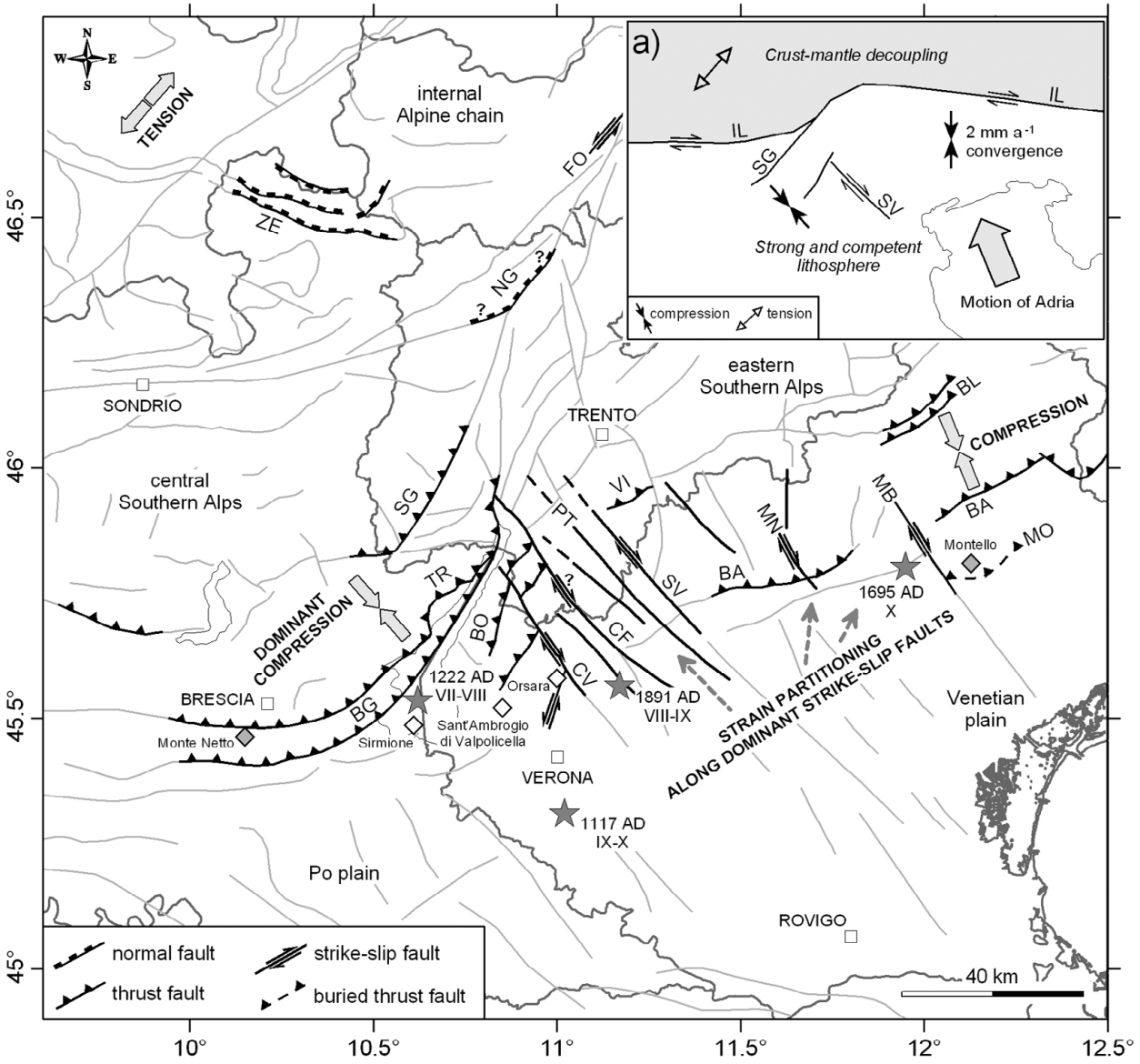

Fig. 5 - Seismotectonic model for the central-eastern Alps (Viganò et al., 2015). Grey stars are most relevant historical earthquakes after the Parametric Catalogue of Italian Earthquakes (CPTI15; Rovida et al., 2016), where Roman numbers are calculated epicentral intensities. Diamonds show the locations of geological sites where Quaternary fault activity along the Southalpine boundary is observed (grey diamonds for compressional tectonics; white diamonds for strike-slip and normal faults). Fault abbreviations are: BA, Bassano; BG, Ballino-Garda; BL, Belluno; BO, Baldo; CF, Campofontana; CV, Cerro Veronese; FO, Forst; MB, Montebelluna; MN, Montagna Nuova; MO, Montello; NG, North Giudicarie; PT, Priabona-Trambileno; SG, South Giudicarie; SV, Schio-Vicenza; TR, Tremosine; VI, Vigolana; ZE, Zebrù. Geodynamic framework in the sketch. (Reprinted from Tectonophysics, 661, Viganò et al., *Earthquake relocations, crustal rheology, and active deformation in the central-eastern Alps (N Italy)*, 81-98, Copyright (2015), with permission of Elsevier).

day deformation of the Southern Alps and the internal Alpine chain is compatible with a northward advancing Adria indenter, with observed and expected strain accumulations (i.e., seismicity) concentrated along the most favourably oriented tectonic structures (Fig. 4). The seismogenic sources of potential important earthquakes are shown in Fig. 6 (DISS Working Group, 2018).

DOI: 10.3301/GFT.2018.01

2. Geology of the Brenta Dolomites

The Brenta Dolomites are a 40 km long and 15 km wide massif, mainly composed of thick successions of Mesozoic dolomite and limestone. The massif can be viewed as a wide, NNE-trending antiform bounded by nearly parallel structures of regional importance such as the Giudicarie and Sabion faults to the west and the Molveno thrust to the east. Within the massif, the N-trending Vedretta dei Camosci fault represents the boundary between two major paleogeographic domains of the Southern Alps, the Lombardian Basin to the west and the Trento Platform to the east (Castellarin et al., 1993) (Fig. 7).

The oldest stratigraphic units of the Brenta Massif are represented by Permian to Middle Triassic sedimentary and volcanic rocks, very similar to the coeval units deposited in the Lombardian Basin. The stratigraphic succession can be observed along the left side of the Rendena Valley, in the southwestern sector of the Brenta Massif, at the hanging-wall of the Sabion fault. Permian volcanics and clastic rocks overlie the Southalpine basement represented by the Rendena schists intruded by the Sabion granite. Intense synsedimentary tectonics of Permian age is testified by sudden thickness variations in both volcanic and sedimentary units and by the occurrence of breccia layers

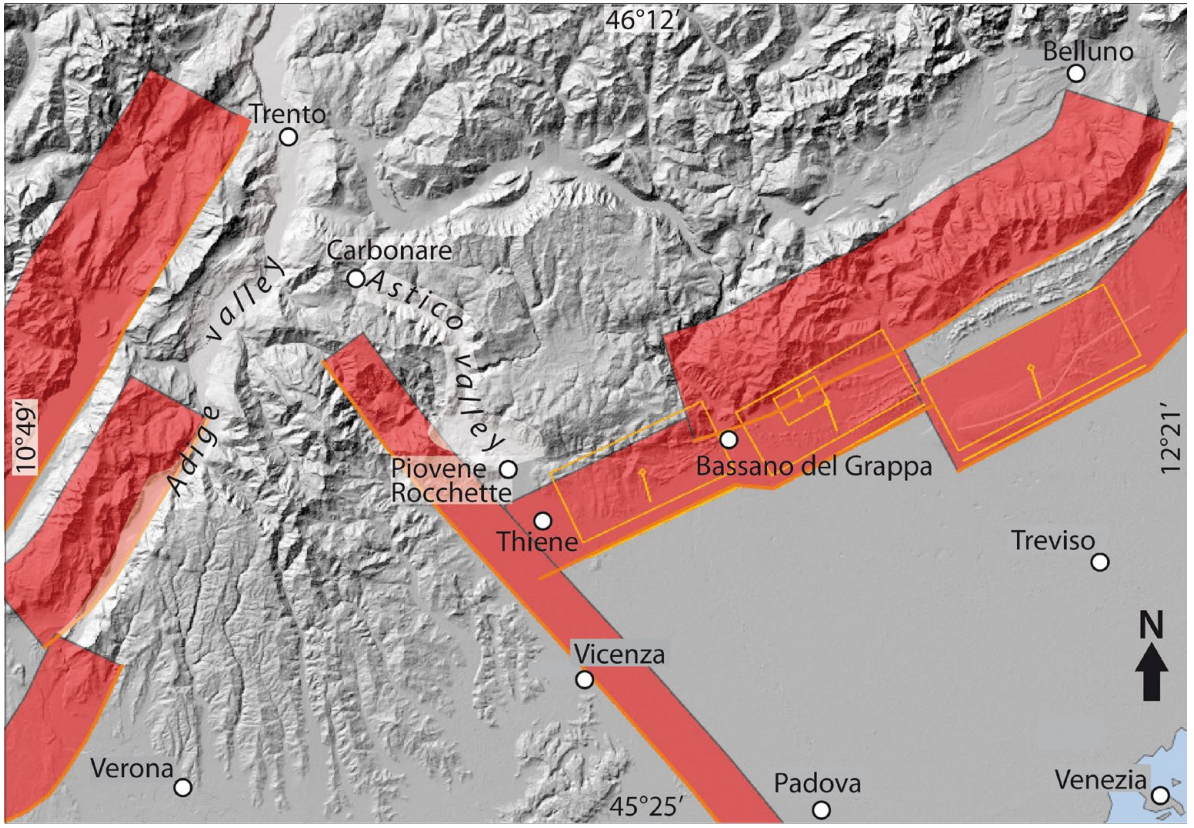

Fig. 6 - Map showing the composite seismogenic sources (in red colour) crossed by the field trip (DISS v. 3.2.1; DISS Working Group, 2018). At the western termination of the eastern Southern Alps front, the ENE-WSW Thiene-Cornuda source (ITCS007) underlies the chain-foreland transition zone. To the left, from south to north the Solferino (ITCS114), the Monte Baldo (ITCS073) and the Giudicarie (ITCS048) composite seismogenic sources trend NNE-SSW. The NW-SE Schio-Vicenza source (ITCS175) bounds the foreland of the eastern Southern Alps. Yellow boxes are individual seismogenic sources.

DOI: 10.3301/GFT.2018.01

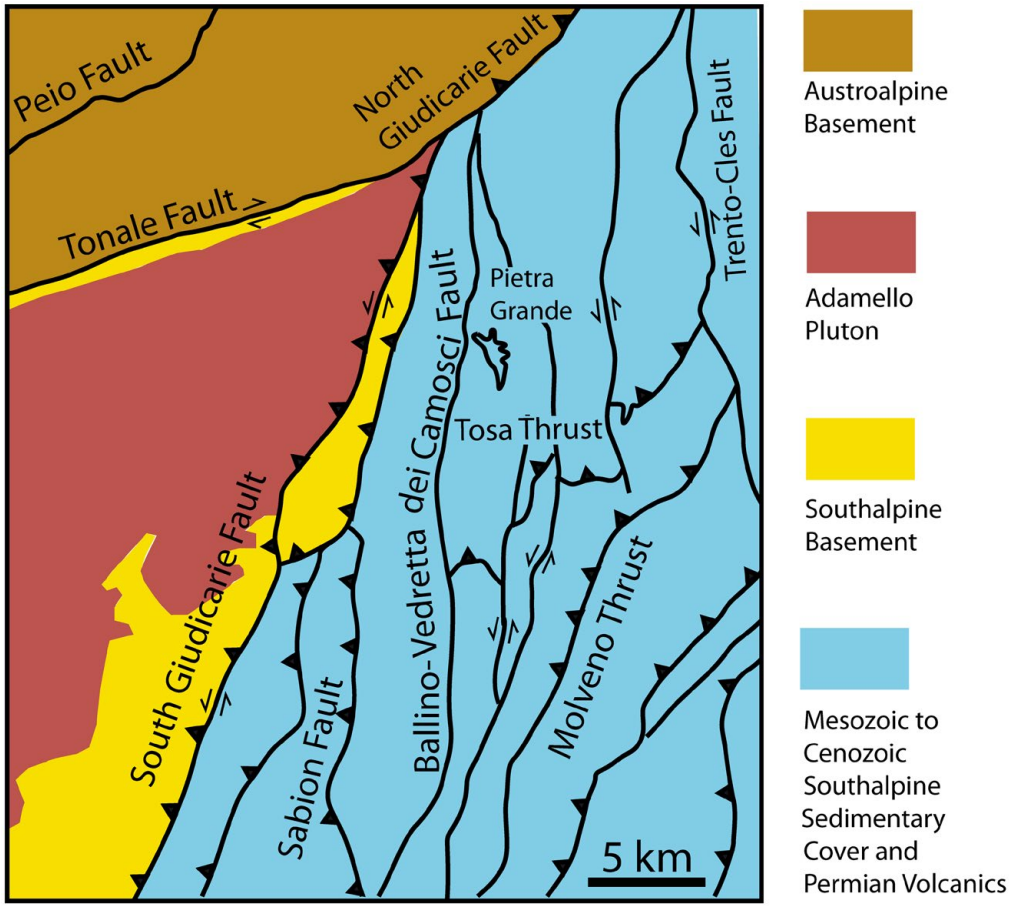

Fig. 7 - Schematic tectonic map of the Brenta Massif.

consisting of clasts of the Rendena schists (Castellarin et al., 2005a).

The backbone of the Brenta Dolomites is made up of an about 2500 m thick carbonate succession of Late Triassic to Early Jurassic age (Fig. 8). It includes the Norian Dolomia Principale (about 1200 m thick), the Rhaetian Calcare di Zu (about 300 m thick) and the Early Jurassic Monte Zugna fm. limestones (about 600 m thick). The presence of clay layers within the Calcare di Zu provides an important décollement level that influenced the geometry of the contractional structures during the Miocene deformation.

The opening of the Lombardian Basin is documented by the presence of basinal facies of Early Jurassic age in the southwestern sector of the Brenta Massif, above the Monte Zugna fm. or resting directly above the Calcare di Zu. This implies the activation of the N-trending Ballino-Vedretta dei Camosci Jurassic fault system (Castellarin, 1972), together with nearly NW-trending transfer faults (i.e., the Forcolotta fault; Castellarin et al., 2005a). In the eastern part of the Brenta Massif carbonate platform sedimentation continued up to the Toarcian with the deposition of oolitic limestones.

After the drowning of the Trento platform, during the Late Cretaceous the Brenta area underwent extensional tectonics, as testified by Scaglia Rossa, filling neptunian dykes within the limestone of the Calcari Grigi Group and forming a syntectonic wedge at the hanging-wall of a Late Cretaceous normal fault. Tectonic activity during the Late Cretaceous-Paleogene times can be also envisaged by the presence of the Val d'Agola fm. (similar to the Lombardian Flysch) along a narrow strip located at the footwall of the Sabion fault.

The present-day structure of the Brenta Dolomites is the result of the Neoalpine shortening events that acted on inherited structures developed during the Mesozoic rifting and the Late Cretaceous extensional tectonics. Neoalpine

DOI: 10.3301/GFT.2018.01

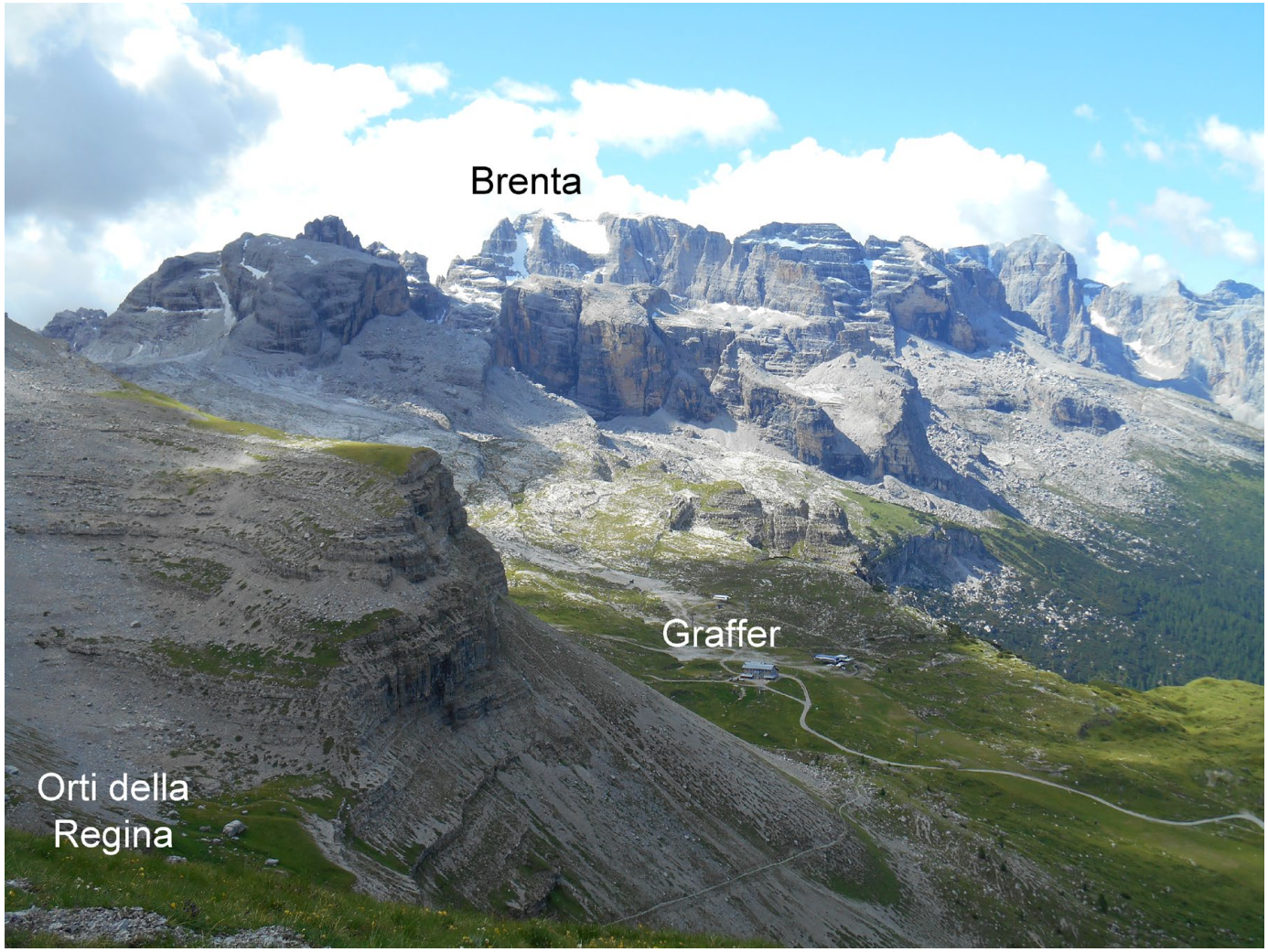

Fig. 8 - The central Brenta Massif, with Orti della Regina on the left and Rifugio Graffer in the lower middle.

contraction took place from the Late Oligocene to the Pliocene-Pleistocene, through a series of tectonic events characterized by variable contraction direction. The major deformation event (Valsugana phase), characterized by SSE-directed shortening, took place during the Middle-Late Miocene (Selli, 1998; Castellarin et al., 2006).

The main contractional structure, occurring in the central part of the Massif, is the Tosa thrust, a low-angle fault, which takes the Dolomia Principale on top of the Calcare di Zu. One major feature of this thrust contact is its segmentation, since it appears dissected by a series of N- to NNE-trending faults, which in most cases reactivate pre-existing Jurassic normal faults. These N- to NNE-trending faults show steeply W-dipping surfaces and mostly display a sinistral kinematics, showing in some cases a contractional component. The Tosa and the Molveno thrusts terminate eastwards against the Trento-Cles line, an important left-lateral transpressive fault that branches from the North Giudicarie fault (Prosser, 1998). The presence of a major décollement level located within the Calcare di Zu explains the occurrence of klippen, made up of Calcare di Zu and Monte Zugna fm. limestones, located on several summits of the Brenta Massif. Klippen

DOI: 10.3301/GFT.2018.01

derive from thin-skinned thrust sheets whose formation is mainly connected to the activity of the major Tosa thrust. The N-vergent Pietra Grande thrust is the largest klippe that can be observed in the Brenta Massif. It formed as an intercutaneous backthrust developed at the hanging-wall of the Tosa thrust.
Here below a summary of the main Neoalpine tectonic phases which affected the Southern Alps and consequently the Brenta Dolomites and the Monte Spinale area (cf. STOP 2.3), according to Castellarin et al. (2006) and references therein:

*** Step 1 Late Oligocene - Early Miocene (Insubric event)**
The right-lateral motion of the Tonale fault implies thrusting of the Austroalpine Units onto the Southalpine Mesozoic cover, along the North Giudicarie fault (Prosser, 1992; 1998). The South Giudicarie fault is active and a Southalpine basement wedge forms between the Sabion thrust and the Giudicarie fault (Picotti et al., 1995). Onset of deformation along the Cima Tosa thrust probably occurs during this step. In the Eastern Dolomites, this event is marked by a NNE-trending compressional axis (Caputo, 1996).

*** Step 2 Middle - Late Miocene (Valsugana event)**
This event is marked by SSE-verging structures, as the main Valsugana thrust with 15 km shortening. In the Brenta Dolomites, deformation involves sinistral transpression along the N- and NNW-trending faults, in part inherited from the Mesozoic rifting event. Transpression along the Giudicarie fault is indicated by apatite fission track ages of the Corno Alto area (Martin et al., 1998). The Vallon-Cima Tosa thrust, with associated klippen (Spinale, Pietra Grande, Turrion and Campa), is also active.

*** Step 3 Messinian - Pliocene (Adriatic event)**
In the eastern Southern Alps, this event is marked by NW-SE compression (Schio-Vicenza fault, Bassano and Montello thrusts). In the Spinale area, the Pozza Vecchia reverse fault (cf. Fig. 60) is activated by E-W compression. The Spinale klippe is reactivated and the Mt. Spinale west-verging breccias are deformed.

*** Step 4 Quaternary**
The WNW-trending extension along the Vedretta dei Camosci normal fault involves the Monte Spinale breccias.

DOI: 10.3301/GFT.2018.01

Day 1: Geology and tectonics of the Astico Valley and southern Trentino: faults, rock-avalanches and seismicity

STOP 1.1: The Southern Alps frontal belt and geomorphology of the Astico frontal moraine system (45.7617 °N, 11.4382 °E)

The geological field trip starts at Piovene Rocchette, in a large service area next to the main road (SP350). For this introductory Stop, the viewpoint is located at the southern termination of the Astico Valley and at the foot of the seismotectonically active front of the eastern Southern Alps belt, between Schio (to the west) and Tricesimo (to the east). At the front of the chain, the stratigraphy of the uplifted sedimentary units forming the Vicentinean plateaux (Asiago, Summano, Pasubio, Tonezza, etc.) will be illustrated (Figs. 9 and 10). In the lower part of the Astico Valley, the evolution of the LGM events of the Astico Glacier have left a prominent imprint on the landscape, including the deep incision of the head of the glaciofluvial Thiene fan. The middle part of the valley is characterized by a rockslide controlled by the structural setting of the slope and possibly triggered by an historical seismic event. In the upper part of the Astico Valley, a prominent fault related to the Early Jurassic extensional tectonics crops out. The effects of the Neogene reactivation with a strike-slip kinematics of these inherited N-S to NNE-SSW trending normal faults are evident in the next stop at the Carbonare Saddle between the Astico and the Centa valleys. Here, the active pop-up structure of the Monte Cornetto di Folgaria is hanging 1000 m over the plateaux level, showing

Fig. 9 - View towards the north from the Vicentinean plain, which belongs to the foreland of the eastern Southern Alps. The ca. 1000 m. high mountain front corresponds to the alignment of the hanging-wall of some NNW-dipping reverse faults with southern vergence (Schio-Piovene and Bassano thrusts). A more southern blind fault segment (Thiene-Bassano), included in the national Database of the Individual Seismogenic Sources (DISS; DISS Working Group, 2018), is believed to be the true frontal structure of this part of the chain (cf. Figs. 6 and 11).

DOI: 10.3301/GFT.2018.01

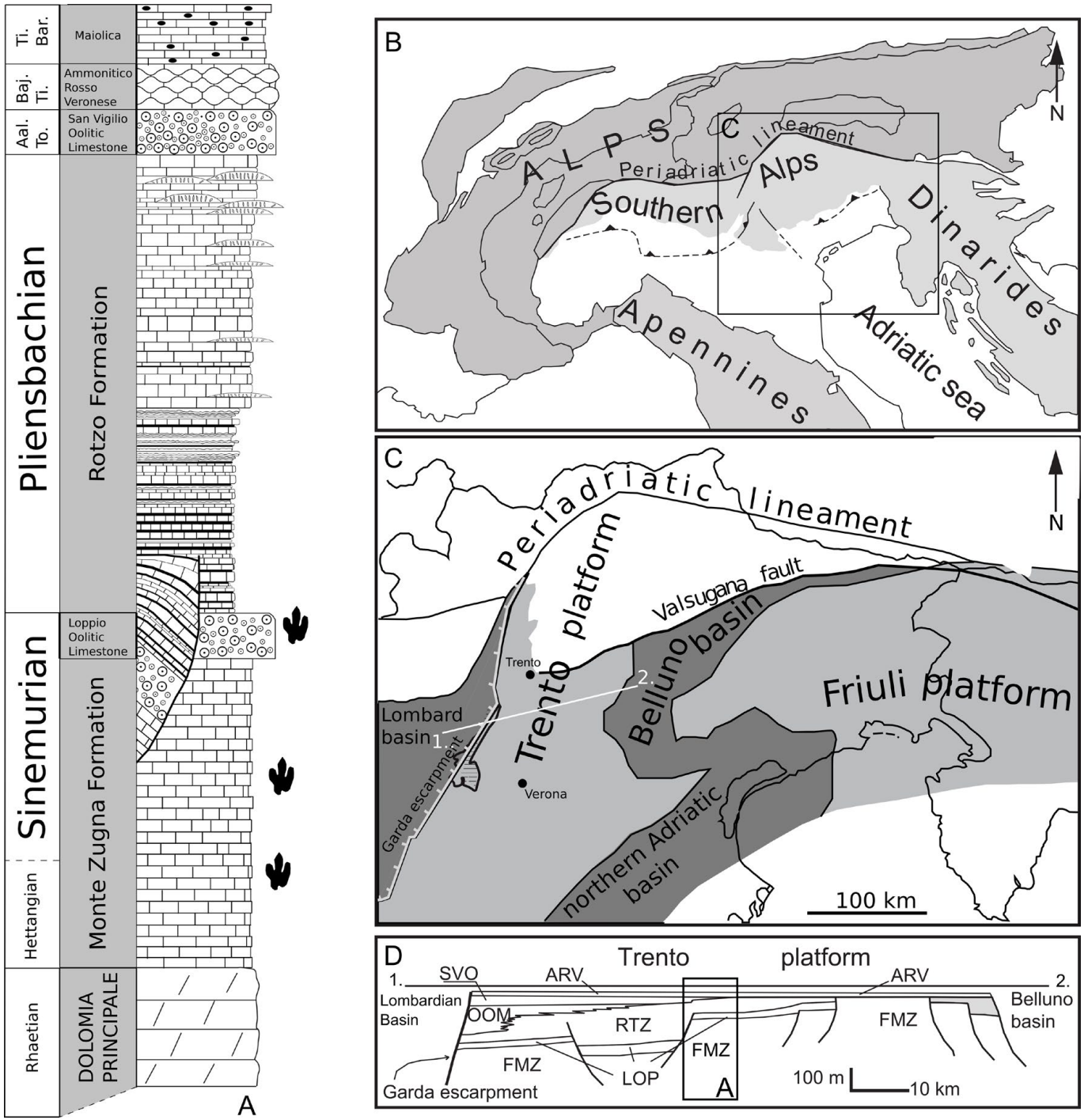

Fig. 10 - A) Schematic stratigraphic column displaying the stratigraphy crossed during Excursion Day 1, along the river Astico Valley up to Carbonare (Fricca Pass). Note the syn-sedimentary tectonics dissecting the Loppio Oolitic Limestone. Approximate stratigraphic position of findings of dinosaur footprints is indicated. B) Location of the Southern Alps. C) Paleogeographic map of the area of the Southern Alps during the Early Jurassic. D) Cross section of the Early Jurassic paleogeographic map showing the stratigraphic relationships between the units displayed in A. Note syn-sedimentary faults cutting the Lower Jurassic series up to the Loppio Oolitic Limestone and inducing thickness variations in the Rotzo fm. FMZ = Monte Zugna fm., LOP = Loppio Oolitic Limestone, RTZ = Rotzo fm., OOM = Massone Oolitic Limestone, SVO = San Vigilio Oolitic Limestone, ARV = Rosso Ammonitico Veronese. (C and D modified from Marine and Petroleum Geology, 79, Martinelli et al., *An extensional syn-sedimentary structure in the Early Jurassic Trento Platform (Southern Alps, Italy) as analogue of potential hydrocarbon reservoirs developing in rifting-affected carbonate platforms*, 360-371, Copyright (2017), with permission of Elsevier).

DOI: 10.3301/GFT.2018.01

accelerated erosional processes acting on the strongly fractured dolostone fault rocks (Fricca Pass).
The presence of the Thiene-Bassano blind thrust is revealed by the Montecchio Precalcino hill, which lies isolated in the Quaternary plain just to the north of Dueville (Fig. 11). On the basis of some 2D seismic sections performed in the seventies, in the 1977 AGIP spa drilled the Villaverla 1 well, just to the north of the Montecchio Precalcino hill (Fig. 12). The well reached the metamorphic basement at 4205 m depth, after crossing a gentle anticline fold, clearly developed in the hanging-wall of a deeper blind thrust. This fault has been included in the DISS, following the papers from Galadini et al. (2005) and Burrato et al. (2008) (Fig. 6).
Westwards, the eastern Southern Alps terminate at Schio, against the Schio-Vicenza fault. This fault separates the foredeep from the Lessini-Berici-Euganei structural high (southern Alpine foreland) and

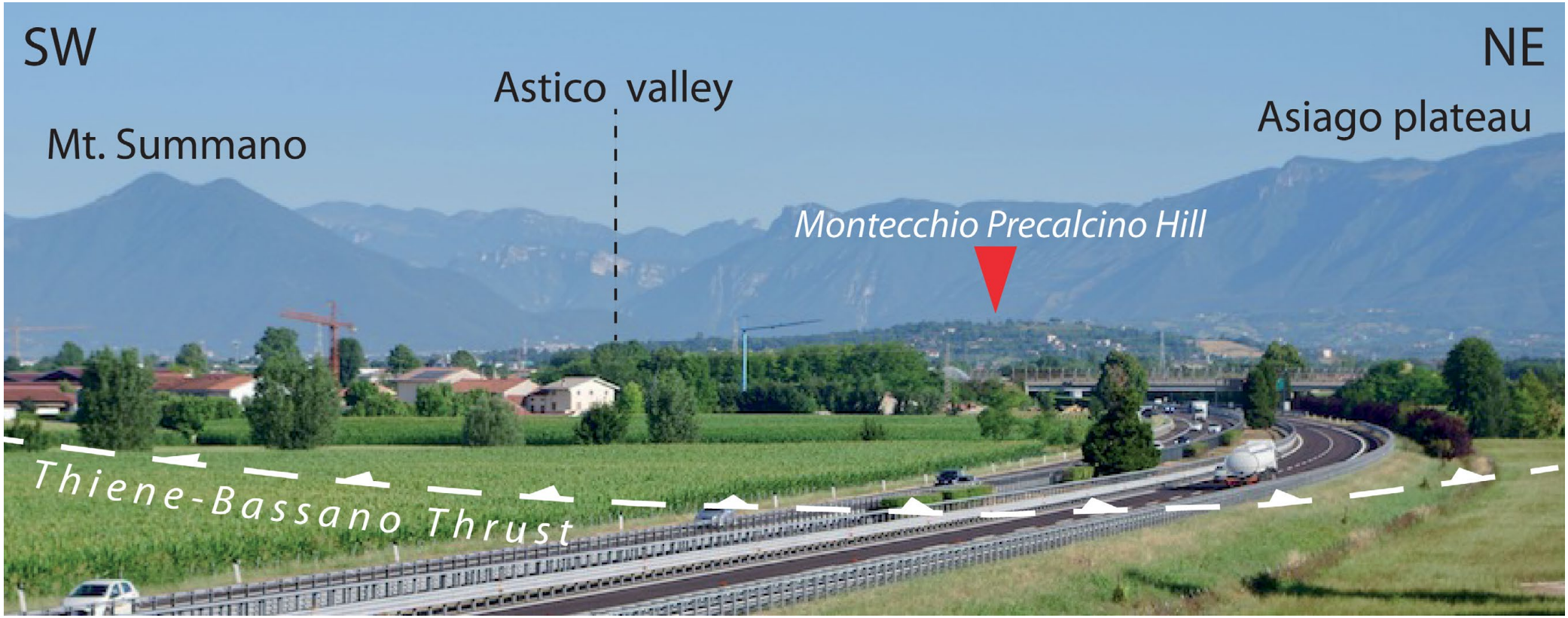

Fig. 11 - The Montecchio Precalcino hill, made of Cenozoic sediments and volcanics, is isolated in the Vicentinean plain. Looking northwest from the plain (near Dueville).

DOI: 10.3301/GFT.2018.01

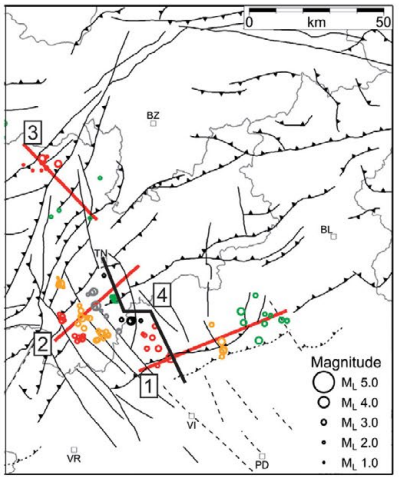

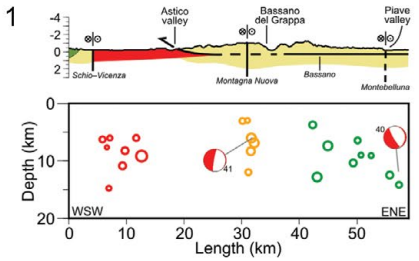

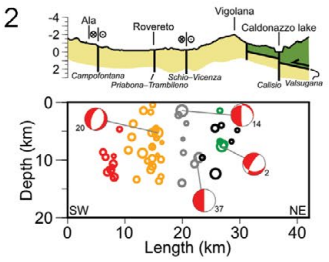

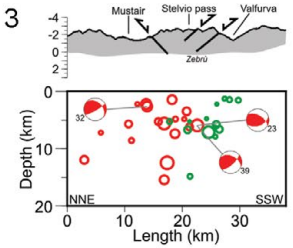

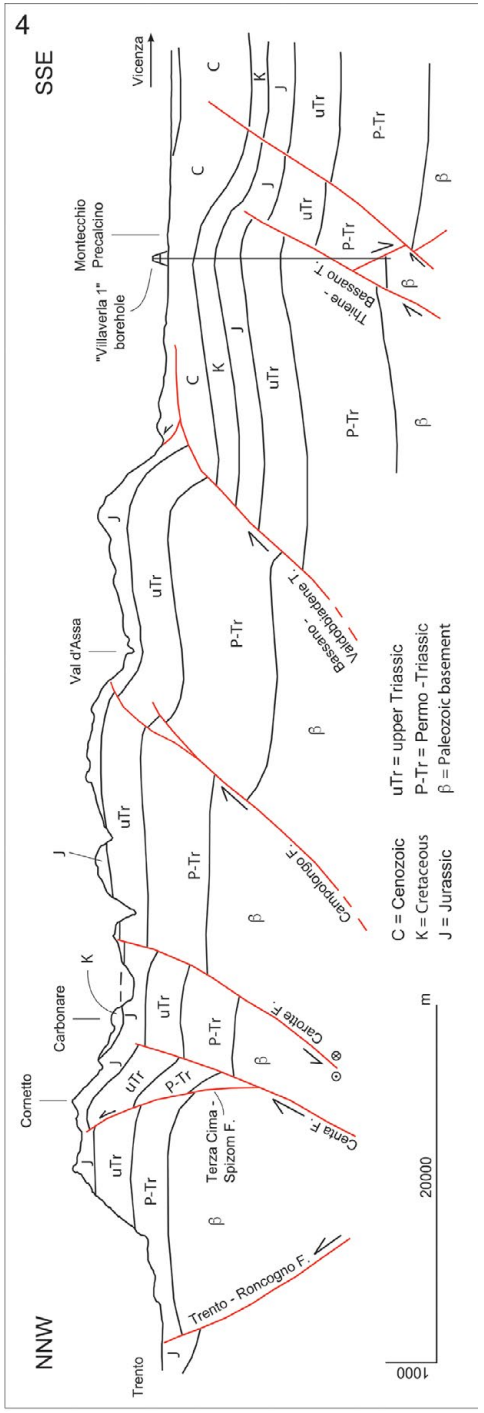

is part of the Schio-Vicenza fault system, oriented at high angle with respect to the chain (Fig. 3). The Schio-Vicenza fault system is composed of some high-angle NW-trending segments, which have been active since the Mesozoic as normal faults (Pola et al., 2014) and are seismically active in the internal chain portion (cf. vertical earthquake alignments in the seismotectonic cross-section 2 of Fig. 12). The present kinematics of the southern part of the Schio-Vicenza segment should be transtensional sinistral, but in the northern part, the seismicity shows a dextral strike-slip activity (see STOP 1.4 for an explanation).

The Piovene Rocchette village lies near the present course of the Astico river, which is the major river course of the north-western Venetian Plain and still influences the Quaternary stratigraphic setting of this area. Two major sedimentary bodies can be identified: the Thiene fan to the east, and the Schio fan to the west (Fig. 13). These alluvial

Fig. 12 - Structural map of the eastern Southern Alps with relocated seismicity of the period 1994-2007 (classified by local magnitude) and the traces of the cross-sections. Sections 1, 2 and 3 show the solutions of the focal mechanisms (modified from Tectonophysics, 661, Viganò et al., *Earthquake relocations, crustal rheology, and active deformation in the central-eastern Alps (N Italy)*, 81-98, Copyright (2015), with permission of Elsevier). Section 4 nearly follows the itinerary of the excursion first day from STOP 1.1 to STOP 1.5. The kinematics of the faults refers to the Neogene-Quaternary deformation phase. Earthquakes shown in cross-sections 1-2: #2, 24 Oct 1994 M_L= 3.2; #14, 26 Apr 1999 M_L= 3.4; #20, 16 Jun 2000 M_L= 3.2; #37, 13 Sep 1989 M_L= 4.7; #40, 4 Dec 2004 M_L= 3.3; #41, 9 Nov 2009 M_L= 3.4.

DOI: 10.3301/GFT.2018.01

fans, likewise the neighbouring Brenta megafan, were deposited mainly during the LGM, when a glacier tongue was flowing into the Astico Valley up to a few kilometers to the NNW of Piovene Rocchette, where a system of LGM terminal moraines is still visible.

Three distinct glacial events were recognized in the middle and lower Astico Valley. The more recent one is attributed to the LGM and the others to the Middle Pleistocene. The related deposits are characterized by the presence of peculiar petrographic signatures, which point to recurrent glacial transfluences of the Adige Glacier through the Carbonare Saddle (see STOP 1.4) into the Astico Valley.

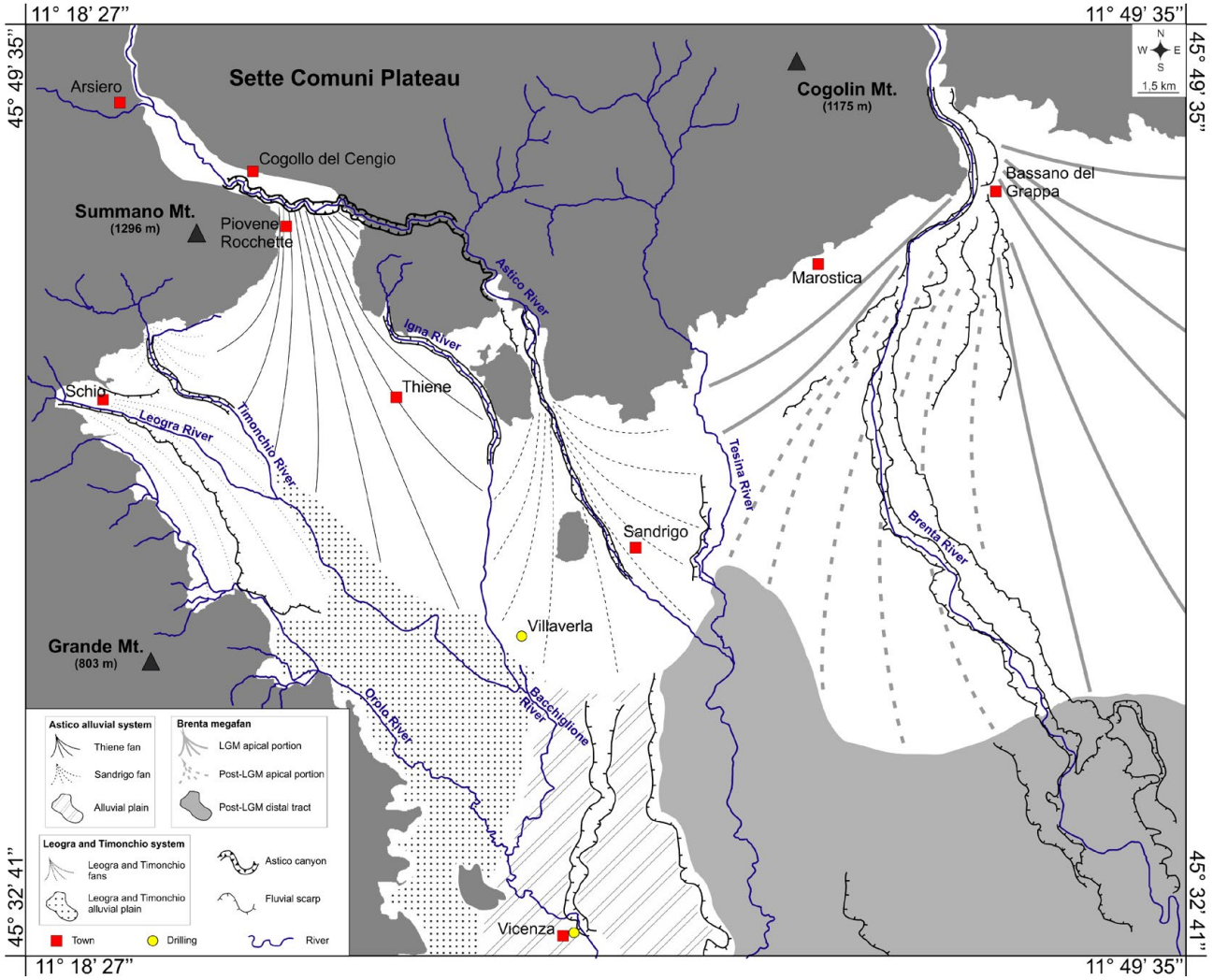

Both Middle Pleistocene glacial advances reached about 6 km down-valley of the LGM terminal moraines (Fig. 14 I-III). This implies that they were related to major glaciations, which could activate the Adige Glacier transfluence through the Carbonare Saddle and allow glacial tongues to reach this marginal prealpine sector. Minor fluctuations of the LGM glacier front led to the formation of several terminal moraines (Figs. 14 IV-V and 15) and conditioned the evolution of the glaciofluvial system in the terminal

Fig. 13 - Geomorphological sketch of the western Venetian plain. (Reprinted from Quaternary International, 288, Rossato et al., *Late Quaternary glaciations and connections to the piedmont plain in the prealpine environment: The middle and lower Astico Valley (NE Italy)*, 8-24, Copyright (2013), with permission of Elsevier).

DOI: 10.3301/GFT.2018.01

valley and the piedmont plain. The more internal position was probably occupied during an event of general withdrawal of the Alpine glaciers at 23-24 cal ka. At the end of the LGM, the collapse of the transfluence from the Adige Glacier led to a rapid decay of the Astico Glacier and to the downcutting at the head of the glaciofluvial Thiene fan (Fig. 14 VI). Local flow conditions led to the activation of an eastern way to the piedmont sector through a gorge cut in bedrock, which fed the Sandrigo fan during the Lateglacial. This mechanism is likely to have occurred multiple times during the Pleistocene, as testified by older deposits, and is probably connected to the presence of tectonic structures/ stratigraphic contacts.

The lower and middle Astico Valley registered even subtle climatic changes during glaciations, allowing the preservation of a significant, though fragmentary, geological record concerning past glacial/ interglacial cycles.

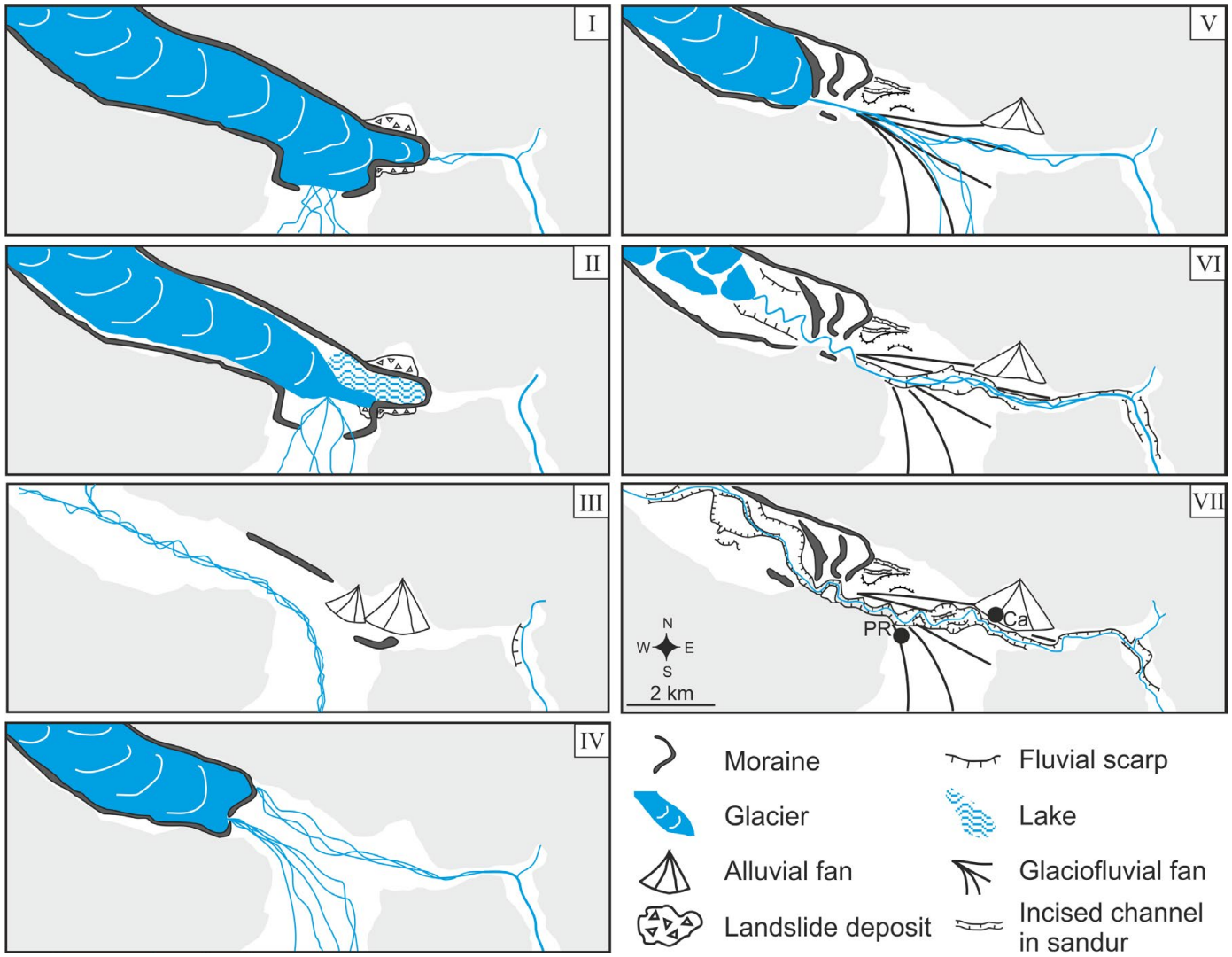

Fig. 14 - Evolution of the middle-lower Astico Valley since the Middle Pleistocene (PR, Piovene Rocchette; Ca, Caltrano). I-III show the penultimate glacial cycle, IV-VI the LGM evolution of the area, and VII is the present situation (Rossato et al., 2013). (Reprinted from Quaternary International, 288, Rossato et al., *Late Quaternary glaciations and connections to the piedmont plain in the prealpine environment: The middle and lower Astico Valley (NE Italy)*, 8-24, Copyright (2013), with permission of Elsevier).

DOI: 10.3301/GFT.2018.01

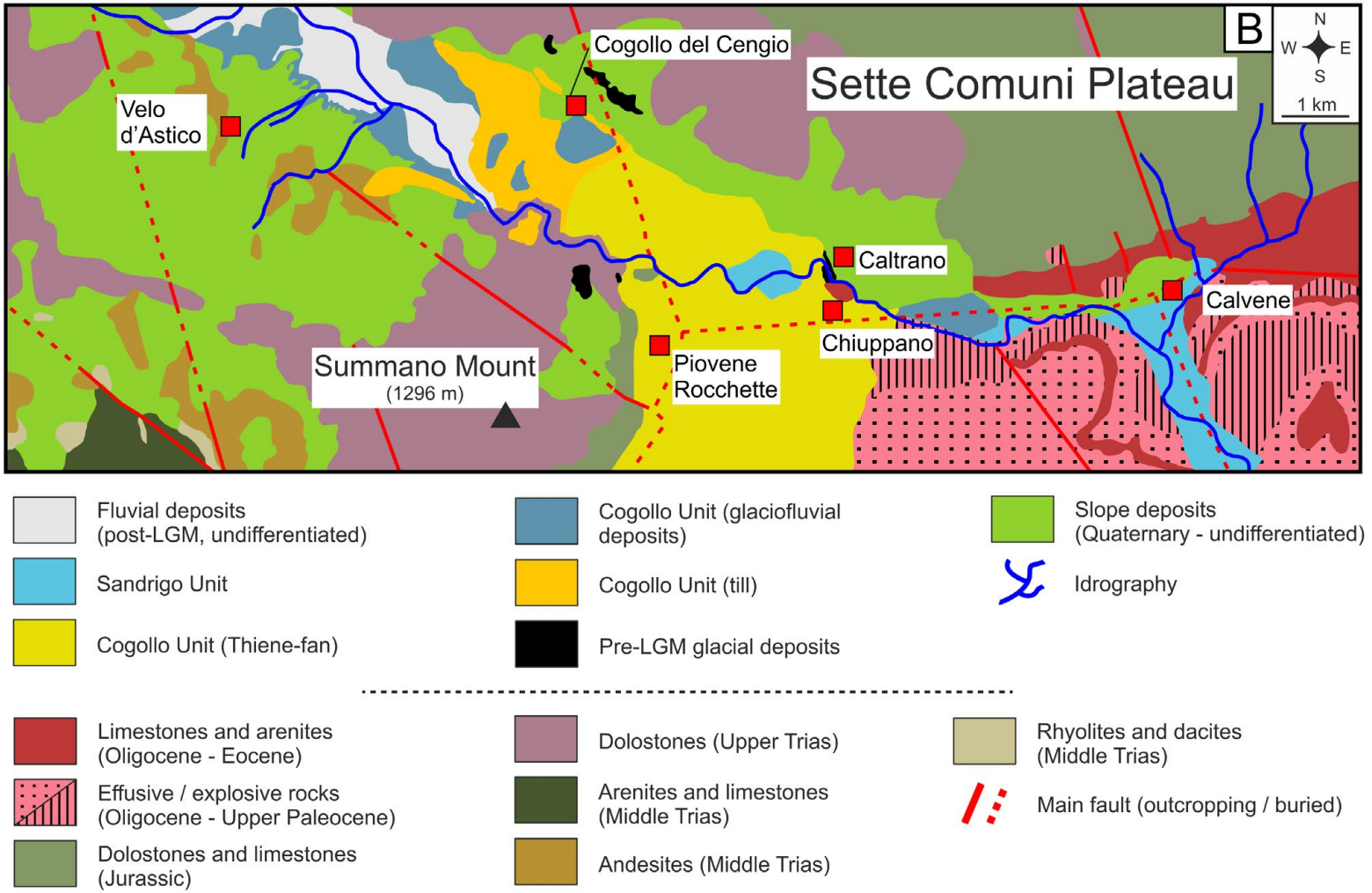

Fig. 15 - Geological sketch of the terminal Astico Valley. The LGM frontal moraine system is also shown (Rossato et al., 2013). (Modified from Quaternary International, 288, Rossato et al., *Late Quaternary glaciations and connections to the piedmont plain in the prealpine environment: The middle and lower Astico Valley (NE Italy)*, 8-24, Copyright (2013), with permission of Elsevier).

STOP 1.2: La Marogna landslide: a structurally controlled collapse (45.8953 °N, 11.3416 °E)

The Stop is located in front of the landslide, on the left valley side and close to the bridge to reach the quarry headquarters. In the middle part of the Astico Valley, where its orientation changes from W-E to N-S, a huge (about 13 x 10^6 m^3) rockslide deposit (La Marogna) was damming the valley (Figs. 16 and 17). The deposit is mainly composed of dolostones and resulted from several rockfall events, the main of which can be possibly referred to an important triggering seismic event (for a detailed discussion see STOP 1.7; cf. Fig. 45).

DOI: 10.3301/GFT.2018.01

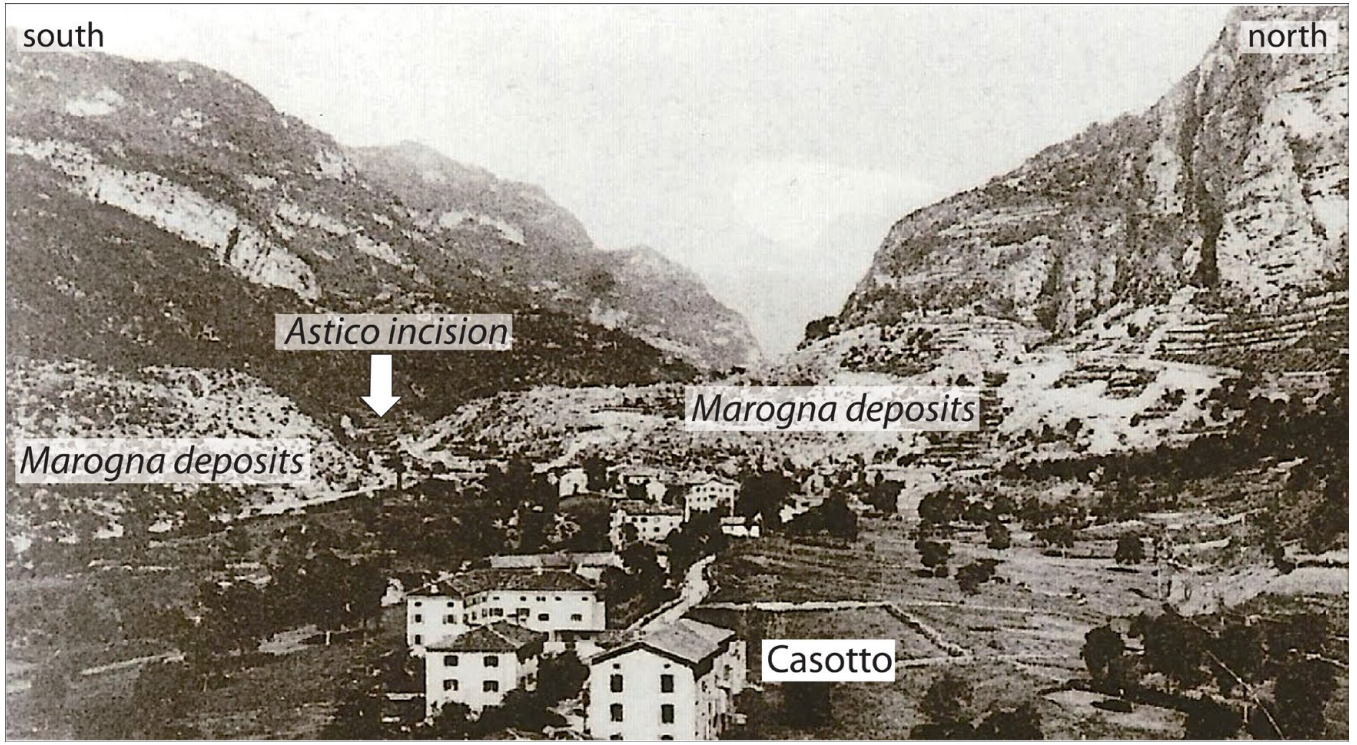

Fig. 16 - Old photo towards the WNE showing the rockslide deposits damming the Astico Valley. The slope failure occurred on the right slope of the valley (left in photo), where the base of the main scarp lies 400 m above the valley floor. In 1278, the natural dam collapsed and the upstream lake vanished.

In recent years, the slide deposits were quarried on the left bank of the Astico creek, while quarrying on the right flank of the valley is still ongoing. This activity has produced a flat area on the valley bottom, which is now suitable for human development. The failure surface corresponds to a fault plane dipping 35° towards the valley floor (Fig. 18); this fault is clearly visible also along the landslide crown (Figs. 19 and 20) (Zampieri and Adami, 2013). The structural features observed at the base of the main scarp (Figs. 19 and 20) would suggest that the La Gioia slope represents a potential geologic hazard and that any development of the valley portion, formerly occupied by La Marogna deposits, should be preceded by an accurate risk assessment.

STOP 1.3: The Jurassic faults across the Vicentinean plateaux (45.9148 °N, 11.2712 °E)

To reach the viewpoint, take the path behind the church (Località Togni) up to the forest edge. The outcrops can be viewed on the opposite valley side.
The route along the Astico Valley goes through a sedimentary succession spanning from the Late Triassic to the Cretaceous. The Dolomia Principale forms the lower portion of the Vicentinean plateaux and it is made of dolostones organized in classical peritidal cycles deposited on a carbonate shelf. At the time of the Dolomia

DOI: 10.3301/GFT.2018.01

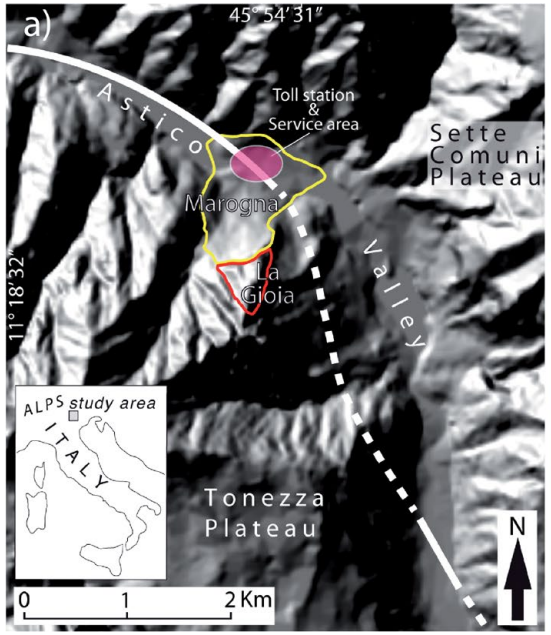

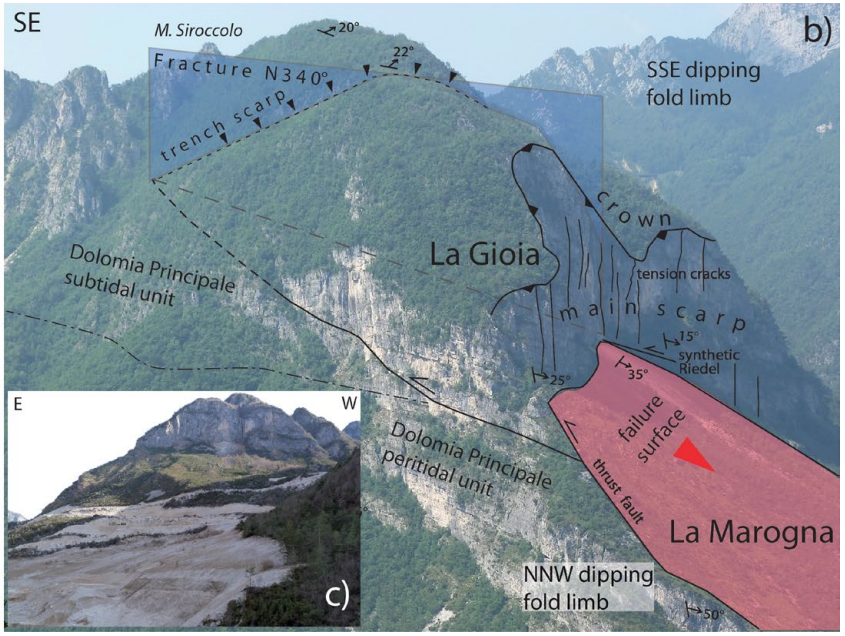

Fig. 17 - **a)** Location of the La Marogna landslide (yellow line); the red line is the contour of the rock mass upstream of the crown (La Gioia), potentially involved by a future landslide. The white line is the designed motorway trace (continuous: surficial; dashed: underground) (Zampieri and Adami, 2013). **b)** Oblique view of the La Gioia upper slope and the upper part of the La Marogna deposit. The rockslide occurred on the northern limb of an anticline (southern limb visible in the background, in the upper right). **c)** Viewing from north, the rockslide main scarp is a 100 m-high face cliff.

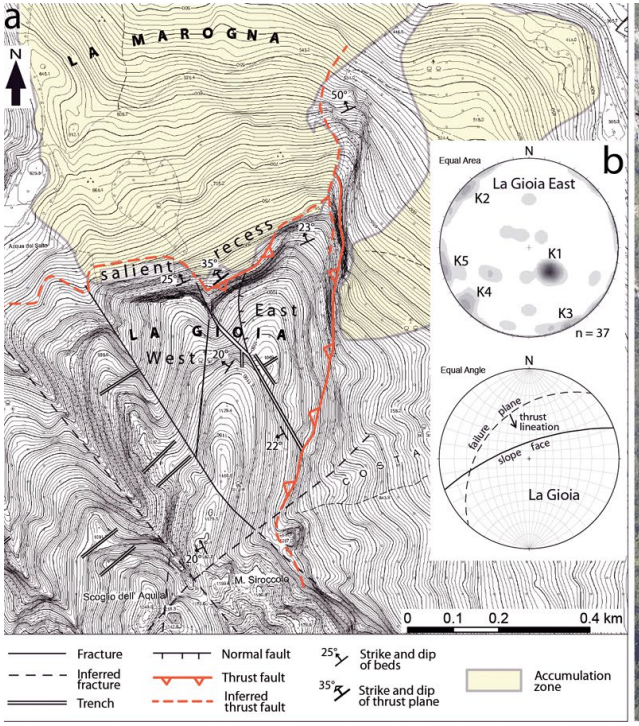

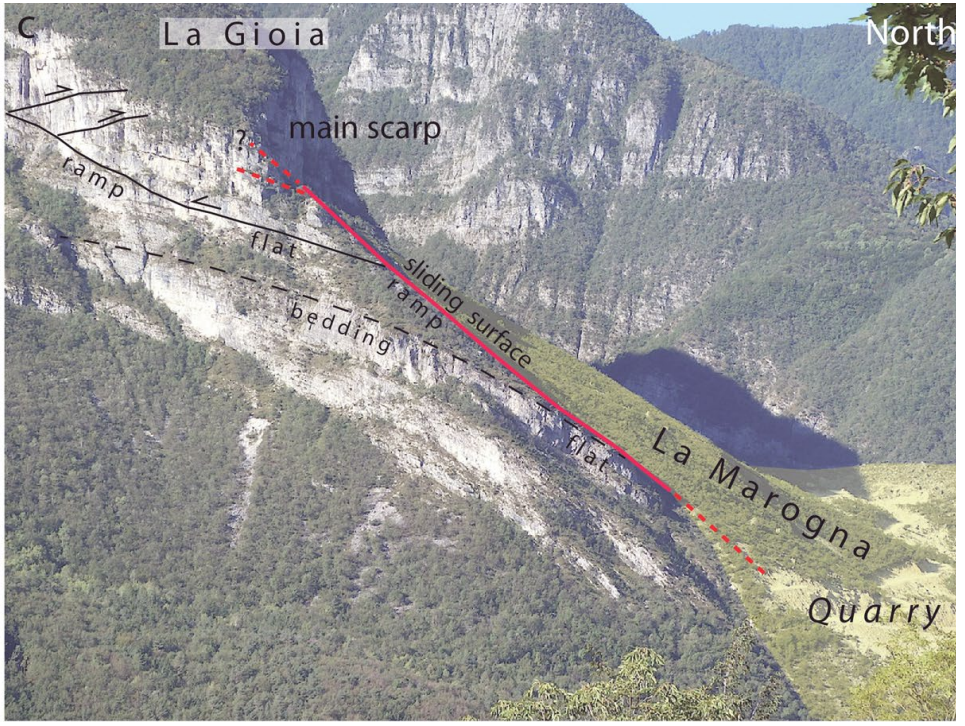

Fig. 18 - **a)** Structural sketch of the La Gioia upper slope. **b)** Plots (lower hemisphere) of the main fracture/fault sets recognized on the eastern sector of the La Gioia upper slope and of the slope face with the failure plane. **c)** Natural cross section of the La Marogna rockslide showing the relationship between bedding and sliding surface (Zampieri and Adami, 2013).

DOI: 10.3301/GFT.2018.01

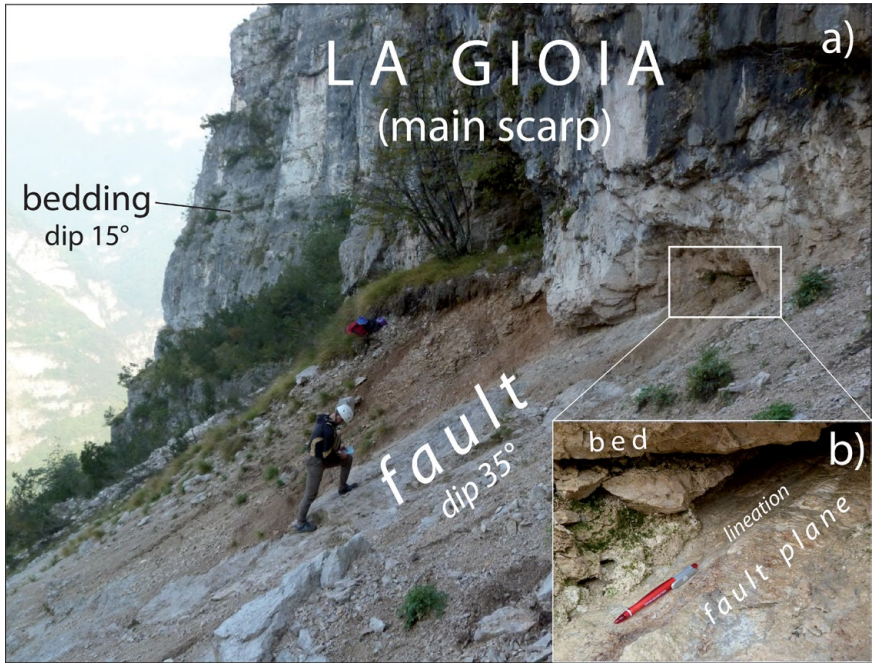

Fig. 19 - a) Base of the La Marogna rockslide main scarp. b) Detail of the fault plane continuing beneath the main scarp wall face.

Fig. 20 - The fault rock is a non-cohesive several dm-thick gouge.

Principale deposition, the Southern Alps were occupied by a wide carbonate platform. This flat paleogeography was progressively fragmented by extensional tectonics connected to the rifting that ultimately led to the break-up of Pangea (Winterer and Bosellini, 1981). Subsidence along extensional faults caused the formation of a series of horsts, where shallow water carbonate platforms persisted, and basins, where deep-water sedimentation occurred. The Trento Platform high was bounded to the E by the Belluno Basin and to the W by the Lombardian Basin, and hosted shallow water carbonate sedimentation (Calcari Grigi Group) until the Toarcian (Masetti et al., 2012 and references therein). The Trento Platform witnessed a complex history as testified by important changes in facies architecture of the units of the Calcari Grigi Group. Major facies changes occur in coincidence with global perturbation of the carbon cycle (Sinemurian-Pliensbachian boundary Event, Franceschi et al., 2014b). Pulses of extensional tectonics since the Sinemurian are testified by syn-sedimentary faulting that induced differential subsidence and caused relevant thickness variations particularly evident in

DOI: 10.3301/GFT.2018.01

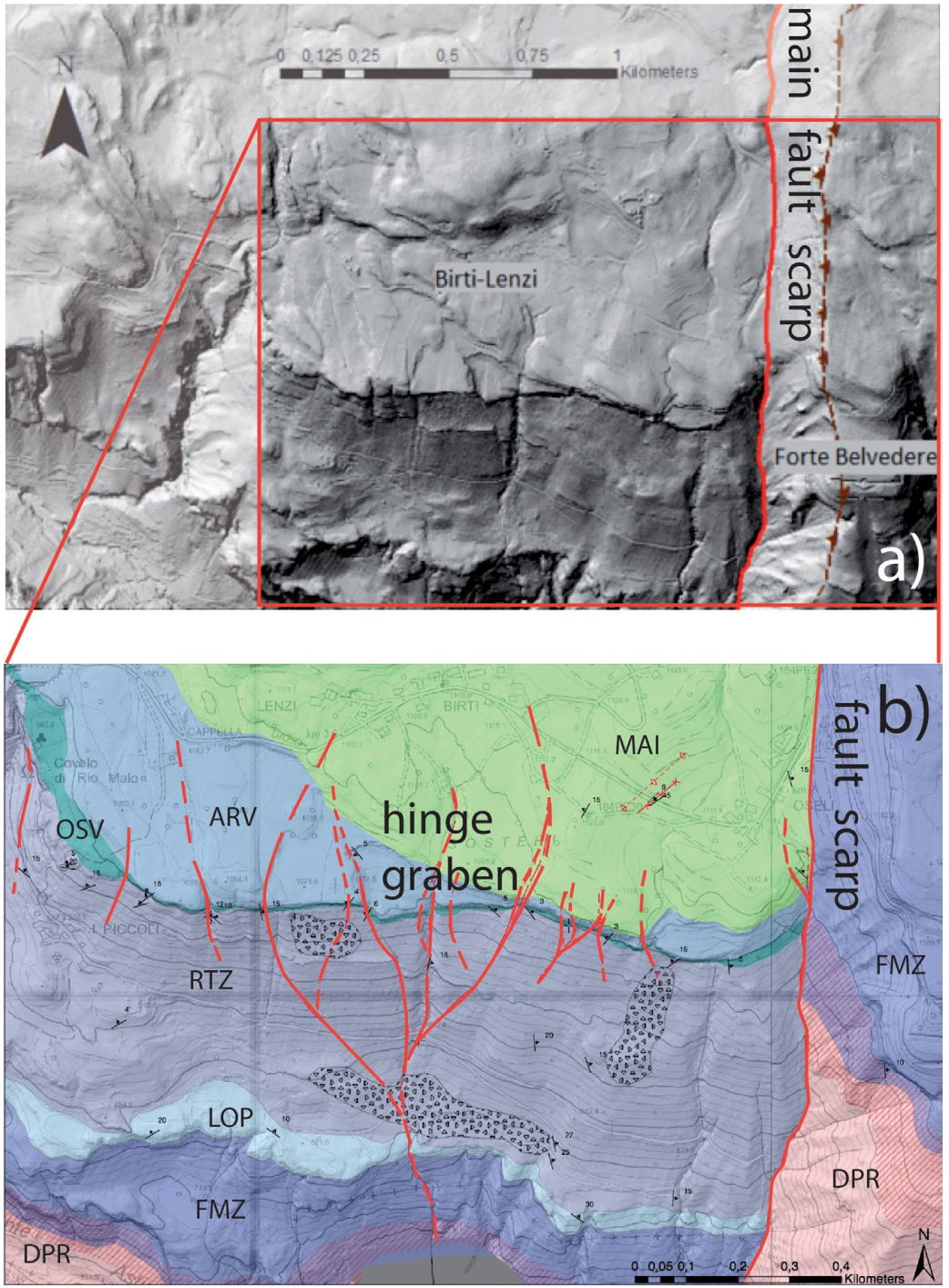

the Rotzo fm. (Franceschi et al., 2014a). The onset of deep-water conditions in the Southern Alps and also in the area occupied by the Trento Platform is marked by a generalized marine transgression (San Vigilio Oolitic Limestone) and by the following deposition of the Rosso Ammonitico Veronese and the cherty limestones of Maiolica.

Along the upper Astico Valley section, the Lavarone plateau (Fig. 21) shows a prominent high-angle W-dipping normal fault (Carotte fault, Fig. 26), which was active during the Pliensbachian (Fig. 22). The syn-sedimentary activity is demonstrated by a hanging-wall rollover anticline, with thickening of the Rotzo fm. towards the fault (Fig. 22).

STOP 1.4: The Cornetto-Becco di Filadonna pop-up (45.9412 °N, 11.2324 °E)

From Carbonare (1076 m; Stop located in a service area along the SS349 road from Carbonare to Lavarone), located on the saddle between the Astico and Centa valleys, the uplift structure of the Cornetto-Becco di Filadonna is prominent (Figs. 23-25). The southern slope of the Cornetto di Folgaria corresponds to the forelimb of the anticline developed in the hanging-wall

Fig. 21 - LiDAR image (a) and geological map (b) of the southern Lavarone plateau and upper Astico Valley. DPR Dolomia Principale, FMZ Monte Zugna fm., LOP Loppio Oolitic Limestone, RTZ Rotzo fm., OSV San Vigilio Oolitic Limestone, ARV Rosso Ammonitico Veronese, MAI Maiolica.

DOI: 10.3301/GFT.2018.01

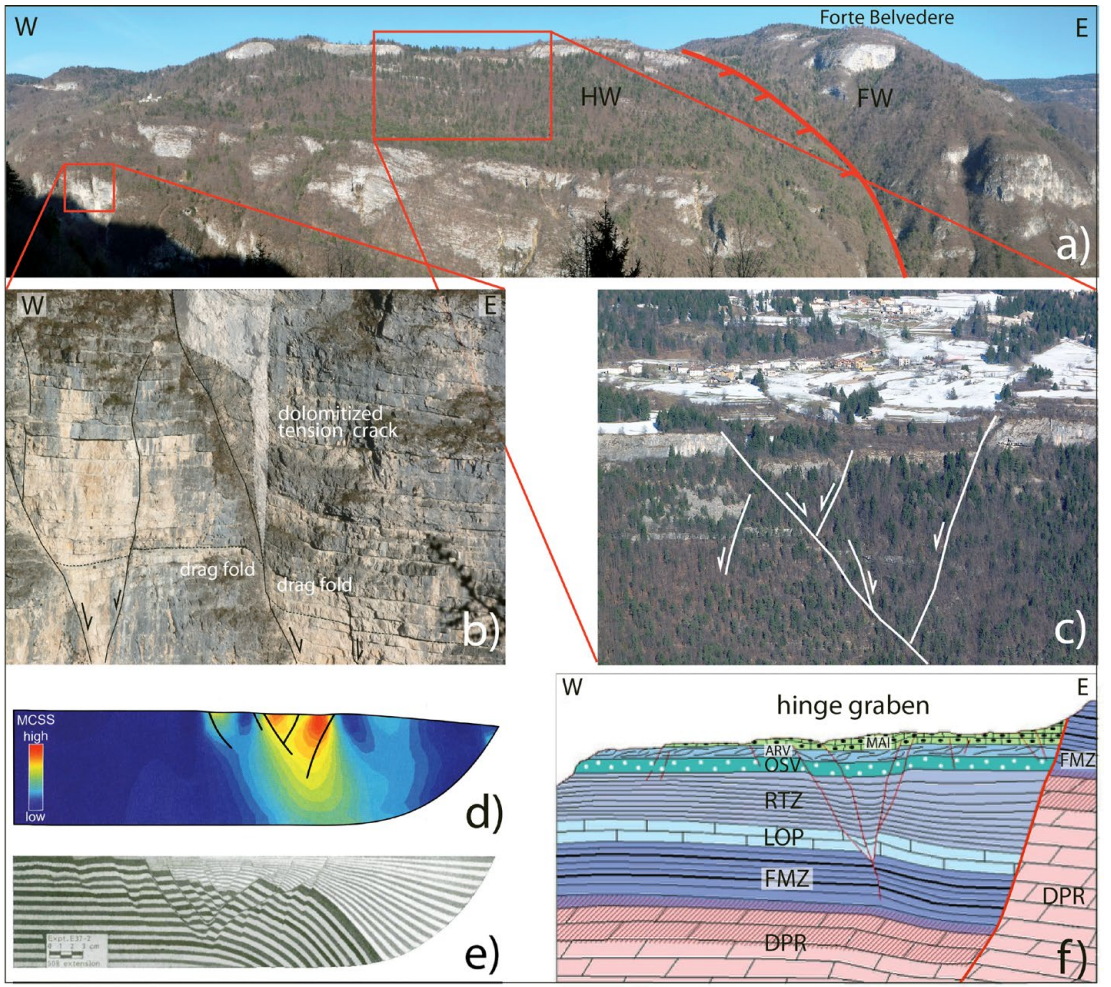

Fig. 22 - a) Left side of the upper Astico Valley with the Jurassic Carotte fault. b) Minor normal faults antithetic to the Carotte fault. c) Graben on the hanging-wall (HW) of the Carotte fault. d) Numerical model of a listric normal fault with rigid footwall block (FW). The Maximum Coulomb Shear Stress (MCSS) results in the hinge of the hanging-wall rollover anticline (Maerten and Maerten, 2006). e) Analogue model of a listric normal fault with rigid footwall block. An active deformation area of the hanging-wall is located in the hinge zone of the rollover anticline (Maerten and Maerten, 2006; cf. McClay, 1990). f) Cross section of the Carotte fault showing the thickening of the Rotzo fm. (RTZ) towards the fault. This permits to infer that the fault activity started during the Pliensbachian, but a syn- or post-Maiolica extensional activity is also present (legend as in Fig. 21b).

of the NW dipping Centa fault, probably a Jurassic fault reactivated as a sinistral transpressional fault (Zampieri et al., 2003).

At the head of the Centa Valley, below Terza Cima, erosion is active on the highly fractured fault rocks produced by the Terza Cima-Spizom reverse fault, a steep backthrust of the Centa fault (Figs. 23 and 24). This prominent structure seems to be active, as suggested by seismicity occurred on October 1994 (Tab. 1) (Viganò et al., 2008; 2015). In particular, the Monte Cornetto area shows dominantly compressive focal mechanisms of relatively shallow earthquakes, while the bordering faults (Schio-Vicenza to the west and Gamonda-Tormeno-Melegnon-Carotte system to the east) show focal mechanisms with dominant strike-slip components (Fig. 26 and Tab. 1). At least in this internal Southern Alps sector, at present the Schio-Vicenza fault shows dextral strike-slip kinematics (Fig. 26) (Viganò et al., 2015). It should be considered that the epicentral position of the 1989 seismic event (pre-1994 seismic network) is surely affected by higher uncertainties than other solutions.

DOI: 10.3301/GFT.2018.01

The Monte Cornetto di Folgaria is a topographic and structural high bounded by two conjugate reverse faults: the Trento-Roncogno fault to the north, and the Centa fault to the south. This uplift has been interpreted as a pop-up localized at the restraining stepover between the presently sinistral Calisio and Schio-Vicenza strike-slip faults, which trend at high angle to the thrust belt (Zampieri et al., 2003). However, the seismicity of the Schio-Vicenza fault in the Pasubio area, i.e. north of Posina, suggests a dextral strike-slip activity, a kinematics confirmed also by the field analysis (Fondriest et al., 2012). The apparent contradictory kinematics of the Schio-Vicenza fault in its different segments could be explained by the pop-up structure development, which requires a dextral activity along its western margin, while the segment south of Posina producing the contractional stepover requires a sinistral activity. This structure could fall within the "sinistral opening zipper" model of Passchier and Platt (2017), where intersecting pairs of simultaneously active faults with different sense of shear merge into a single fault, via a zippered section (extraction fault) eventually experiencing no displacement.

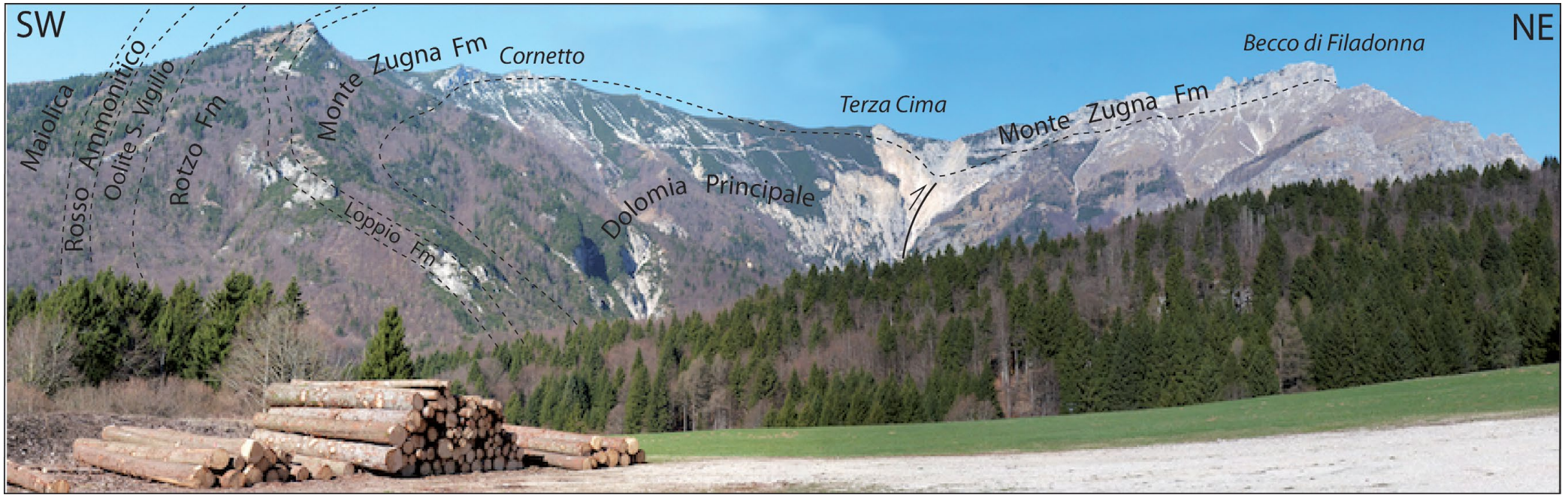

Fig. 23 - Panoramic view of the Cornetto di Folgaria (from Carbonare, towards NW).

DOI: 10.3301/GFT.2018.01

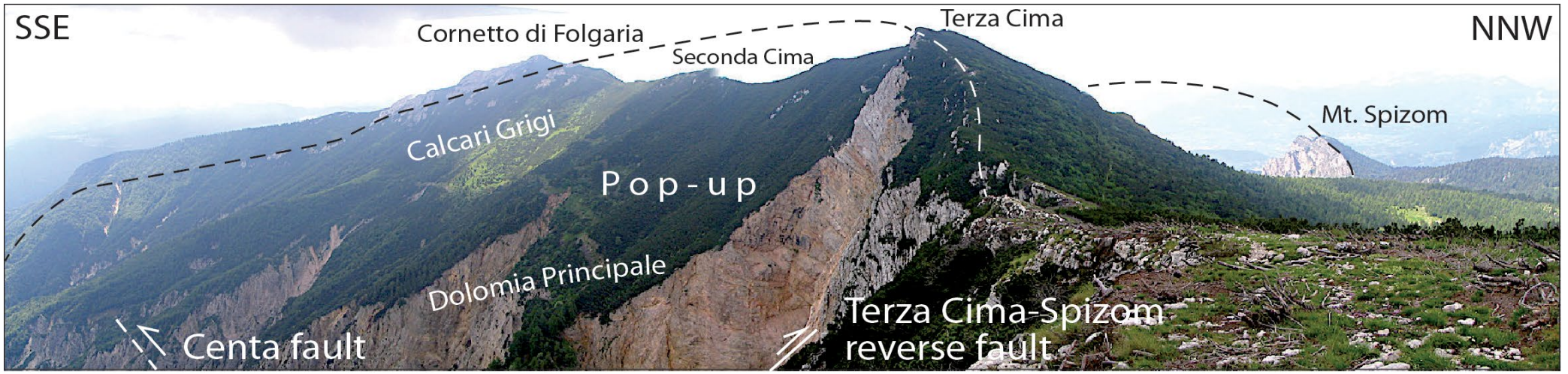

Fig. 24 - The Cornetto di Folgaria pop-up structure seen from the ridge between the Cornetto di Folgaria and Becco di Filadonna (view towards WSW).

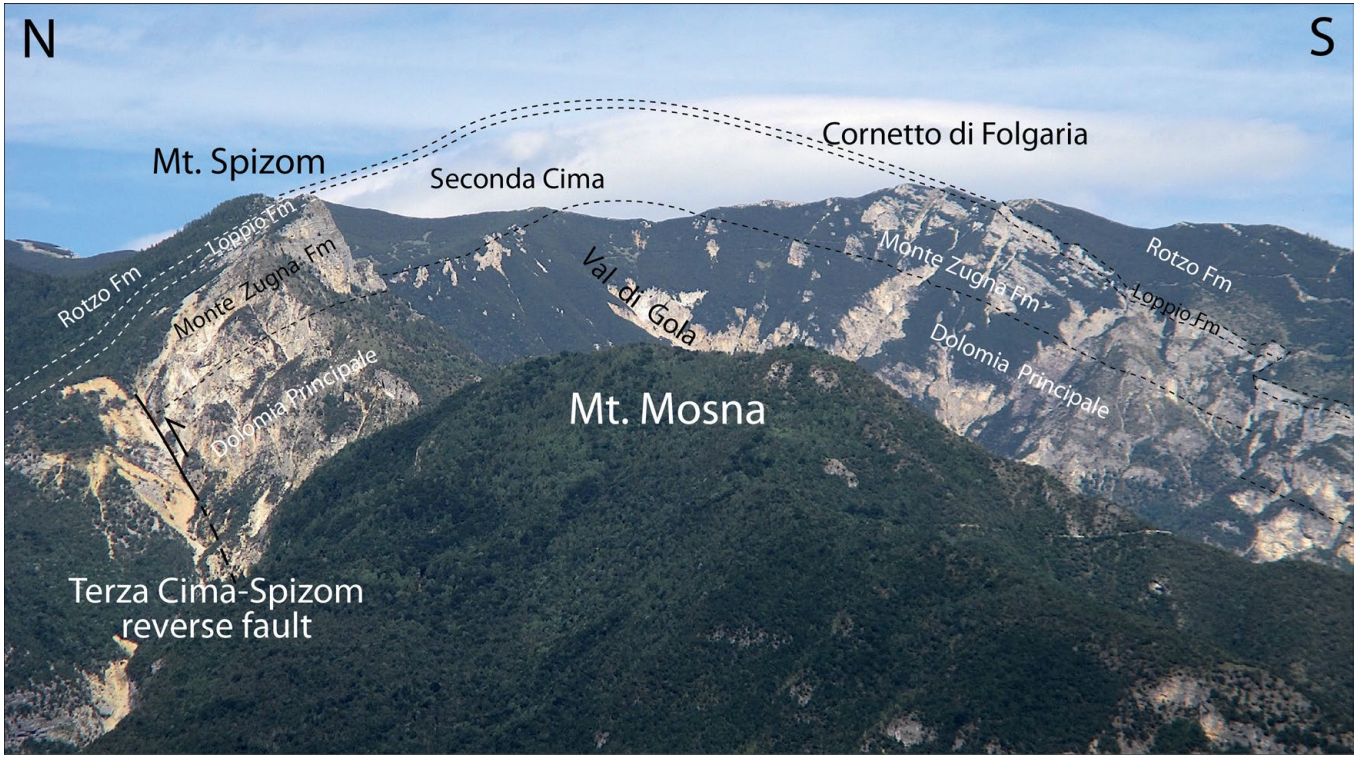

Fig. 25 - From Castel Barco (Savignano) in the Adige Valley, the Cornetto-Spizom pop-up appears deformed in a wide anticline, deeply incised by the Val di Gola. To the left, the S-dipping Terza Cima-Spizom reverse fault crops out.

DOI: 10.3301/GFT.2018.01

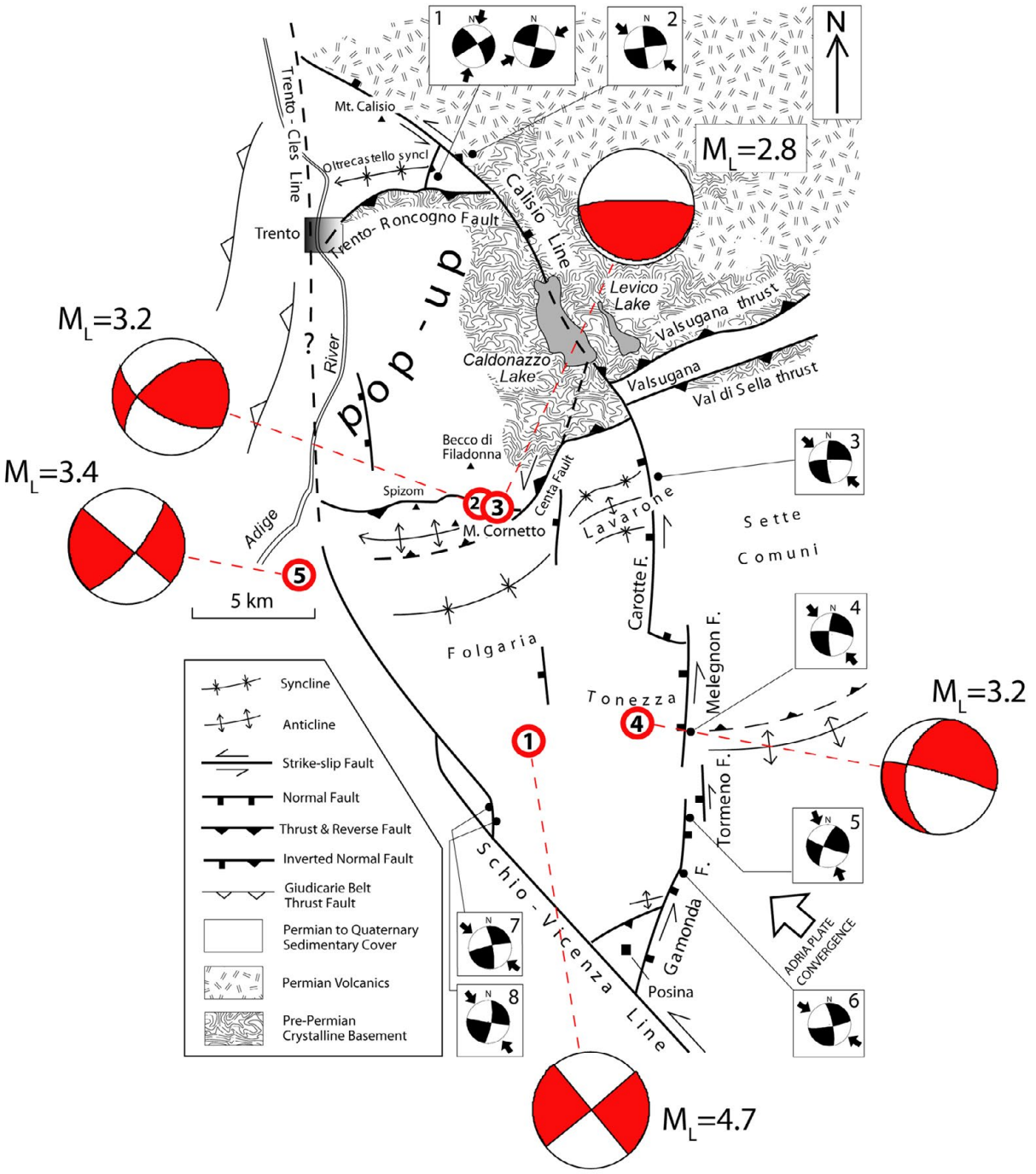

STOP 1.5: Fault rocks at Fricca Pass (45.9476 °N, 11.2070 °E)

Laboratory tests on rock samples of fault zones and their host rocks provide useful data for geotechnical and mechanical models at different scales (e.g., Gudmundsson, 2004; Heap et al., 2010). Strength and Young's moduli measurements were conducted on rock samples from the Fricca-Scanuppia area (Fig. 27), which is characterized by sets of well-exposed brittle faults in carbonates (cf. Zampieri et al., 2003).

The study area includes two sites belonging to the Cornetto-Becco di Filadonna pup-up (see STOP 1.4). A first site is located at Fricca Pass (STOP 1.5, along the abandoned road starting near the entrance to the gallery), where the Centa fault zone crops

Fig. 26 - Seismotectonic sketch of the area with focal mechanisms from Viganò et al. (2008; 2015). M_L is local magnitude. Compare with earthquake data in Tab. 1. The B/W pseudo focal mechanisms are calculated from fault slip data. (Modified from Eclogae geologicae Helvetiae, 96, Zampieri et al., *Strike-slip contractional stepovers in the Southern Alps (northeastern Italy)*, 115-123, Copyright (2003), with permission of the Swiss Geological Society).

DOI: 10.3301/GFT.2018.01

Tab. 1 - Earthquakes occurred in the study area (cf. Fig. 26).

ID	Date	Time (UTC)	Latitude (°N)	Longitude (°E)	Depth (km)	M_L
1	13 Sep 1989	21:54:01	45.860	11.210	9.1	4.7
2	24 Oct 1994	23:22:48	45.938	11.188	7.6	3.2
3	25 Oct 1994	15:09:36	45.937	11.195	7.3	2.8
4	22 Oct 1998	00:58:50	45.866	11.262	12.4	3.2
5	26 Apr 1999	02:53:46	45.916	11.096	1.5	3.4

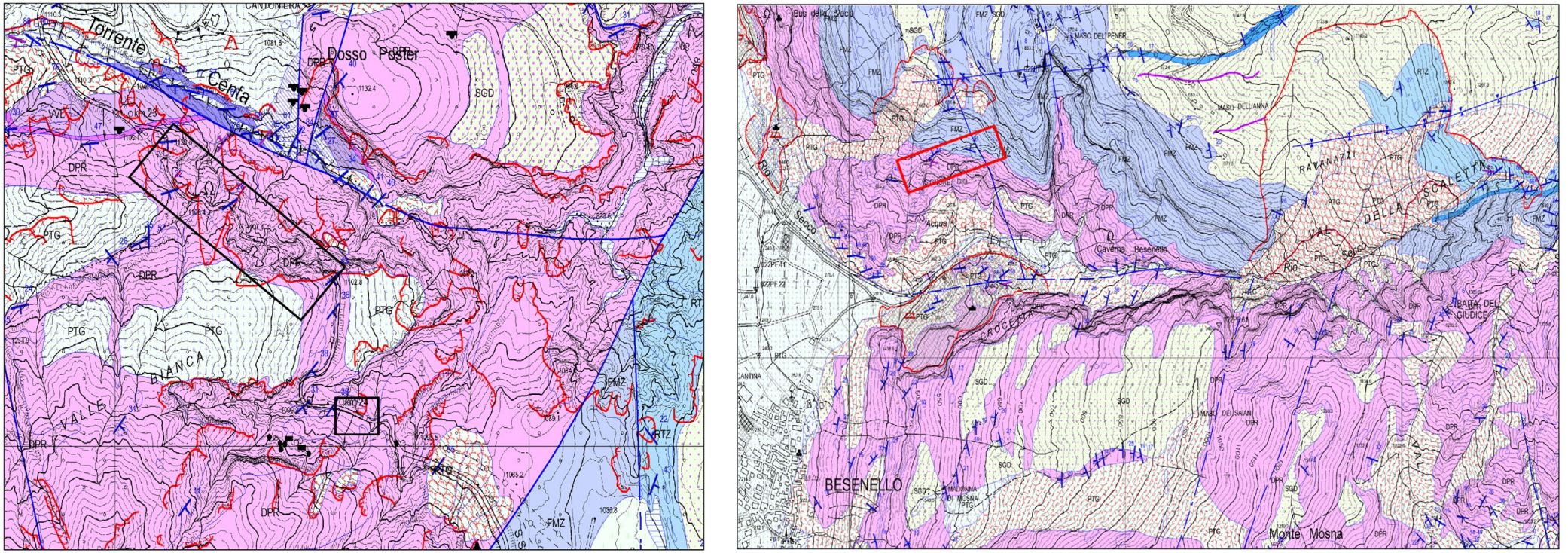

Fig. 27 - Geological map of the Fricca (left) and Scanuppia (right) study areas (CARG project database; courtesy of the Geological Survey of the Autonomous Province of Trento). Sampling sites are inside the areas marked by black and red rectangles. For scale, the gray grid on the maps has 1 km spacing. Stratigraphic units: VVL calcari della Val Vela (Ladinian-Carnian), DPR Dolomia Principale (Carnian-Norian), FMZ Monte Zugna fm. (Sinemurian), RTZ Rotzo fm. (Pliensbachian).

DOI: 10.3301/GFT.2018.01

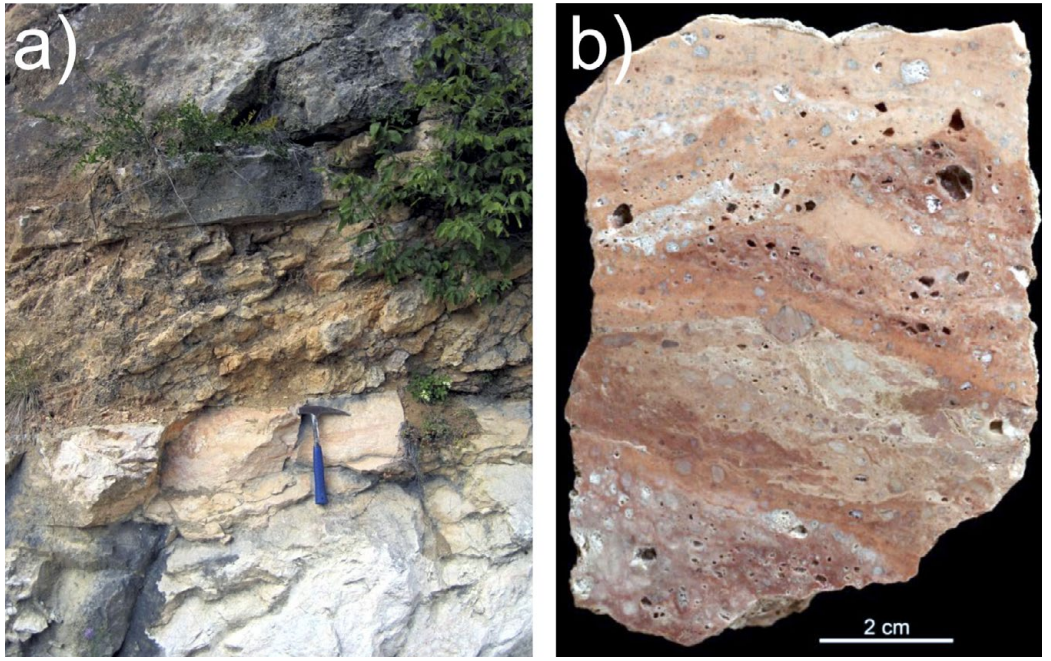

Fig. 28 - a) Fault core with subsidiary shear planes, at Scanuppia. b) Typical banded cataclasites of Scanuppia (courtesy S. Adami).

out (Figs. 26 and 27); a second site is located along the Scanuppia slope close to the Terza Cima-Spizom reverse fault (Figs. 25, 26 and 27).
The tested rocks are: (i) hosting dolomites (Dolomia Principale, Centa fault at Fricca Pass) and limestones (Monte Zugna fm., Scanuppia area); (ii) cohesive fault cataclasites (Scanuppia area); (iii) fault gouge of dolomitic composition (Centa fault). In addition, a sample of dolomitic breccia was studied, as belonging to the host rocks of the Centa fault system.

Fig. 28 shows a typical fault core sampled in Scanuppia. Cohesive fault cataclasites are strongly banded, with some layers showing very fine grained matrix and flow structures (Fig. 28).
Densities of the studied rocks range from 2.6 to 2.7 g cm^{-3} for host dolomites and limestones, and from 2.3 to 2.5 g cm^{-3} for cataclasites. Uniaxial and triaxial failure compressive tests were conducted on intact rock cylinders (54 mm diameter, Fig. 29) at room

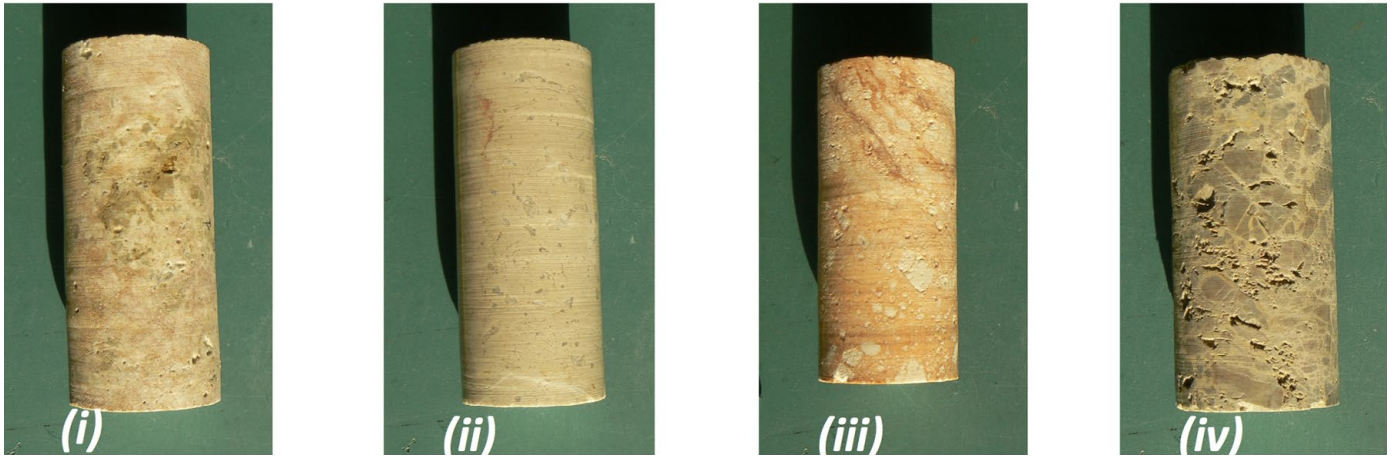

Fig. 29 - Examples of specimens tested in this study: (i) host dolostones of Centa fault at Fricca Pass (Dolomia Principale); (ii) host limestones of Scanuppia (Monte Zugna fm.); (iii) cohesive fault cataclasites of Scanuppia; (iv) breccia, belonging to the host rocks of the Centa fault system. For scale, the diameter of specimens is 54 mm.

DOI: 10.3301/GFT.2018.01

temperature under confining pressure up to 30 MPa, corresponding to shallow burial depths (~1 km). Tensile strength analyses (Brazilian tests) on the same samples were also performed.
The strength envelope of cataclasites is significantly different from the strength envelopes of host rocks (Fig. 30). The same difference is significant also considering the Young's moduli (Fig. 31). In terms of friction angle and apparent cohesion we obtained 48.9° and 7.5 MPa for host dolostones, 52.6° and 9.1 MPa for host limestones, and 46.6° and 4.1 MPa for cataclasites.
Particle size analyses by sieving have been carried on three fault gouge samples of soils from the Fricca Pass (Centa fault). The granulometric composition is quite similar, with dominant sand (~50-60%) and minor gravel (~10-20%) (Fig. 32). The 63 μm passing percentage is between 21% and 41%. A gouge fine soil sample coming from Scanuppia has been classified as clay of medium plasticity, according to Atterberg limits.
These geotechnical results form an initial experimental database in order to better understand the rock mechanics for this seismotectonically active Southern Alps sector. Nevertheless, because of its intrinsic limits (e.g. difficulty in sampling very deformed fault rocks and/or preparing representative specimens), the methodology here applied cannot be used to completely and definitely characterize the studied fault system.

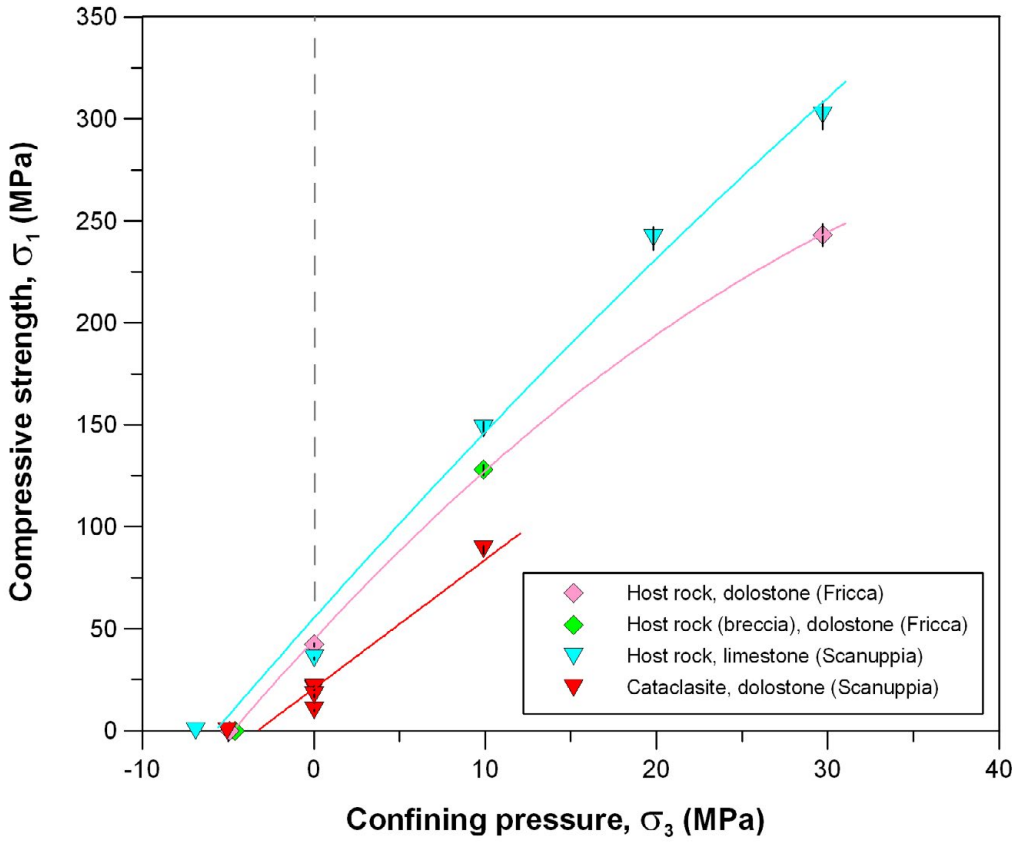

Fig. 30 - Strength values of host and fault rocks at Fricca Pass and Scanuppia area. The corresponding envelopes are obtained by fitting individual data points from Brazilian, uniaxial and triaxial tests (i.e., for confining pressures lower than, equal to, or higher than 0 MPa, respectively). Fitting equations are: $y = -0.031\ x^2 + 9.432\ x + 55.140$ (light blue); $y = -0.081\ x^2 + 9.095\ x + 44.576$ (pink); $y = 6.307\ x + 20.676$ (red).

DOI: 10.3301/GFT.2018.01

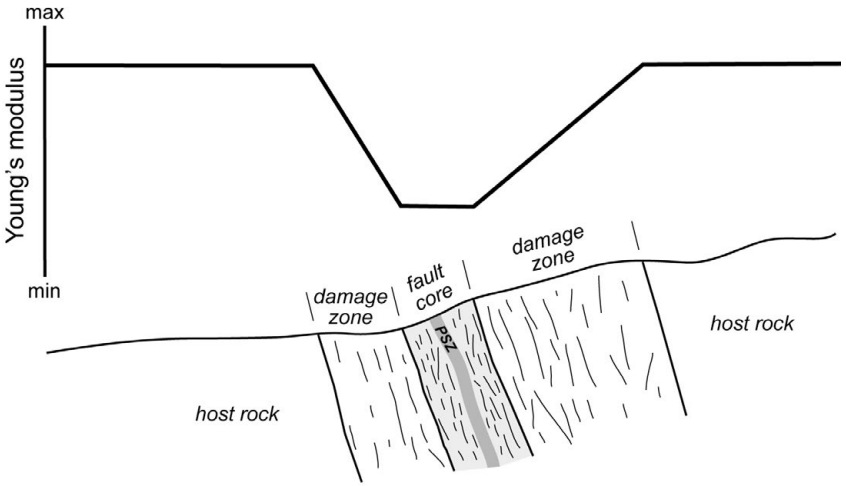

Rock type	Host rock			Fault rock (cohesive cataclasites)
Lithology	Dolostone	Dolostone (breccia)	Limestone	Dolostone
Site	Fricca Pass	Fricca Pass	Scanuppia	Scanuppia
Young's modulus (GPa)	43 53	42	46 49	12 18 28 32

Fig. 31 - Major fault zones are composed of two principal mechanical units: a fault core and a fault damage zone. Fracture frequency commonly increases gradually towards the core, decreasing the effective stiffness towards the central parts of the fault zone (PSZ, Principal Slip Zone). As the fault zone develops, these units gradually become thicker and mostly control the displacement on the fault, which is primarily along the core or its contact with the damage zone (cf. Gudmundsson, 2004). The distribution of Young's moduli follows these main mechanical units, as depicted by the scheme and confirmed by experimental data in table.

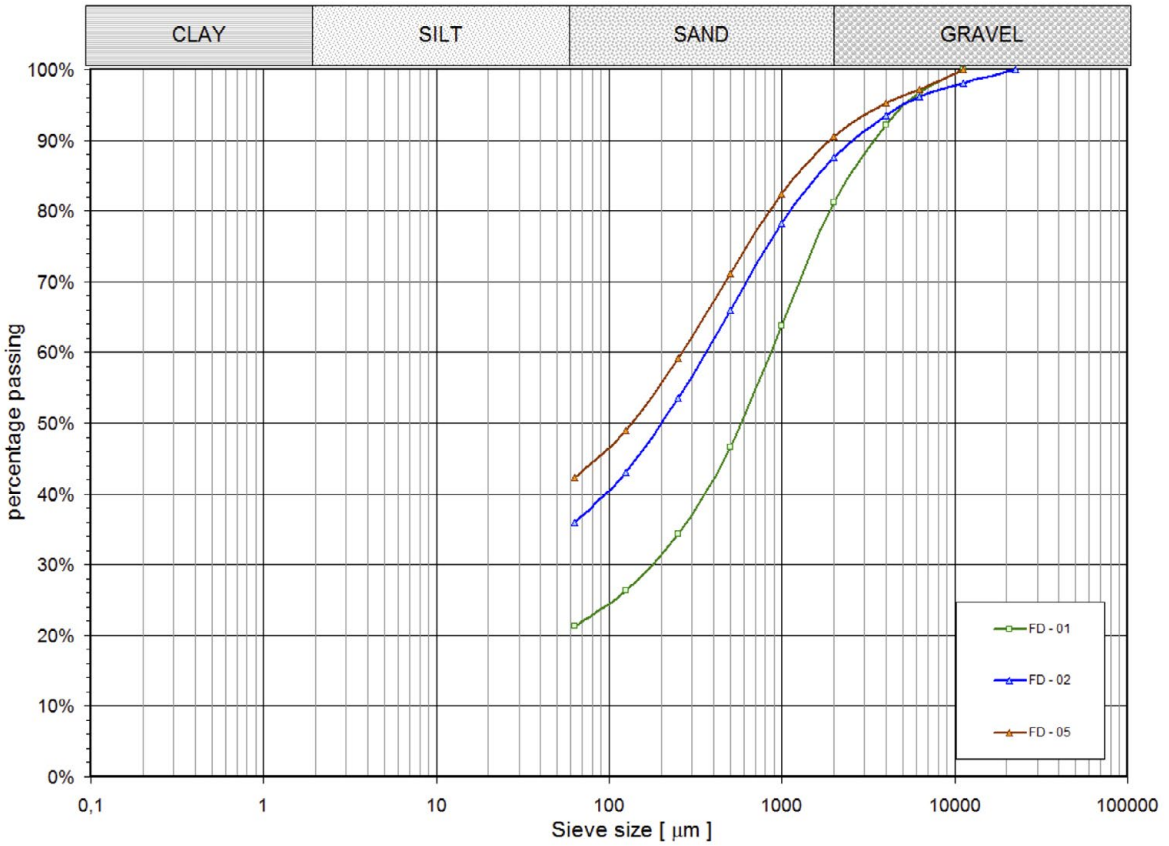

Fig. 32 - Particle size distribution of three different fault gouge samples from the Fricca Pass.

DOI: 10.3301/GFT.2018.01

STOP 1.6: The Castelpietra and Lavini di Marco rock-avalanches in the Adige Valley: ages and earthquake triggering

In Trentino many landslides are present (Fig. 33). Some of them, including Lavini di Marco, Marocche di Dro and Castelpietra, are rock avalanches, i.e. huge volumes of collapsed rock (>10^6 m^3) that flow very rapidly (cf. Hungr et al., 2001).

Before the availability of isotopic dating, it was generally accepted that the largest gravitational collapses in the Alps occurred right after deglaciation (e.g., Abele, 1974). As more and more Alpine landslides were isotopically dated, it became apparent that most occurred during the Holocene, thus 6000 years or more after the withdrawal of glaciers from the alpine valleys (e.g., Prager et al., 2009; Ivy-Ochs et al., 2017b).

The three rock avalanches described during the field trip (see below) are major post-glacial collapses, occurred in the middle Adige Valley (Castelpietra – Stop 1.6.1 and Lavini di Marco – Stop 1.6.2) or in the lower Sarca Valley

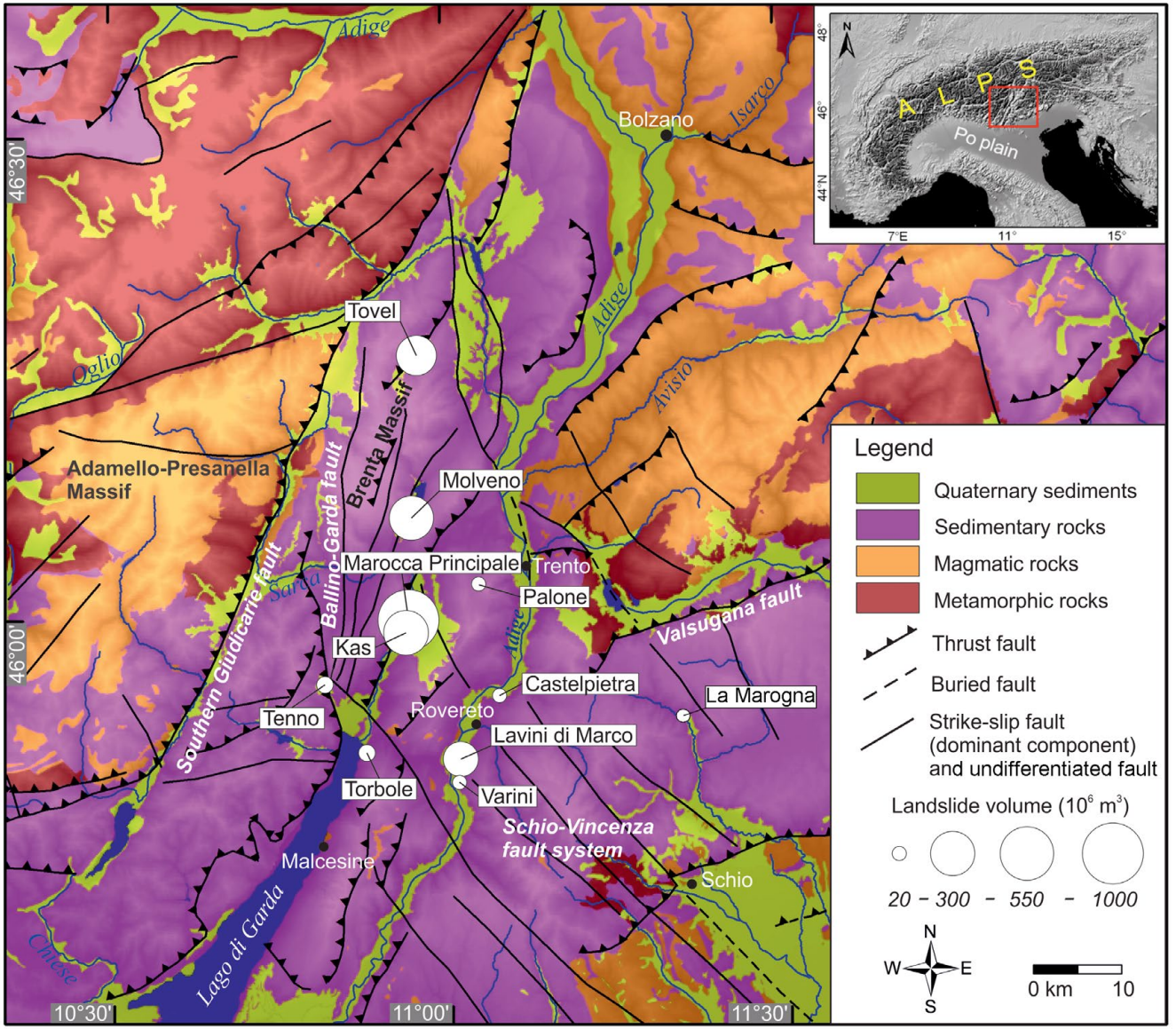

Fig. 33 - Simplified geological map with the main landslides in the study area. Circle sizes are proportional to landslide volumes. (Modified from Quaternary Science Reviews, 169, Ivy-Ochs et al., *Geomorphology and age of the Marocche di Dro rock avalanches (Trentino, Italy)*, 188-205, Copyright (2017), with permission of Elsevier).

DOI: 10.3301/GFT.2018.01

(Marocche di Dro, see STOP 1.7) (Fig. 33). Stop 1.6.1 is a service area along the SP59 road, between Calliano and Nomi. STOP 1.6.2, the viewpoint is located along the cycle lane on the right bank of the Adige River, at the bridge near the Mori train station (SS240 road).

Stop 1.6.1: Castelpietra (45.9273 °N, 11.0815 °E)

The Castelpietra deposit is located at the foot of a reddish rock wall named Cengio Rosso (920 m a.s.l.), which is 300 m high and 2 km long. The NE-SW oriented main head scarp is composed of Dolomia Principale overlain by the Calcari Grigi Group (Fig. 34). Bedding planes dip 30-45° to the W and WNW, forming a dip slope. The scarp is cut by NNE-trending fractures, E-W oriented open fractures, and by NW-SE fault planes related to the Schio-Vicenza system (Fig. 34). A second detachment is located at about 450 m a.s.l. It is 70 m high and 800 m long, within Dolomia Principale.

The deposit covers about 1.2 km^2, between 400 and 200 m a.s.l. It includes boulders up to 20 m in diameter, dominated by Dolomia

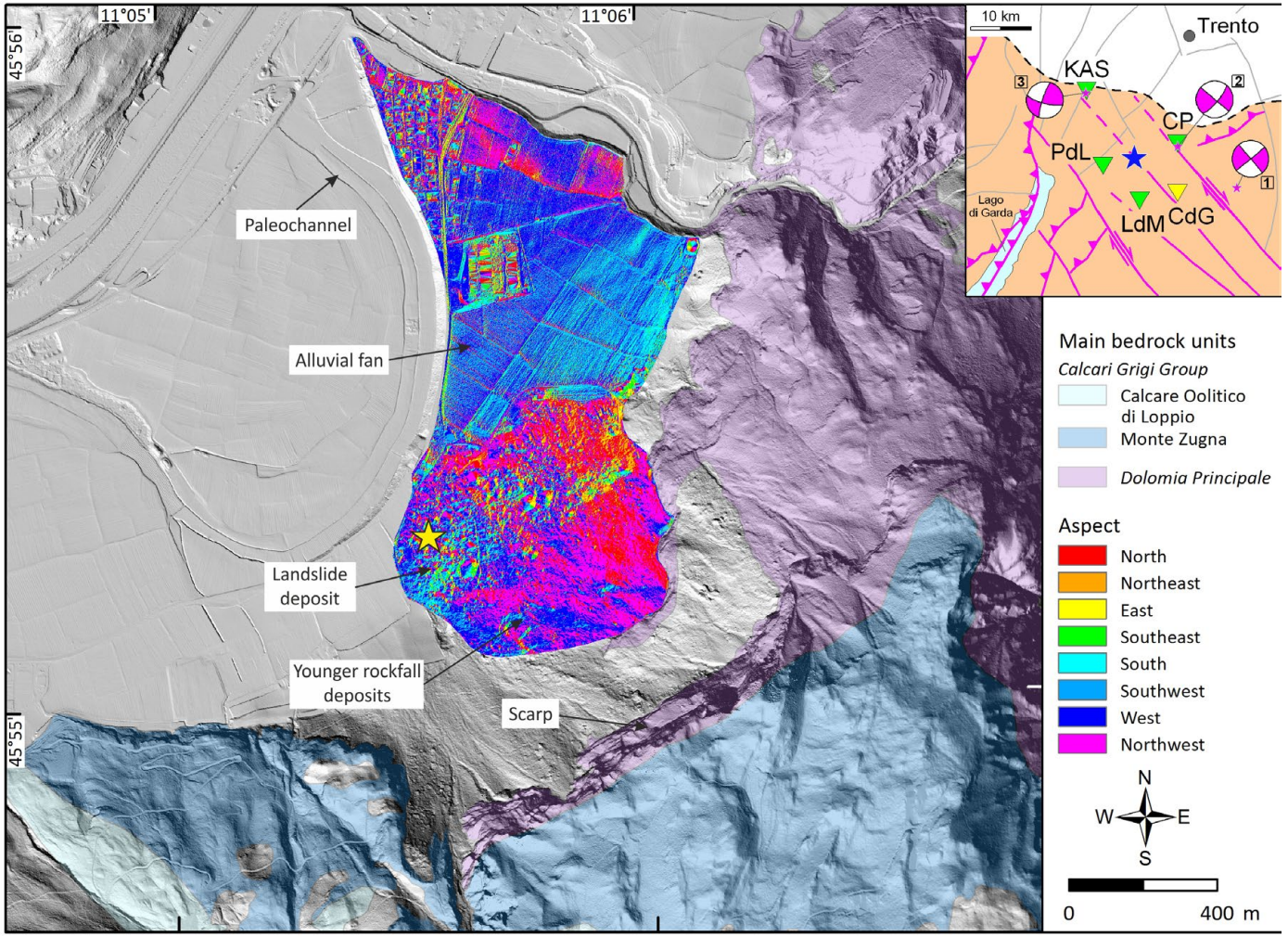

Fig. 34 - Hillshade map of Castelpietra (sun azimuth 225°). Landslide and fan deposits shown with aspect map. Geology from the Geological Survey of Trento, CARG project database. The star marks the position of dated boulders. For inset map, see Fig. 46. (Reprinted from Advancing Culture of Living with Landslides, *Geomorphology and age of large rock avalanches in Trentino (Italy): Castelpietra*, 2017, 347-353, Ivy-Ochs et al., with permission of Springer).

DOI: 10.3301/GFT.2018.01

Principale and Calcari Grigi dolomitic limestone. The travel distance of debris of the blocky deposit is 0.7 km. A steep angle of reach of 42° was calculated by Abele (1974). Fig. 34 shows that the river meandered quite close to the toe of the landslide, but was not deflected by the event.
The Castelpietra castle was built sometimes before 1206 AD right on landslide debris (Ivy-Ochs et al., 2017a and references therein).
A ^{36}Cl surface exposure age of 1060 ± 270 AD (non-weighted mean) was obtained from two boulders of the main blocky debris (Ivy-Ochs et al., 2017a).

Stop 1.6.2: Lavini di Marco (45.8626 °N, 10.9983 °E)

The Lavini di Marco were mentioned by Dante Alighieri, the Italian Poet who interpreted the Lavini di Marco deposits as the result of a slope instability ("sostegno manco") perhaps related to an earthquake ("tremoto") (Alighieri, 1314): «*Qual è quella ruina che nel fianco di qua da Trento l'Adice percosse, o per tremoto o per sostegno manco, che da cima del monte, onde si mosse, al piano è sì la roccia discoscesa, ch'alcuna via darebbe a chi sù fosse…*».
The Lavini di Marco rock avalanche deposit lies along the left side of the middle Adige Valley (western slope of Monte Zugna Torta), south of the town of Rovereto and about 10 km south of Castelpietra (Fig. 33). Among the seven individual identified rockslides, these deposits consist of the main Lavini di Marco and the minor Costa Stenda separated by the Costa Stenda ridge (Figs. 35 and 36). The two rock avalanches cover an area of 6.8 km^2, with a length of about 4.8 km and width of 1.8 km, for an estimated volume of about 200 x 10^6 m^3 (Martin et al., 2014). Altitudes range between 170 m a.s.l. for the lower deposit that has spread out on the flood plain of the Adige River, to a maximum altitude of 1260 m a.s.l. at the head scarp. Abele (1974) calculated an angle of reach of 12° and estimated a ~4.8 km long run-out distance.
The Lavini di Marco rock avalanche developed within the Lower Jurassic carbonate rocks of the Calcari Grigi Group, mainly including here the Monte Zugna, Loppio Oolitic Limestone and Rotzo formations (Fig. 36). Monte Zugna and Loppio Oolitic Limestone formations were directly involved in the Lavini di Marco rock avalanche. Here, the Calcari Grigi Group rocks form a massif elongated in a N-S direction, with WNW dipping slopes, that is cut by several NW-trending faults belonging to the Schio-Vicenza system (Fig. 33). These faults bound carbonate blocks along scarps and counterscarps. One of these is 50 m high and extends from the town of Lizzana up to Monte Zugna Torta, where it is only a few meters high and forms the eastern wall of the release area of the Lavini di Marco rockslide (Figs. 35 and 36).

DOI: 10.3301/GFT.2018.01

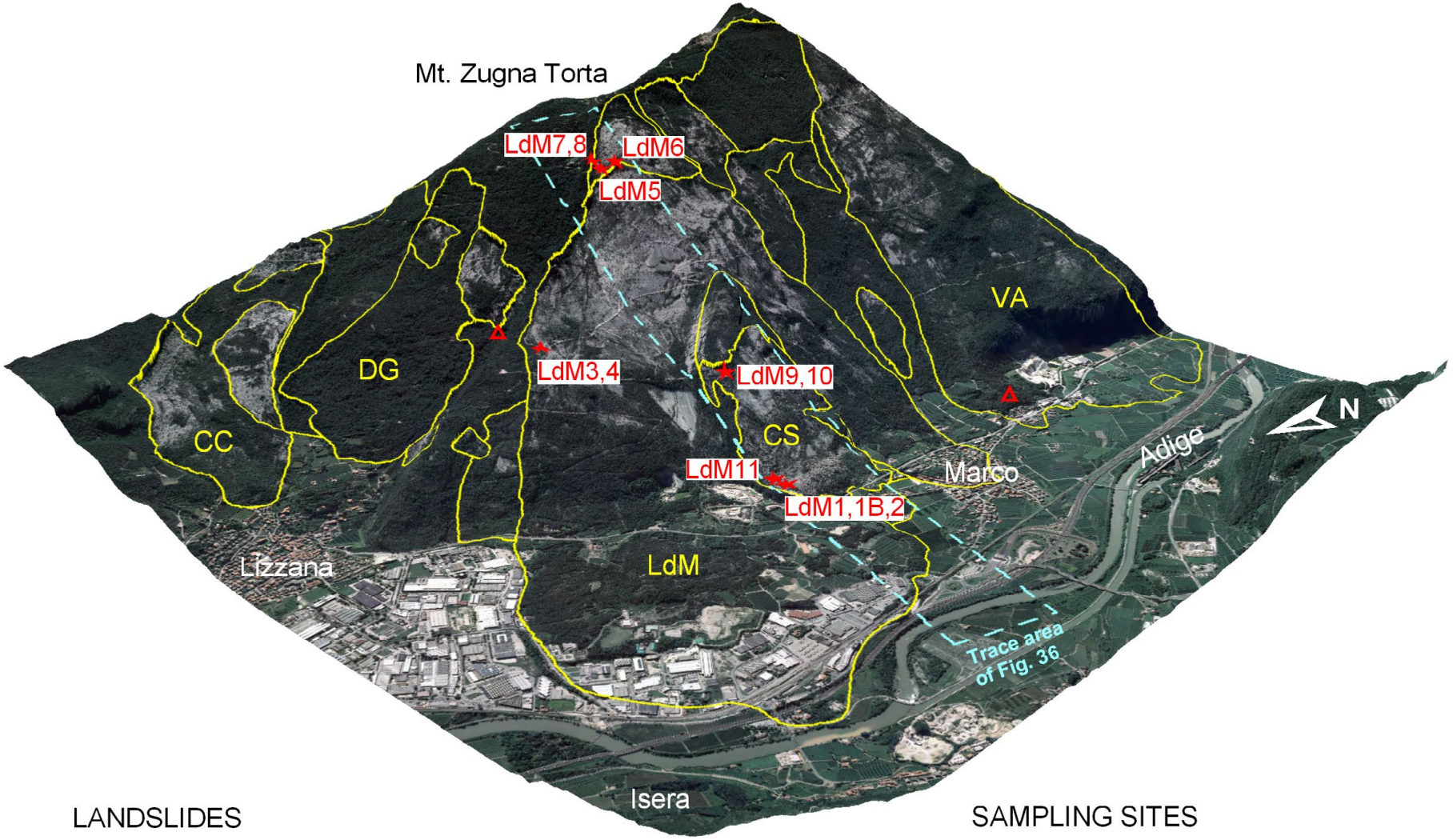

Fig. 35 - Landslide scarps and deposits along the western slope of Monte Zugna Torta near Rovereto. Stars mark the ^{36}Cl dated samples for the Lavini di Marco and Costa Stenda (cf. Fig. 38). Triangles mark where ^{14}C-dated organic material was found under the respective landslide (Orombelli and Sauro, 1988). The blue rectangle is the trace of Fig. 36. (Modified from Quaternary Geochronology, 19, Martin et al., *Lavini di Marco (Trentino, Italy): ^{36}Cl exposure dating of a polyphase rock avalanche*, 106-116, Copyright (2014), with permission of Elsevier).

DOI: 10.3301/GFT.2018.01

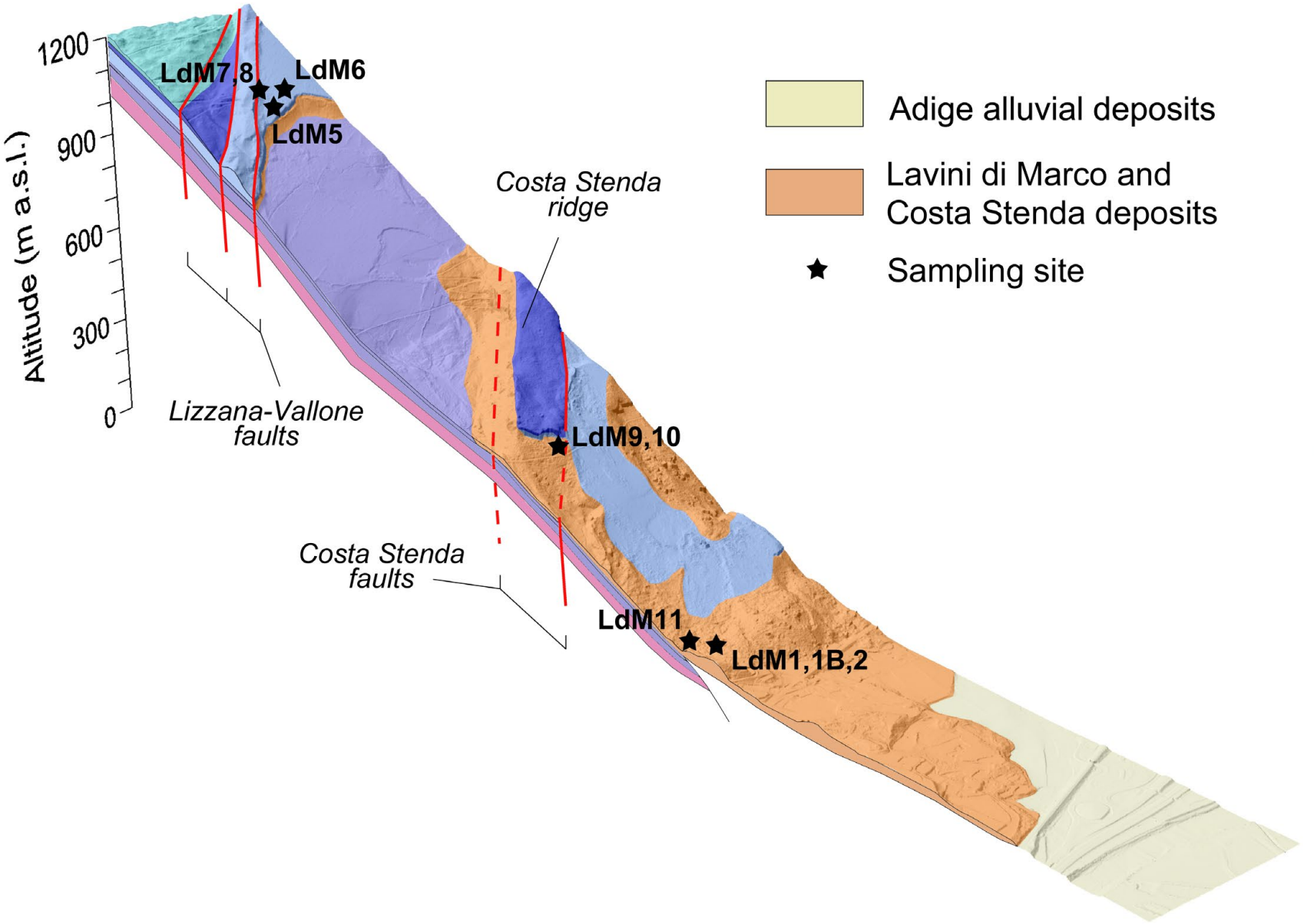

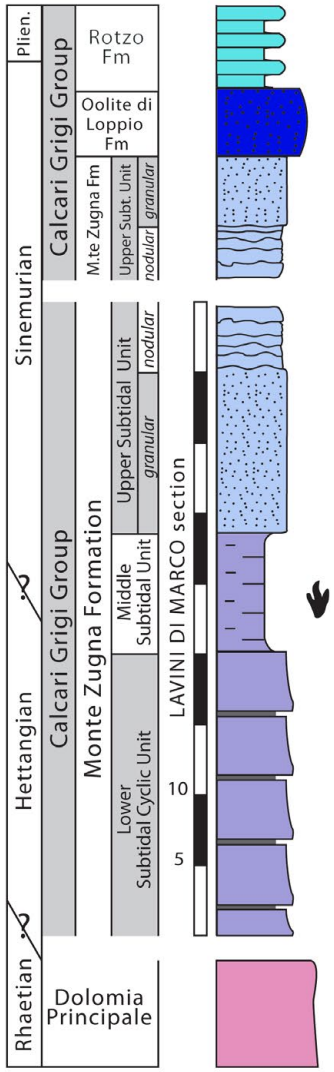

Fig. 36 - Schematic geological section based on digital terrain model along the Lavini di Marco and Costa Stenda scarps and deposits (trace in Fig. 35). The stratigraphy is modified after Avanzini et al. (2006). Samples collected along the profile are shown (cf. Fig. 35). (Reprinted from Quaternary Geochronology, 19, Martin et al., *Lavini di Marco (Trentino, Italy): ^{36}Cl exposure dating of a polyphase rock avalanche*, 106-116, Copyright (2014), with permission of Elsevier).

DOI: 10.3301/GFT.2018.01

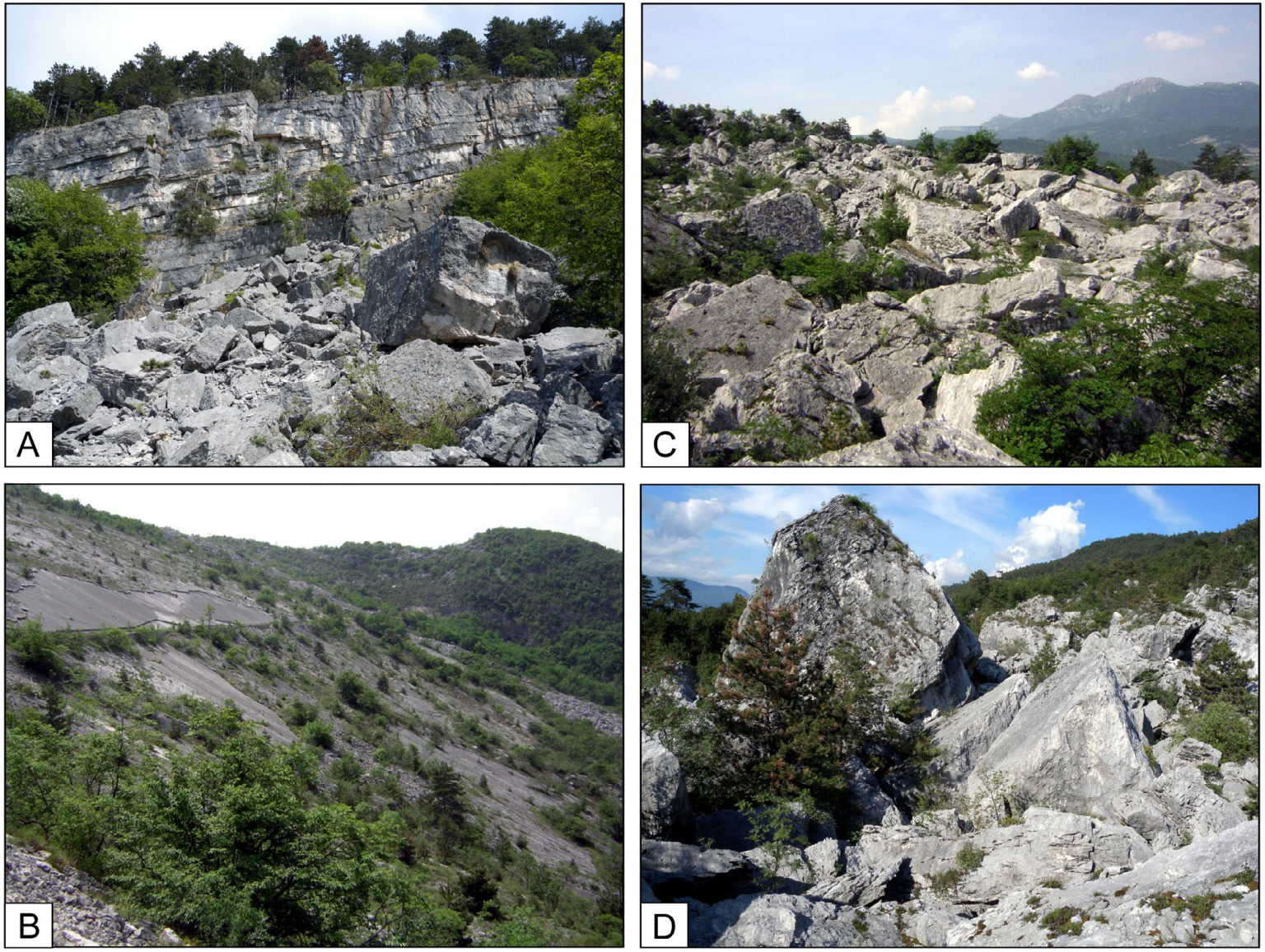

Fig. 37 - Photographs of the Lavini di Marco (A, B) and Costa Stenda rock avalanches (C, D). A) Release area upper scarp with boulder deposit at base. B) Dip slope 'sliding' plane with minor detachments. C-D) Landslide deposits, block diameters up to several meters. (Reprinted from Quaternary Geochronology, 19, Martin et al., *Lavini di Marco (Trentino, Italy): ^{36}Cl exposure dating of a polyphase rock avalanche*, 106-116, Copyright (2014), with permission of Elsevier).

Between the head scarps and deposits clear bedding planes (about 20° to NW), which acted as sliding planes, can be observed (Fig. 37). Shear planes are evidenced by uplift (up to 10 cm) of the rock sheets in their lower portion, allowing a downward sheet superposition. Boulders with an average diameter of 1.5 m cover the surface of the deposit. The Costa Stenda deposit was released along the base of the Costa Stenda ridge and moved downslope only a few hundred meters due to block detachment and translational sliding (Fig. 37). Debris accumulated at the foot of the slope on the Adige River flood plain with a marked concentric outer ridge that is made up of the largest boulders. The Costa Stenda deposits are topographically higher and overlie the Lavini di Marco deposits. From

DOI: 10.3301/GFT.2018.01

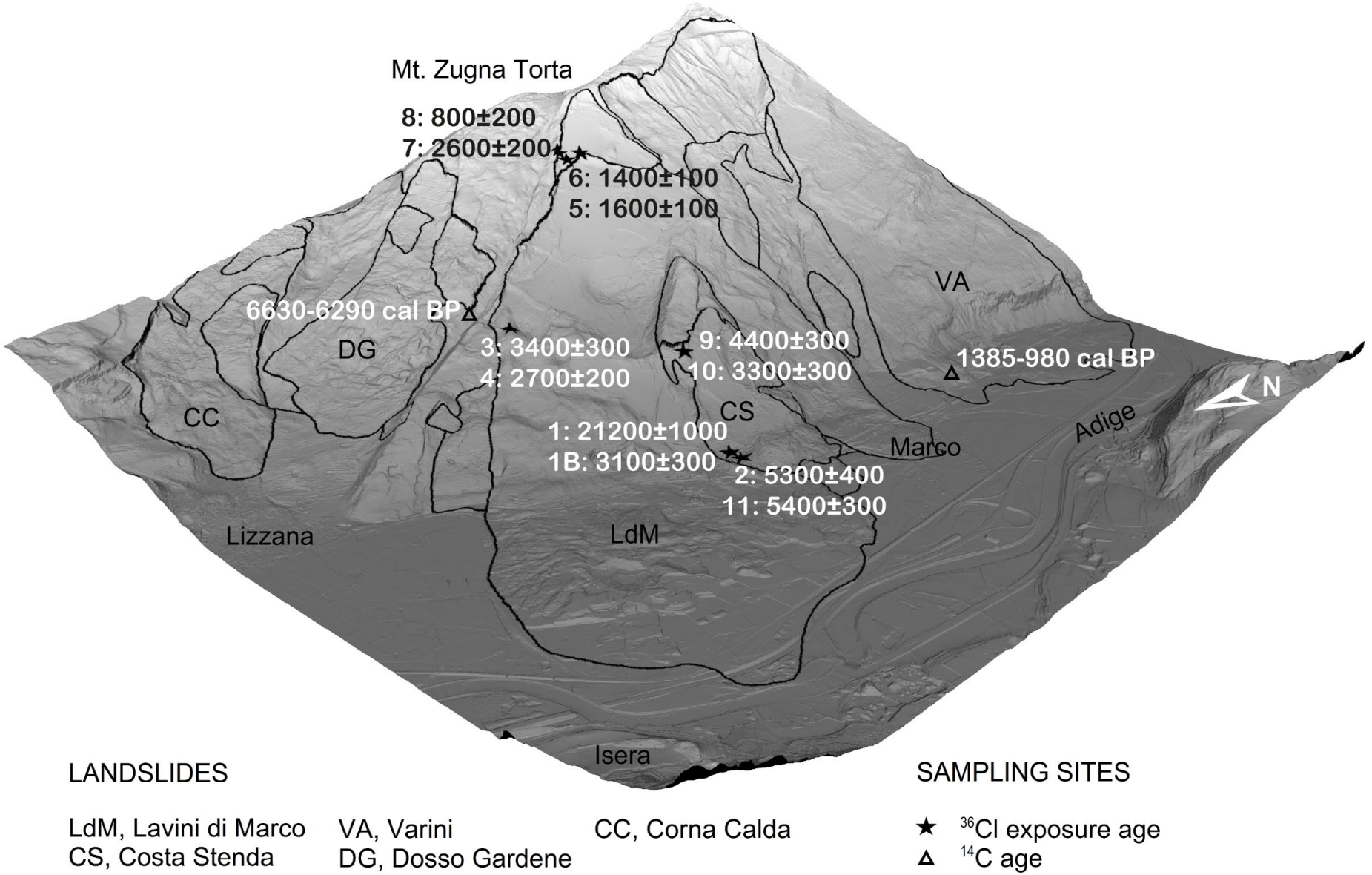

Fig. 38 - Distribution of ^{36}Cl exposure ages (stars) for boulders and bedrock of the Lavini di Marco and Costa Stenda rock avalanches (sample number: age ± uncertainty). Radiocarbon sites and calibrated ^{14}C ages (triangles) from Orombelli and Sauro (1988). (Modified from Quaternary Geochronology, 19, Martin et al., *Lavini di Marco (Trentino, Italy): ^{36}Cl exposure dating of a polyphase rock avalanche*, 106-116, Copyright (2014), with permission of Elsevier).

DOI: 10.3301/GFT.2018.01

geomorphological evidence, they are thus interpreted as the most recent deposit of Lavini di Marco.
Boulders in both the Lavini di Marco and Costa Stenda deposits were sampled for ^{36}Cl surface exposure dating (Figs. 35 and 37). Samples were also taken from bedrock surfaces. All samples belong to the Calcari Grigi Group, in particular to the basal Monte Zugna fm.
Lavini di Marco and Costa Stenda boulder ages cluster around 3000 years. We calculate a mean age for the Lavini di Marco and Costa Stenda rockslides of 3000 ± 400 years (Fig. 38). Within the uncertainties of our data the two slides were simultaneous. For the bedrock sliding plane we obtained significantly younger ages, 1600 ± 100 and 1400 ± 100 years, and for the head scarp 800 ± 200 years.
Based on our dataset, the Lavini di Marco rock avalanche occurred during a period of increased landslide activity of the Subboreal that has been recognized all across the Alps (Ivy-Ochs et al., 2017b and references therein). This time period roughly corresponds to the warm and humid climatic conditions of the Subboreal (e.g., Prager et al., 2008; Borgatti and Soldati, 2010). The ^{36}Cl exposure dates for Lavini di Marco and Costa Stenda boulders, with a mean age of 3000 ± 400 years, fall well within this time interval, suggesting climatic conditions with high precipitation.
Finally, the younger ages record small-scale reactivation, which seems to overlap in time with a catastrophic flood event of the Adige River in Verona in 883 AD, and possibly other events (cf. Fig. 45).

STOP 1.7: The Marocche di Dro rock-avalanches in the Sarca Valley: revisiting a reference case study (45.9837 °N, 10.9414 °E)

STOP 1.7 is the parking area located along the small road that connects the SP84 road to Drena and the Cavedine Lake (about 900 m coming from the first hairpin turn to Drena).
The Marocche di Dro of the middle reach of the lower Sarca Valley are some of the most famous and most beautiful of Alpine rock avalanche deposits (Fig. 39). Along this reach of the Sarca River as many as 12 different landslides, including five from Marocche di Dro, have been discussed (e.g., Trener, 1924). Based on fieldwork, remote imagery analysis, and ^{36}Cl surface exposure dating, we subdivide the Marocche di Dro into two landslides, the Marocca Principale and the younger overlying Kas (Fig. 39).
The Sarca River originates in the Adamello-Presanella tonalitic massif and, after a curvy course in the internal Giudicarie belt and the Sarca Valley, flows into Lago di Garda (the largest glacial lake of the Italian Alps). Along the eastern side of the lower Sarca Valley, the Sarca River flows along the western valley side through the

DOI: 10.3301/GFT.2018.01

landslide deposits. Farther to the south, the Sarca River passes through a marked bedrock narrow between Moletta and Arco before flowing out onto the Arco fan and the alluvial plain north of Lago di Garda. The Lago di Garda bedrock structure, and its northern prolongation into the lower Sarca Valley, suggests a very deep, steep-walled valley formed during the Late Miocene related to desiccation of the Mediterranean (Bini et al., 1978; Felber et al., 1998) (Fig. 39).

The release areas of the studied landslides are sourced in the steep towering walls of the Mt. Brento-Mt. Casale group along the western side of the valley. The area is dominated by rocks of the Calcari Grigi Group, which were deposited on the Trento carbonate platform during the Early Jurassic (Castellarin et al., 2005a; 2005b). The rock units exposed along the Mt. Brento-Mt. Casale rock wall are described herein

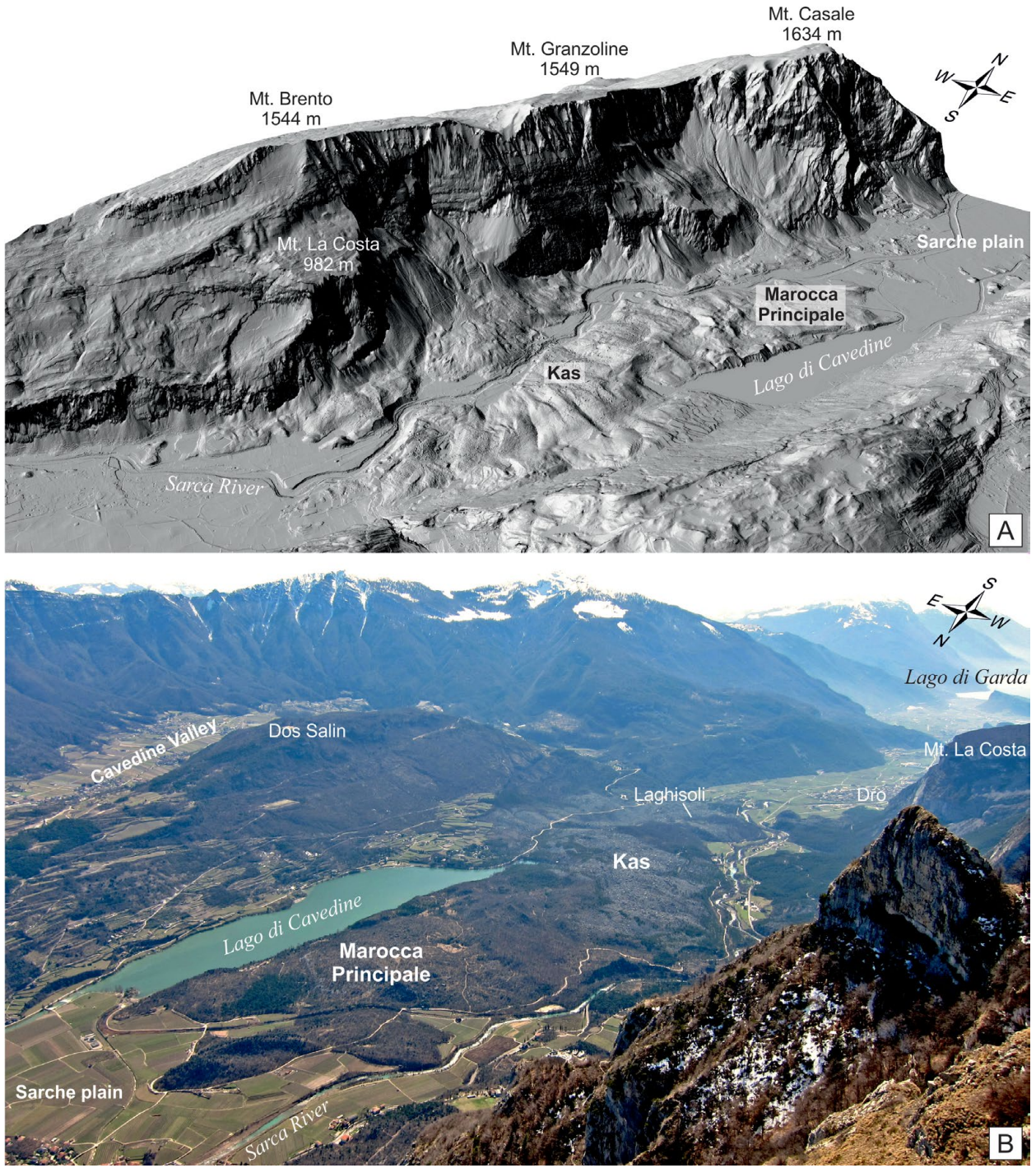

Fig. 39 - A) Hillshade view of the lower Sarca Valley and the Marocche di Dro deposits. B) Photo of the lower Sarca Valley. (Reprinted from Quaternary Science Reviews, 169, Ivy-Ochs et al., *Geomorphology and age of the Marocche di Dro rock avalanches (Trentino, Italy)*, 188-205, Copyright (2017), with permission of Elsevier).

DOI: 10.3301/GFT.2018.01

in stratigraphic order from bottom to top (Castellarin et al., 2005b; Avanzini et al., 2010) (Fig. 40). The Monte Zugna fm. (FMZ) consists of peritidal dolomitic limestones with fenestrae and stromatolites, as well as micritic limestones (mudstone and wackestones) rich in fossils, such as bivalves and algae (age: Rhaetian?- Sinemurian). Overlying the FMZ, lies the Loppio Oolitic Limestone (LOP), which is characterized by cream-colored grainstones with ooids and botroids and common intra- and bioclasts (age: Sinemurian). The Rotzo fm. (RTZ) comprising subtidal micritic limestones, intercalated with dark to greenish marly levels, follows this unit. Biocalcarenites can be present at the top of the formation (Sinemurian to Pliensbachian). The Tovel member of the Rotzo fm. (RTZ_1) consists of alternating gray micritic sediments mostly mudstone and wackestone, and gray to yellow packstone/ wackestone with bioclasts and algae. In the upper part, chert nodules are present (Sinemurian to Pliensbachian). The next unit is the Massone Oolitic Limestone (OOM), an oolitic micritic limestone with gray sparry calcite cement with cross and parallel lamination. Oolites and oncoids are relatively large; they are dominant over bioclasts (upper Pliensbachian). The OOM is followed by the San Vigilio Oolitic Limestone (OSV), which typically consists of radial oolitic grainstone with crinoids and encrinites (Toarcian-Aalenian). The uppermost unit at Mt. Casale is the Rosso Ammonitico Veronese (ARV) in the study area. These comprise pink to red nodular micritic limestones (Bajocian-Tithonian).

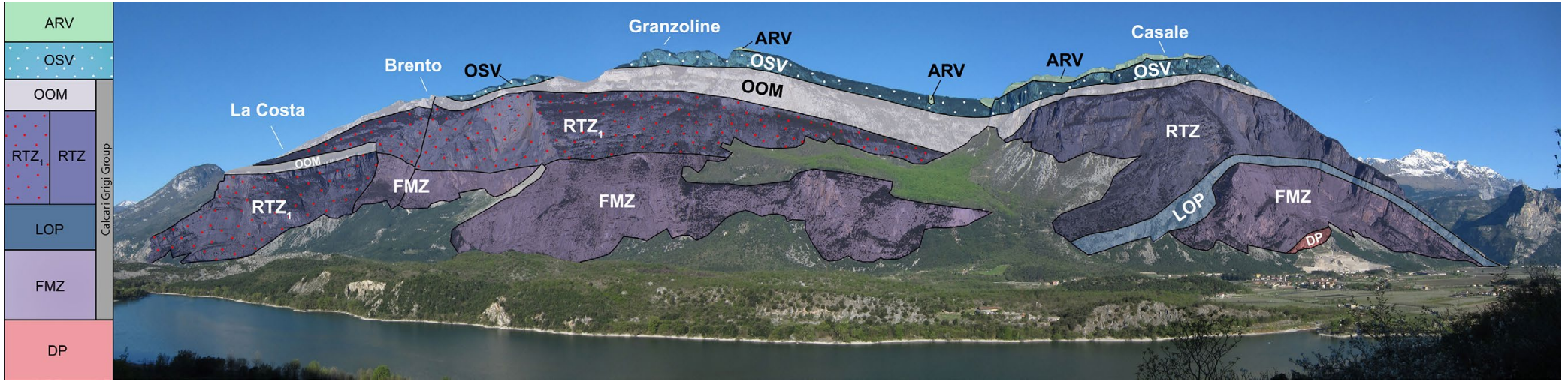

Fig. 40 - Photo of the Monte Brento to Monte Casale eastern wall with bedrock units identified (modified from Castellarin et al., 2005a; 2005b). (Reprinted from Quaternary Science Reviews, 169, Ivy-Ochs et al., *Geomorphology and age of the Marocche di Dro rock avalanches (Trentino, Italy)*, 188-205, Copyright (2017), with permission of Elsevier).

DOI: 10.3301/GFT.2018.01

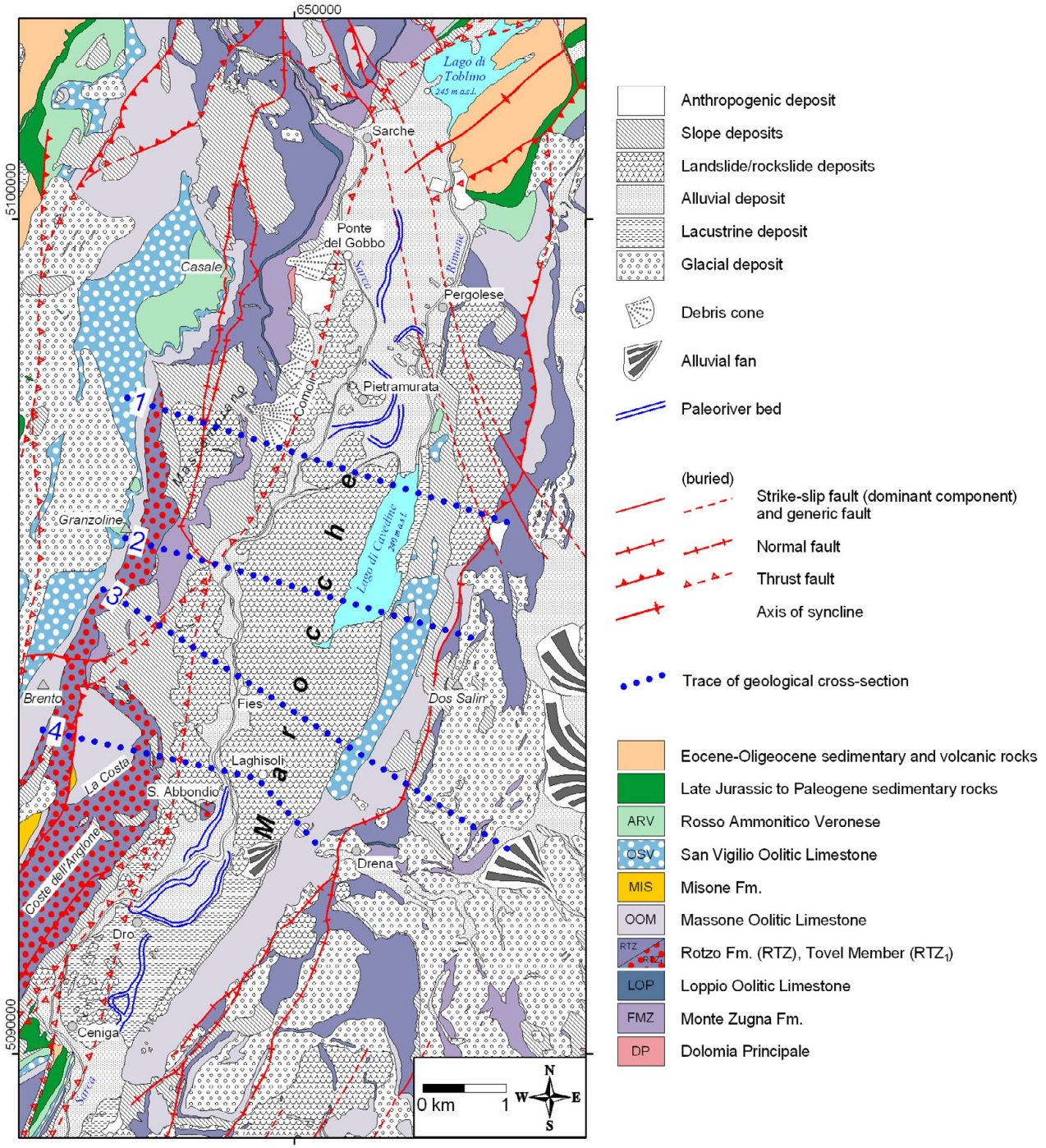

The NNE-SSW oriented Giudicarie fold-and-thrust belt, resulting from a polyphase deformation history (Picotti et al., 1995), dominates the lower Sarca Valley and Lago di Garda region (Fig. 41). The Neoalpine compression, which inverted the Mesozoic N-S oriented normal faults, acted during two stages, the Valsugana (Middle-Late Miocene) and the Schio-Vicenza phases (Late Miocene-Pliocene) (Castellarin et al., 2006). Decametric folds with axes about ENE-WSW oriented, due to the first phase, are visible along the Mt. Brento-Granzoline-Casale eastern faces (Fig. 40). NNE-SSW oriented structures, with out-of-sequence and strike-slip reactivations along the Giudicarie and Schio-Vicenza fault systems (due to the SE-NW to SSE-NNW oriented compression, second

Fig. 41 - Geological map of the lower Sarca Valley (data from the Geological Survey of Trento, CARG project database; Castellarin et al., 2005a, 2005b). Dotted lines show traces of Fig. 42 geological cross-sections. (Modified from Quaternary Science Reviews, 169, Ivy-Ochs et al., *Geomorphology and age of the Marocche di Dro rock avalanches (Trentino, Italy)*, 188-205, Copyright (2017), with permission of Elsevier).

DOI: 10.3301/GFT.2018.01

phase) can be recognized in the geological map (Fig. 41). The Giudicarie fold-and-thrust system is characterized by an ESE-to-SE vergence, evidenced by asymmetric folds, which in turn caused an asymmetric morphology to the lower Sarca Valley. A syncline can be recognized at the base of the Mt. Casale where the Dolomia Principale (DP) overthrusts Eocene marly rocks. In the whole area, evident NW-SE oriented nearly vertical strike-slip faults cut across the Giudicarie thrust system displacing originally adjacent structural blocks. Widespread N-S oriented normal faults and fractures record a late post-compressional deformation (Fig. 41).

The Marocca Principale rock avalanche deposits extend from Pietramurata village in the north to S. Abbondio hill in the south (Fig. 41). The total length of the Marocca Principale is about 5 km and its width varies from 1.5 to 2 km in the southern sector near S. Abbondio to about 3 km near Lago di Cavedine. The areal extent right after failure (before being buried in its southern half by the Kas event) was approximately 10 km^2 (Ivy-Ochs et al., 2017b).
The suggested thickness of about 130 m for the Marocca Principale indicates an approximate volume of at least 1 km^3.
The Marocca Principale release area extends from Mt. Casale to Mt. Granzoline, and likely continues over to Mt. Brento (Fig. 39). Based on the difference between the highest elevation in the release area (estimated 1480 m a.s.l.) and elevation of the top of the deposit (estimated 200 m a.s.l.) at the southern extent of the deposit (to the east of S. Abbondio) and the total horizontal distance travelled to S. Abbondio toma (estimated 5800 m), an angle of reach of 12° is obtained (Ivy-Ochs et al., 2017b). Run-up of the rock avalanche on the opposite side of the valley reached up to several hundred meters as shown by rock avalanche deposits found along the ridgeline of the Dos Salin ridge above Lago di Cavedine (Figs. 41 and 42).
The Marocca Principale deposit surface is relatively smooth with the areas between boulders filled in by developing soil (Fig. 43). Areas with gigantic boulders are infrequent, found notably in the NE sector and just to the west of the Lago di Cavedine. Broad ridges, tens of meters long and 3-5 m high, dominate the surface topography especially in the middle sector just north of the contact with Kas deposits (Ivy-Ochs et al., 2017b). Their orientation, ESE, suggests the direction of movement directly outwards from the huge niche above the Massampiano (Fig 39).
The boulders of the Marocca Principale are dominated by micritic massive to peloidal in some cases oolitic RTZ limestones, many with 5-10 cm deep rillenkarren (Fig. 43). Trener (1924) and Bassetti (1997) also reported the presence of OSV and FMZ boulders. In the Pietramurata area, boulders of the Rosso Ammonitico Veronese are prevalent.

DOI: 10.3301/GFT.2018.01

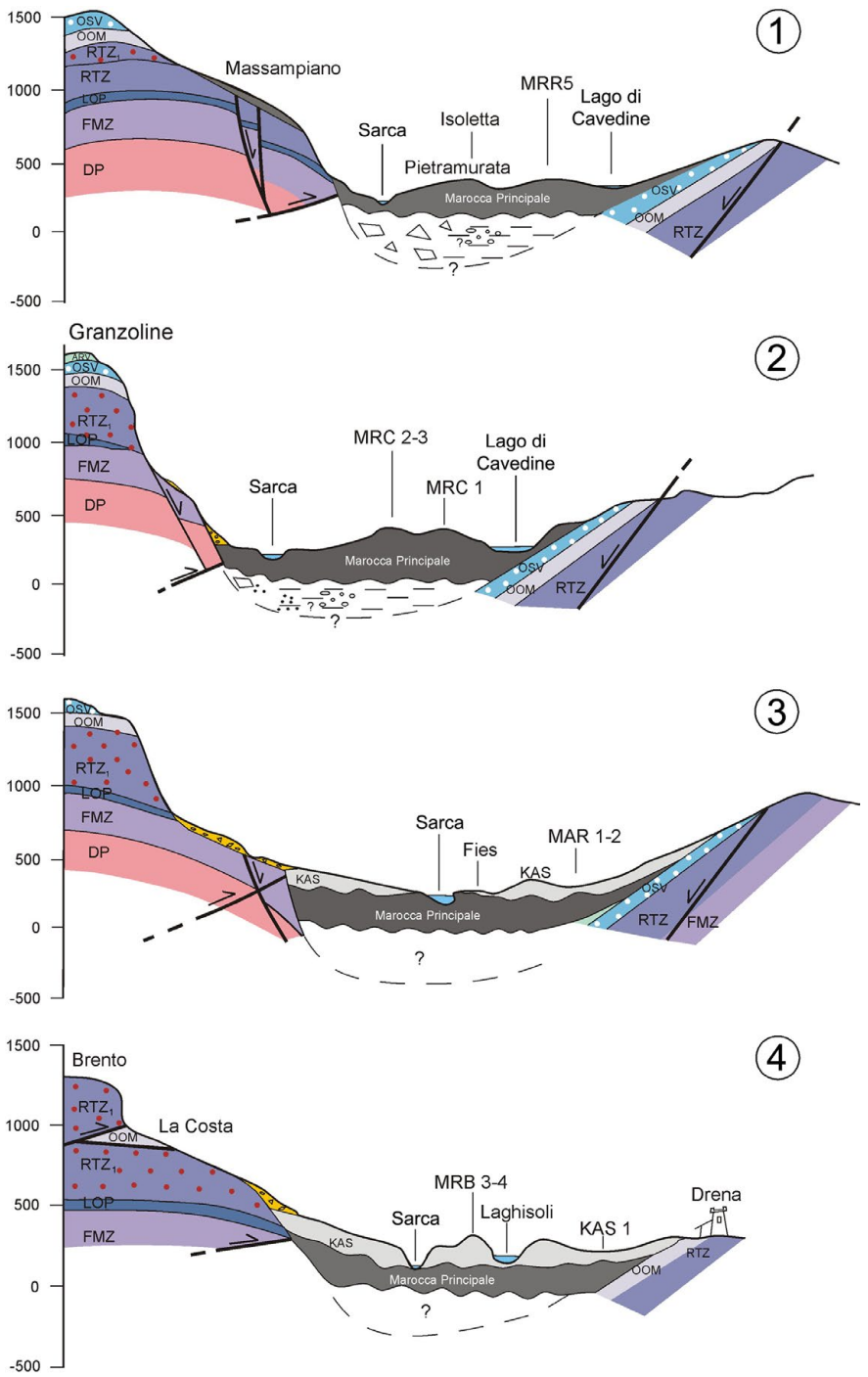

The ^{36}Cl surface exposure ages for the Marocca Principale boulders range from 4310 ± 320 yr to 6220 ± 560 yr (Fig. 44). As all ages overlap within uncertainties, we take the average and obtain 5300 ± 860 yr.

Kas deposits are approximately 3 km long and vary in width from 0.5 to 1.5 km, corresponding to an area of about 3.5 km^2. We estimate a thickness of ca. 80 m based on the difference in elevation of the top of the Marocca Principale deposits and the elevation of the Kas debris hills. An estimated volume of ca. 300 X 10^6 m^3 is obtained (Ivy-Ochs et al., 2017b). The Kas rock avalanche originated from the fresh appearing niche on the face of Mt. Brento and from right below Mt. La Costa (Fig. 39).

The elevation of the furthest Kas deposits along the southeastern side is 200 m a.s.l. Based on total horizontal distance of 3500 m (not precisely travel distance as much of the horizontal distance was covered during the collapse from the rock wall), an angle of reach of 17° is obtained.

The Kas rock avalanche deposits comprise distinctly barren, chaotic, blocky debris completely devoid of vegetation (Fig. 43). House-size, angular boulders (up to 20 X 20 m) are especially abundant on the surface of the Kas deposits, especially near Laghisoli (Figs. 39 and 43). While the sediment below the blocky carapace consists of shattered and comminuted very angular rock fragments ranging down to silt size. Blocks of a

Fig. 42 - Schematic E-W cross-sections across the lower Sarca Valley (traces shown in Fig. 41). (Reprinted from Quaternary Science Reviews, 169, Ivy-Ochs et al., *Geomorphology and age of the Marocche di Dro rock avalanches (Trentino, Italy)*, 188-205, Copyright (2017), with permission of Elsevier).

DOI: 10.3301/GFT.2018.01

white-weathering limestone with yellow and black lenses or bands of chert (MRB3, MRB4) belonging to the Tovel member (RTZ_1) are scattered on top of the Laghisoli hills, which are topographically higher than the rest of the deposit.

Six boulders of the Kas deposit were ^{36}Cl exposure dated. Four boulders located in the deposits mapped as Kas and two from the area previously mapped as the Laghisoli landslide (Fig. 44). The data show that if the Laghisoli landslide did occur as a separate event, its age is indistinguishable from the Kas landslide. As the two oldest ages do not overlap within uncertainties, we consider them as outliers

Fig. 43 - A) View across the Kas deposits towards Mt. Brento. B) Kas boulders around Laghisoli. C) Boulder MRB3 (Kas rock avalanche). D) Boulder MRR5 (Marocca Principale). E) Boulder MRC2 (Marocca Principale) exhibiting 5-10 cm deep rillenkarren. F) Boulder MAR3 (Kas) showing chert bands (several cm across) standing < 1 cm proud. G) Boulder on the left MRB4 (Kas). H) Boulder MRC3 (Marocca Principale). See also Fig. 44 (reprinted from Quaternary Science Reviews, 169, Ivy-Ochs et al., *Geomorphology and age of the Marocche di Dro rock avalanches (Trentino, Italy)*, 188-205, Copyright (2017), with permission of Elsevier).

DOI: 10.3301/GFT.2018.01

that contain inherited ^{36}Cl. We take the mean age of the remaining boulders, which is 1080 ± 160 yr, as the age of the Kas landslide (Ivy-Ochs et al., 2017b).

Figure 45 shows the ages of the three dated landslides here discussed, compared with other catastrophic events; all are located within a maximum distance of 20 km from each other (Ivy-Ochs et al., 2017a; 2017b and references therein). This coincidence in time and space (Fig. 46) strongly suggests a seismic origin (cf. Prager et al., 2008).
Based on available compilations of historical seismicity (Guidoboni et al., 2007; Rovida et al., 2016), two strong earthquakes struck southern Trentino and the central Po plain around 1000 AD. They are the "Middle Adige Valley" event dated to 1046 AD (estimated epicentral intensity IX MCS, Mercalli-Cancani-Sieberg scale; Guidoboni and Comastri, 2005; Guidoboni et al., 2007) and the "Verona" earthquake, which occurred in 1117 AD (estimated epicentral intensity IX MCS; Guidoboni et al., 2007).
Although there are significant uncertainties associated with the epicentral coordinates of the 1046 AD earthquake, its location (Guidoboni and Comastri, 2005) is considerably closer to the representative Castelpietra and Kas sites (about 6 and 11 km of epicentral distance, respectively) than the

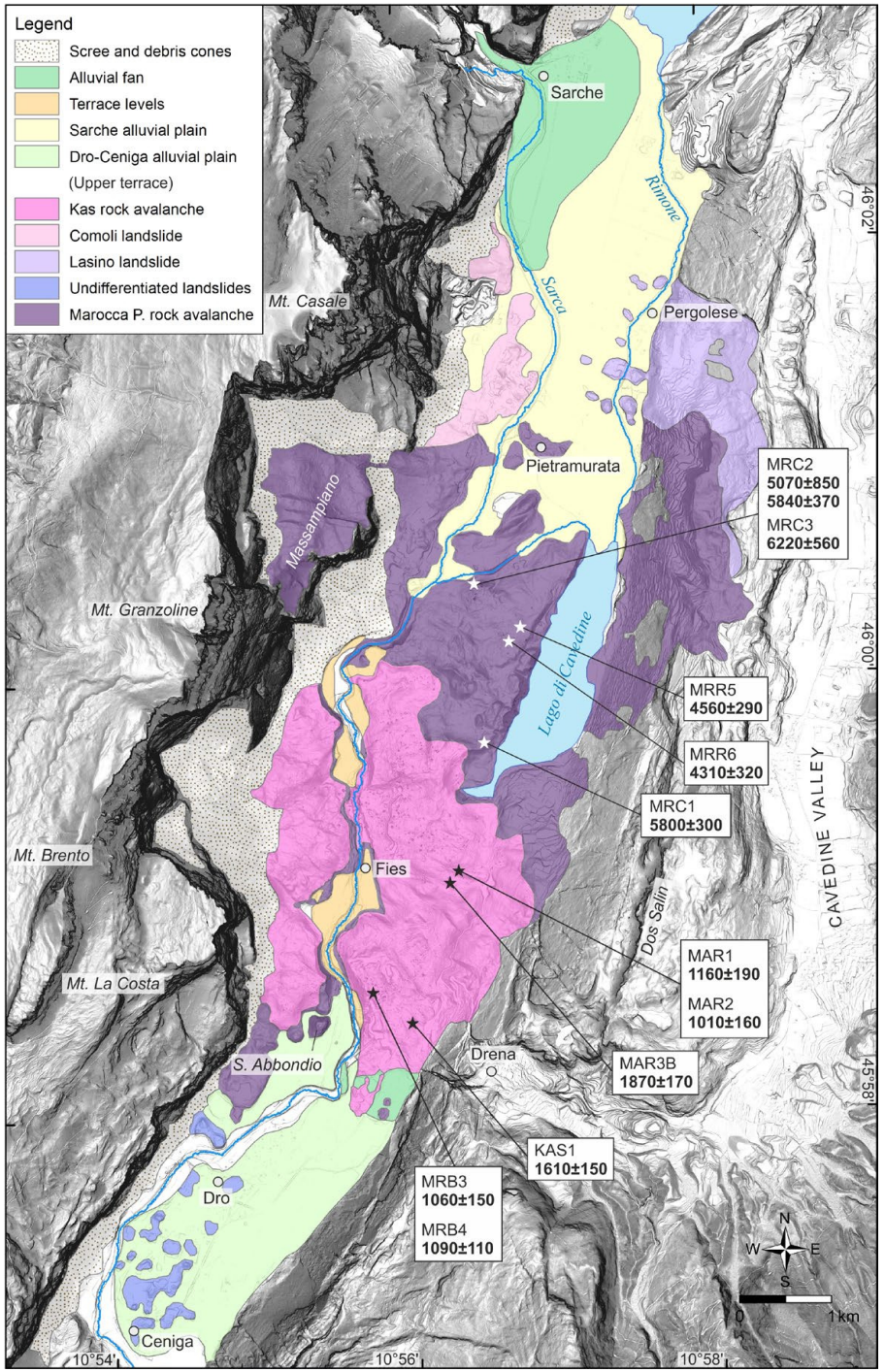

Fig. 44 - Sketch map of the main geomorphological units of the lower Sarca Valley, with cosmogenic ^{36}Cl exposure ages for all the analyzed boulder samples. (Modified from Quaternary Science Reviews, 169, Ivy-Ochs et al., *Geomorphology and age of the Marocche di Dro rock avalanches (Trentino, Italy)*, 188-205, Copyright (2017), with permission of Elsevier).

DOI: 10.3301/GFT.2018.01

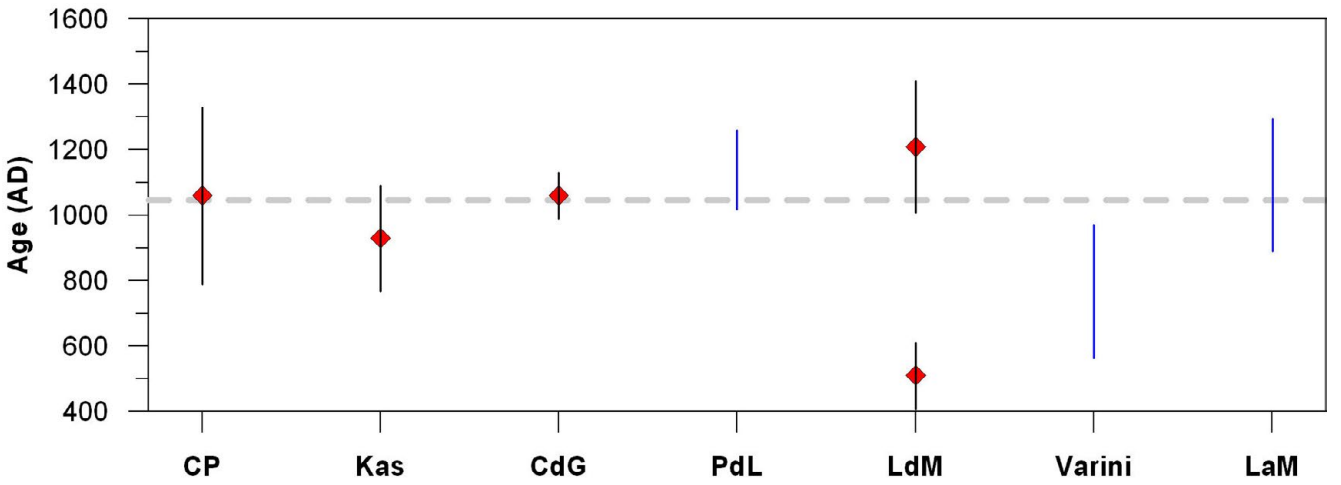

Fig. 45 - Ages of landslides discussed in the text (CP Castelpietra, Kas of Marocche di Dro, PdL Prà da Lago, LdM Lavini di Marco [only younger ages, see below], Varini near Lavini di Marco, LaM La Marogna) and Cogola di Giazzera cave (CdG). Red diamonds are ^{36}Cl ages and U/Th dating (CdG), with uncertainties. Blue bars are radiocarbon dating (PdL, Varini and LaM). The gray dotted line marks the "Middle Adige Valley" 1046 AD earthquake. See also STOP 1.2 and STOP 1.6. LaM ^{14}C calibrated ages courtesy of S. Ivy-Ochs (ETH Zürich) and M. Cucato.

1117 AD earthquake (about 72 and 80 km, respectively) (Fig. 46). Based on an epicentral intensity of IX MCS (Guidoboni et al., 2007) and a distance of about 10 km, the Peak Ground Acceleration (PGA) for the 1046 AD event can reasonably be considered to have exceeded the threshold proposed by Guo et al. (2015) for triggering a landslide on a slope. In contrast, a much greater distance from the seismic source (the distance between Castelpietra and Kas and the 1117 AD epicenter is more than six times greater) would have yielded considerably lower PGA values. In light of the non-linear decrease of co-seismic ground acceleration with distance (Boore et al., 2014 and references therein), we can therefore suggest a possible correlation between the 1046 AD seismic event and both the Castelpietra and Kas landslides, and possibly the Prà da Lago, Varini and La Marogna events as well. About the event recorded by the Cogola di Giazzera stalagmite, Frisia et al. (2005) already proposed linkage to a major seismic event.

Several factors contribute to the prevalence of rock slope failures in the Sarca Valley. One is extreme relief of more than one kilometer attributable to Miocene downcutting amplified by undercutting by the Adige Glacier during Quaternary glaciations (Ivy-Ochs et al., 2017b and references therein). The active tectonic setting plays a decisive role in the repeated failure along Mt. Brento e Mt. Casale. Post-compressional N-S oriented normal faults and fractures facilitated backwall detachment; strike-slip faults of the Schio-Vicenza system focused lateral constraints for detaching blocks. For the two events (Marocca Principale and Kas), failure was initially translational, which quickly evolved to massive collapse and complex failure, followed by run-out across the valley and run-up on the eastern slope.

DOI: 10.3301/GFT.2018.01

In the Alps three periods of apparent enhanced rock slope failure have been recognized (Ivy-Ochs et al., 2017b and references therein): 10-9 kyr, 5-3 kyr, and 2-1 kyr, the latter especially for the Southern Alps. No deposits of the first temporal cluster are found at Marocche di Dro. The age of Marocca Principale at 5300 ± 860 yr broadly coincides with the recognized period of increased frequency of failure events at the transition from the middle to the late Holocene when a shift to a wetter, colder climate occurred. Nevertheless, a seismic trigger cannot be excluded. Although the Verona earthquake (1117 AD) may have had a great regional impact, we suggest that the "Middle Adige Valley" (1046 AD) earthquake, whose epicentral distance is much closer to the Sarca Valley, triggered the Kas rock avalanche (1080 ± 160 yr) (see STOP 1.6 and Fig. 45).

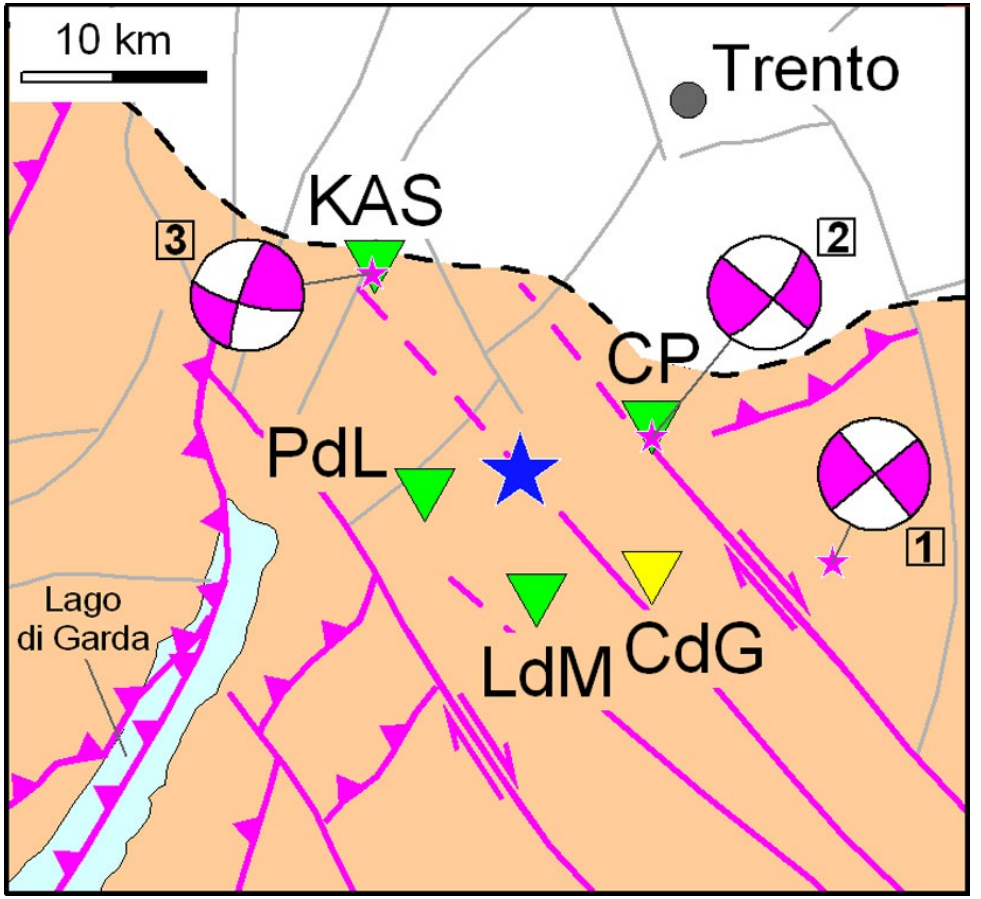

Fig. 46 - Seismotectonic sketch with the high-seismicity area south of Trento (orange shading), major faults in gray and active faults in magenta. Green triangles are Castelpietra (CP), Kas (at Marocche di Dro, see STOP 1.6), Lavini di Marco (LdM), and Prà da Lago (PdL) landslide deposits, and yellow triangle is the Cogola di Giazzera cave (CdG). The blue star marks the location of the 1046 AD earthquake epicenter from Guidoboni and Comastri (2005). Epicenters and focal mechanisms from Viganò et al. (2015): 1) 13 September 1989, local magnitude 4.7; 2) 26 April 1999, local magnitude 3.4; 3) 16 June 2000, local magnitude 3.2 (cf. also Tab. 1, but with different event numbering).

DOI: 10.3301/GFT.2018.01

DAY 2: Geology and structures of the central Brenta Dolomites

STOP 2.1: Tectonics around Grostè Pass

The Brenta Dolomites stratigraphy is strongly influenced by synsedimentary Norian-Early Jurassic normal faults related to Mesozoic continental rifting. These faults existed before the drifting stage that led to the break up and opening of the Ligurian Ocean during the Middle Jurassic times. The Brenta Massif is located at the Trento Platform - Lombardian Basin transition, corresponding to a set of N-trending normal faults, which permitted a high subsidence rate in the western sectors (Fig. 47).
In the Non Valley the Norian-Lower Jurassic sedimentary cover is typical of a structural high, as indicated by a thin succession of Dolomia Principale and Rhaetian beds (only 300 m) and the absence of the Calcari Grigi Group limestone on top. This structural high coincides with the core of the Trento Platform and includes the Sella Group in the Dolomites.

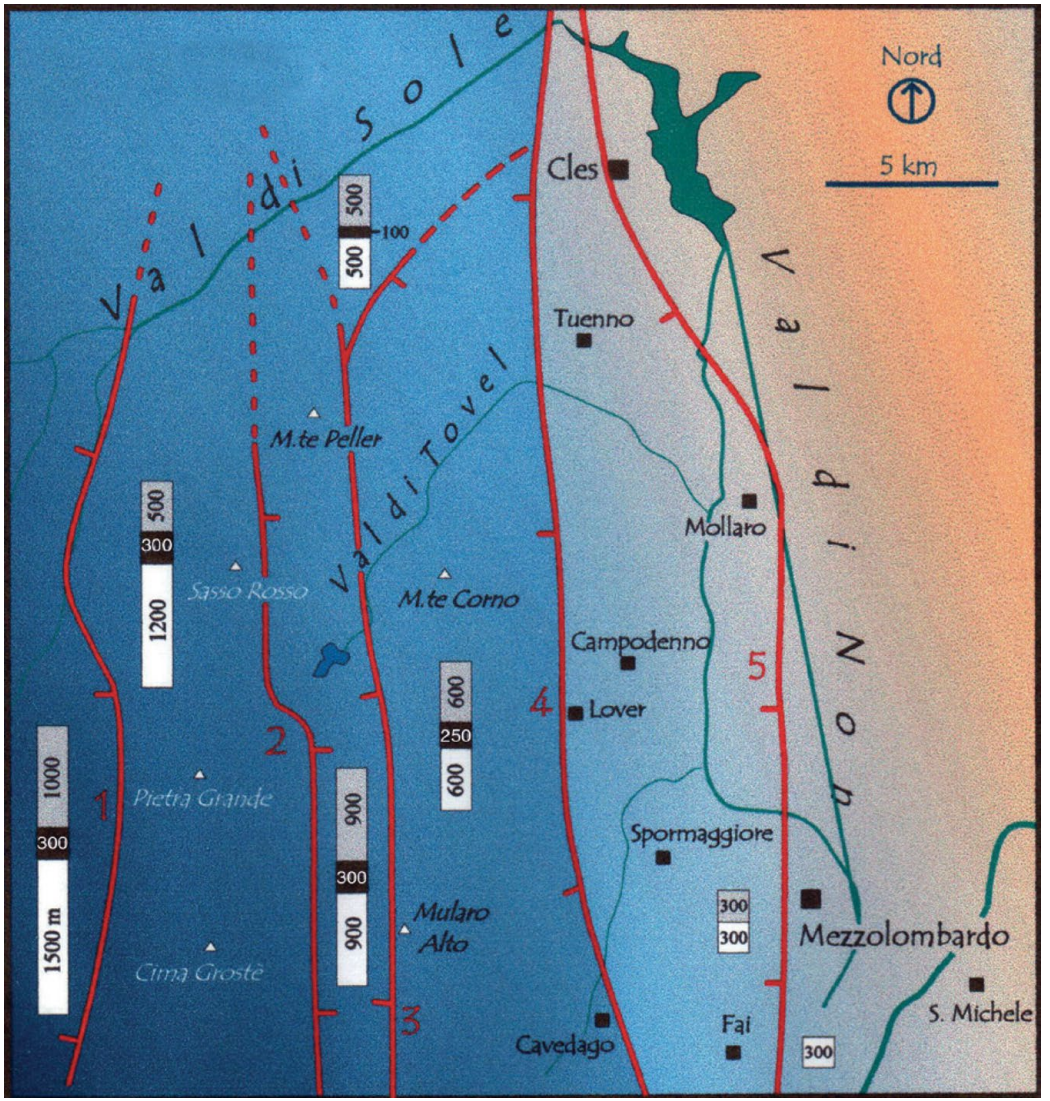

Fig. 47 - Palaeostructural map showing the central Southern Alps between Non Valley and Brenta Dolomites. The Norian-Early Jurassic syn-rift N-S trending normal faults are shown: (1) Vedretta dei Camosci, (2) S. Maria di Flavona, (3) Val Strangola, (4) Trento-Cles, (5) Mezzolombardo-Taio. The blue colours represent the subsiding sectors and the orange ones the structural highs. The synthetic stratigraphic columns show the thicknesses of Dolomia Principale (white), Calcare di Zu (black) and Calcari Grigi Group (grey). (Dal Piaz et al., 2007; courtesy of the Geological Survey of the Autonomous Province of Trento)

DOI: 10.3301/GFT.2018.01

Stop 2.1.1: (46.2145 °N, 10.9029 °E)

In the area comprised between the Vedretta dei Camosci line (fault 1 in Fig. 47) and the Non Valley, subsidence rates increased from the east to the west, without significant facies changes in the peritidal platform carbonates. Here, the maximum thickness of peritidal limestones is up to 2500 m. In the western sector, located at the hanging-wall of the Vedretta dei Camosci line (Figs. 47 and 48), opening of the Lombardian Basin is shown by the syn-rift cherty limestones of the Tofino fm.

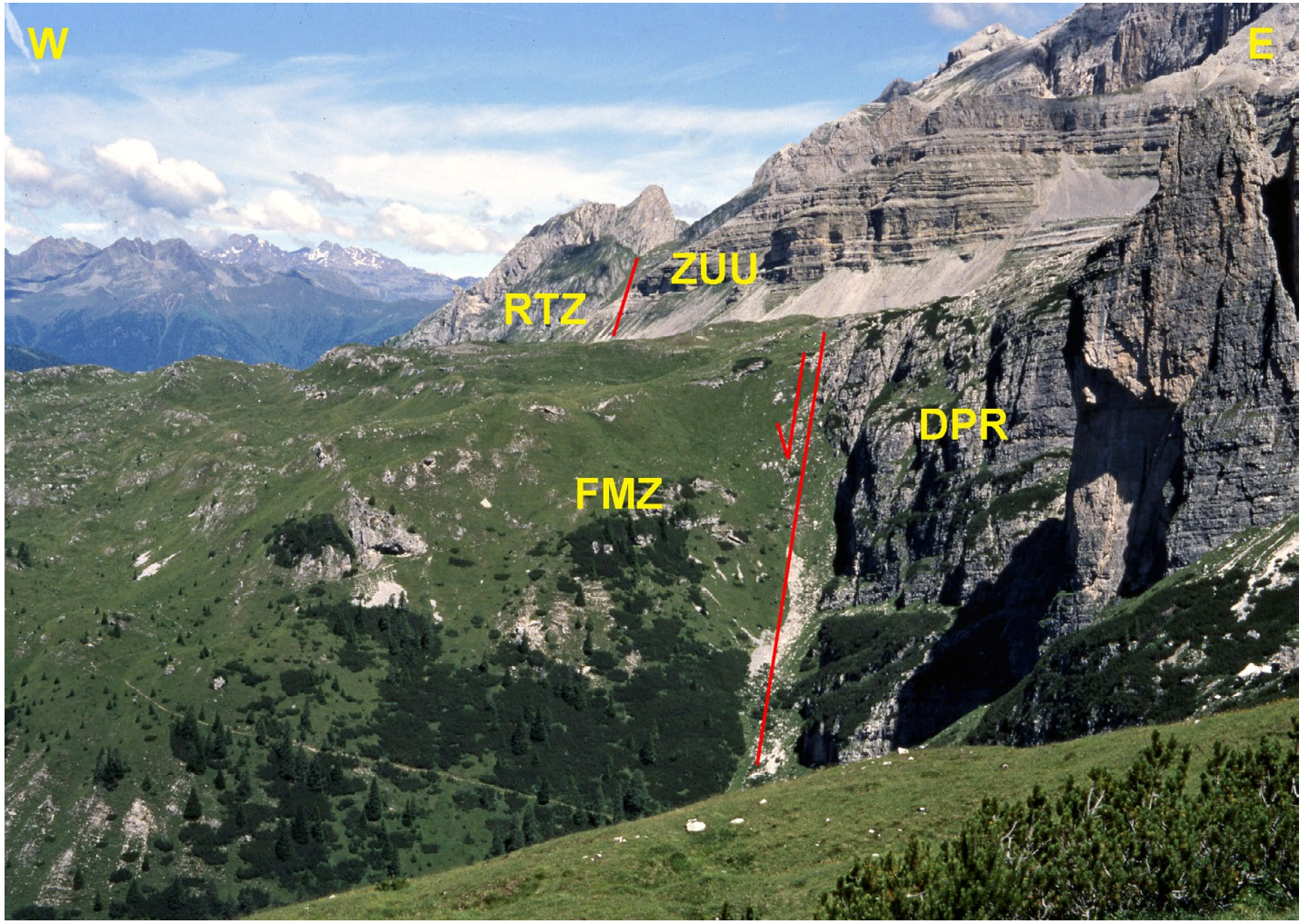

Fig. 48 - The Vedretta dei Camosci line, with the Norian Dolomia Principale in the footwall and the Lower Jurassic Calcari Grigi Group in the hanging-wall.

During the Miocene inversion, the syn-rift normal fault were reactivated as left-lateral transpressive lateral ramps combined with short south-verging frontal ramps. In the hanging-wall of these thrusts (Vallon, Cima Tosa, Passo Clamer) north-verging intercutaneous wedges detached along black shales of the Calcare di Zu (Fig. 49). Later, erosion produced klippen structures, which mark the present-day relief of the Brenta Group around the Grostè Pass (Fig. 50). These are, from the west to the east, the Spinale, Pietra Grande, Turrion and Campa Massif klippen (Figs. 51 and 52).

DOI: 10.3301/GFT.2018.01

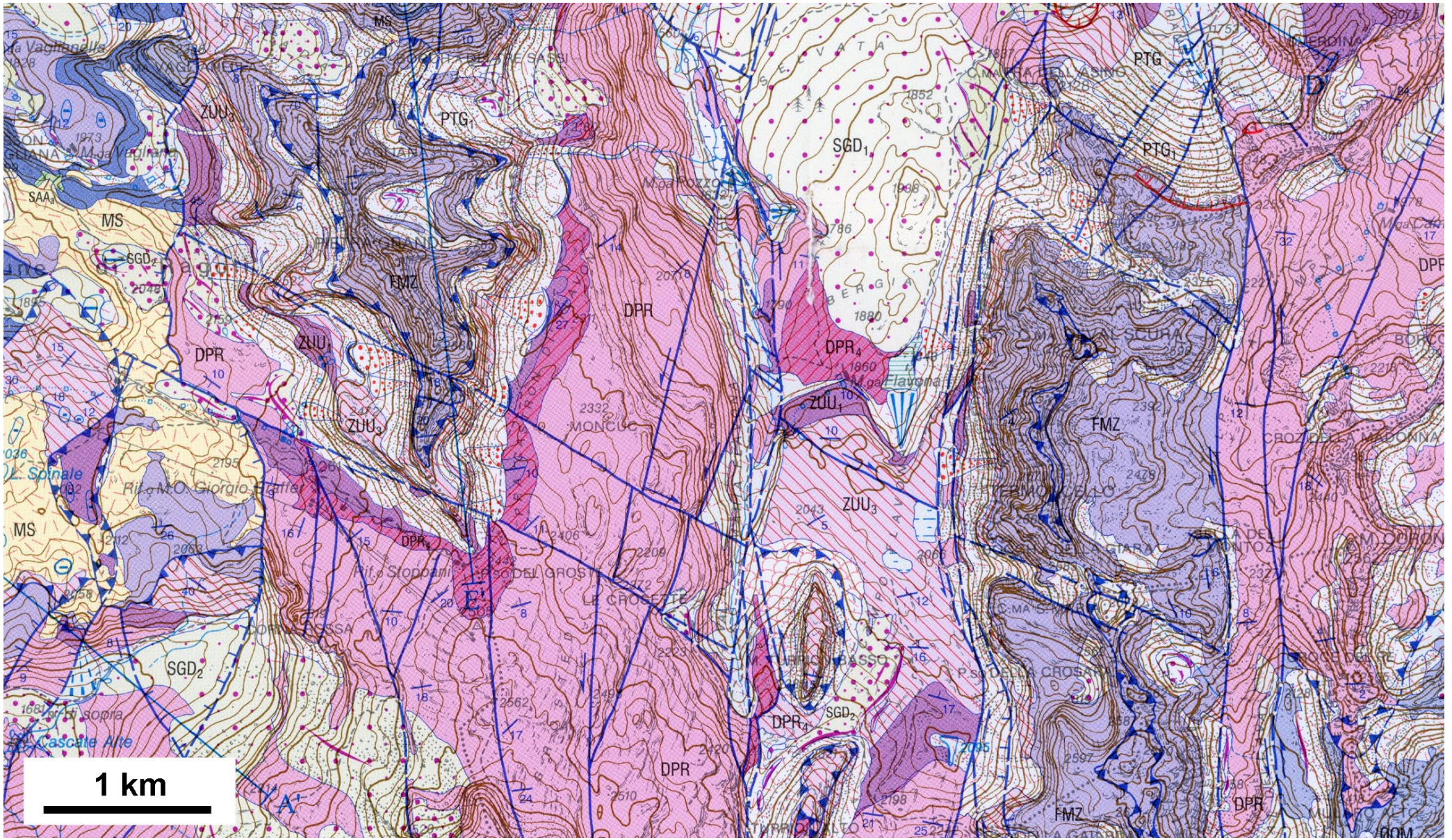

Fig. 49 - Geological map of the central Brenta Massif. DPR Dolomia Principale (Carnian-Norian), DPR_4 Flavona mb. (Norian), ZUU_1 Calcare di Zu Grostè mb. (Rhaetian), ZUU_3 Calcare di Zu Tremalzo mb. (Rhaetian), FMZ Monte Zugna fm. (Sinemurian), LOP Loppio Oolitic Limestone (Sinemurian), RTZ Rotzo fm. (Pliensbachian), MS Monte Spinale breccias (Plio-Pleistocene). Note the system of north-verging klippen. (Dal Piaz et al., 2007; courtesy of the Geological Survey of the Autonomous Province of Trento)

DOI: 10.3301/GFT.2018.01

Stop 2.1.2: The Pietra Grande thrust (46.2282 °N, 10.8950 °E)

The Pietra Grande thrust is a sub-horizontal north-vergent décollement connected with the major Cima Tosa thrust (Castellarin et al., 1993) (Figs. 53 and 54). This thrust propagated within the limestones of Late Triassic-Early Jurassic age and mainly separates the massive Monte Zugna fm. limestones (upper part; FMZ in Fig. 54) from the stratified Calcare di Zu limestones with intercalated marls (lower part; Tremalzo mb. ZUU_3 in Fig. 54).
Along the Pietra Grande thrust, unusual indications of co-seismic deformations can be observed (Viganò et al., 2011; 2013b).

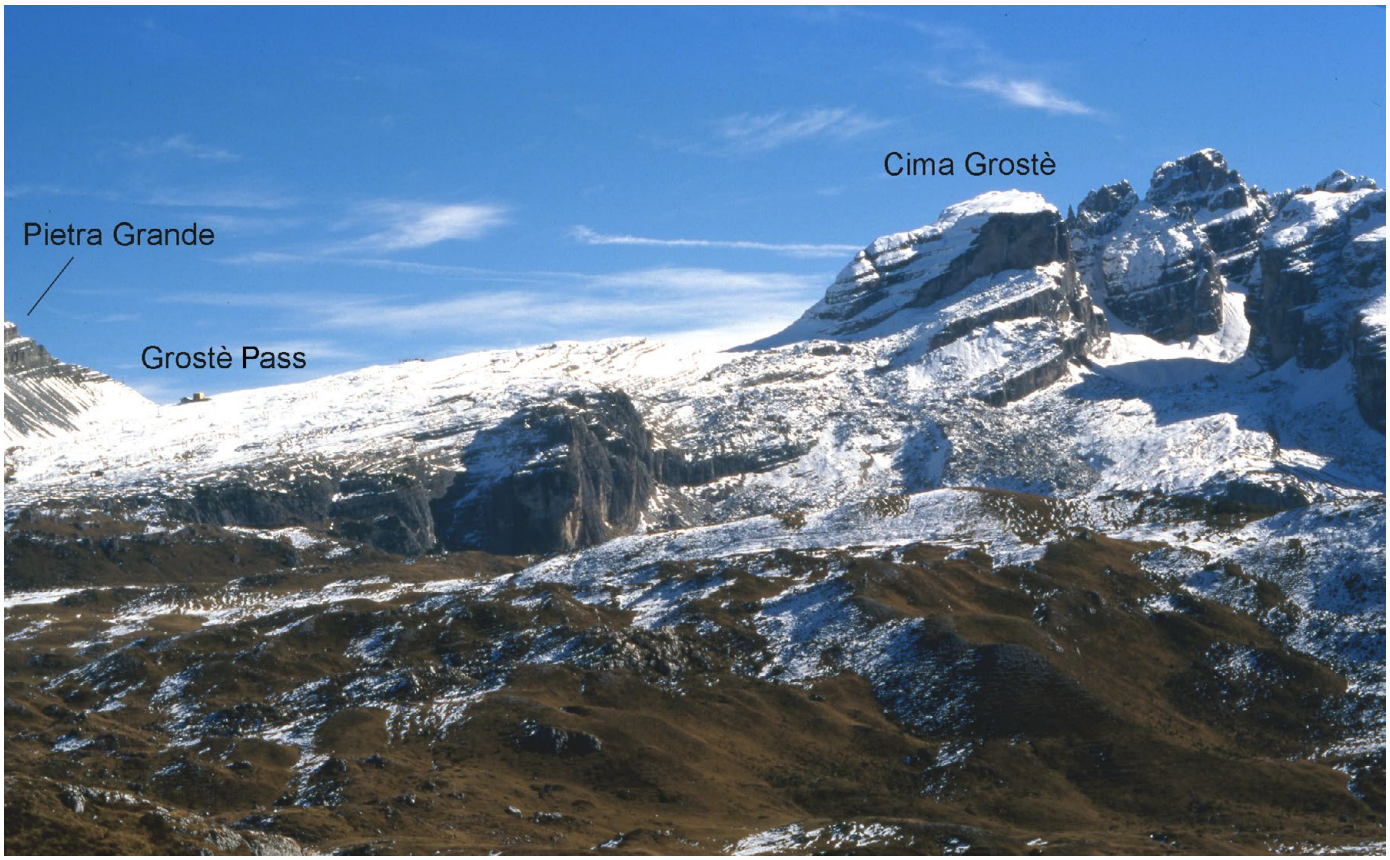

Fig. 50 - Starting from north (on the left): the slope of the Pietra Grande, Grostè Pass and Cima Grostè. Northward dipping beds of Dolomia Principale are located at the hanging-wall of the Cima Tosa thrust.

STOP 2.2: Panoramic view of the Adamello-Presanella and Cevedale Massifs (46.2300 °N, 10.8888 °E)

We can appreciate a wide panoramic view of the central Southern Alps and the southern Austroalpine Units. Our view spans from the Carè Alto peak (Adamello Massif) to the SW, to the Cevedale Massif to the N (Figs. 55 and 58). The geological features that can be recognized in the area are summarized in Figs. 56, 57 and 59 (modified from the geological maps cited below; courtesy of the Geological Survey of the Autonomous Province of Trento).

DOI: 10.3301/GFT.2018.01

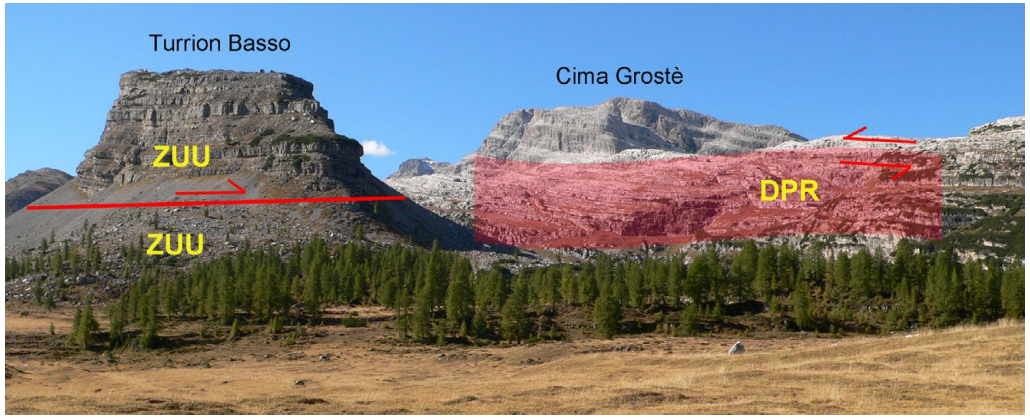

Fig. 51 - The Turrion klippe (view from NNE). The steep slope in the right side of the picture marks the S. Maria di Flavona left-lateral fault, along which the Grostè area is uplifted of about 600 meters.

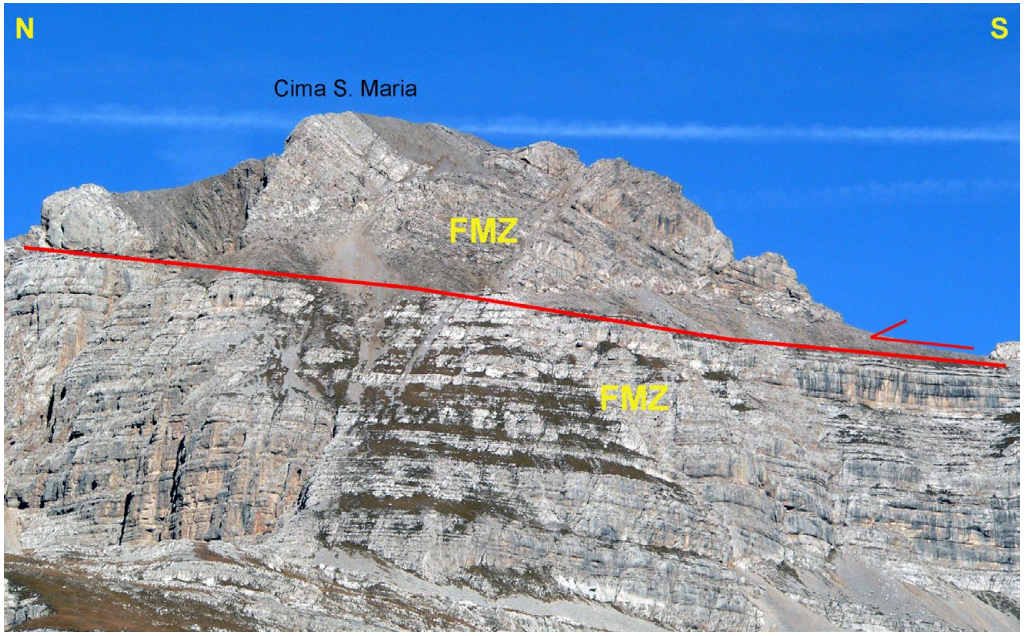

Fig. 52 - One of the klippen of the Campa Massif can be observed at the Cima S. Maria. The structure is similar to the Spinale, Pietra Grande and Turrion klippen.

Fig. 53 - Panoramic view from S to N of the western slope of Pietra Grande. The Pietra Grande thrust is clearly marked by the sub-horizontal ledge (Vidi path at close-up).

DOI: 10.3301/GFT.2018.01

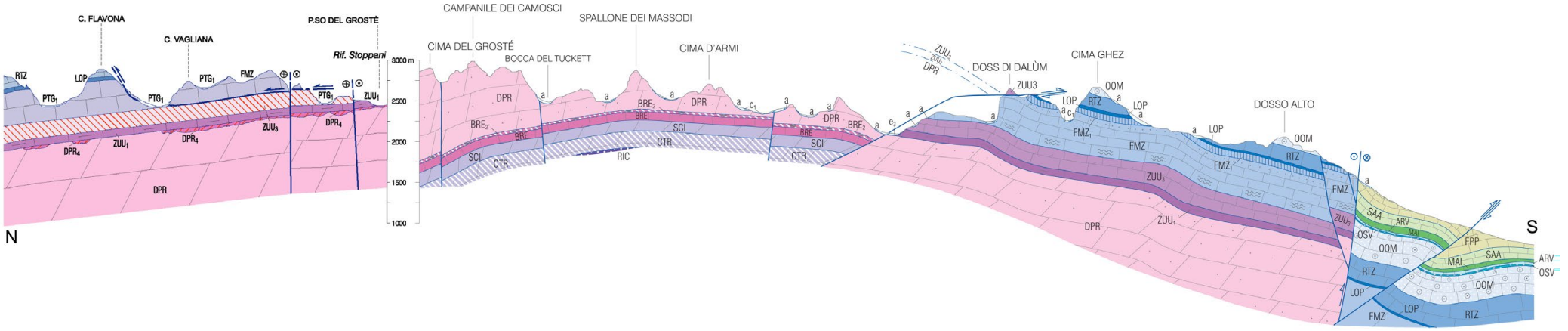

Fig. 54 - Geological cross-section along the Brenta Massif between Cima Flavona and San Lorenzo Dorsino, showing the Pietra Grande thrust and its relation with the Cima Tosa thrust (visible in the middle part of the cross-section). (Modified from Castellarin et al., 2005a and Dal Piaz et al., 2007; courtesy of the Geological Survey of the Autonomous Province of Trento).

Immediately in front of us, down in the valley, the Mt. Spinale can be observed. It consists mainly of the Monte Zugna (FMZ) and Calcare di Zu (ZUU) limestones (Dal Piaz et al., 2007). Limestone at Mt. Spinale is covered by the Mt. Spinale breccia (MS), hosting different lithologies, some of which, as the Scaglia Rossa and the Loppio Oolitic Limestone, are not present anymore in the Pietra Grande area (Castellarin et al., 2005a).
Looking southwestward, beyond Val Rendena and the terminations of Val Nambrone and Val di Genova, large portions of the Adamello Massif are visible. The highest peak of Caré Alto is made up of the Central Adamello tonalite (TAC, Upper Eocene) in the upper part and of the Re di Castello tonalite (RCT, Upper Eocene) in the lower part. These plutons are intruded within the Rendena schists (SRE), with intercalated orthogneiss, exposed in the Breguzzo and San Valentino valleys (Brack et al., 2008).
Westward, the Sabion fault separates the carbonate sequence of M.te Spinale (Dolomia Principale, Calcare di Zu and Monte Zugna fm.) from the basement of the Southern Alps, consisting of the Rendena schists (SRE) intruded by Permian granitoids (GLM; Martin et al., 1996). This structure can be observed in the area of the Passo Campo Carlo Magno and northwards in the Meledrio Valley (Figs. 55 and 56). To the east, the Giudicarie fault separates the Southalpine basement from the Mt. Nambrone-Mt. Nambino foliated leucotonalite (PPN; Oligocene) and the Presanella and Cima Palù tonalite (PPC; Oligocene). Along the Mt. Nambrone-Mt. Nambino topographic high a set of NNE-trending faults and fractures, parallel to the Southern Giudicarie and Sabion faults, can be detected within the foliated leucotonalite.

DOI: 10.3301/GFT.2018.01

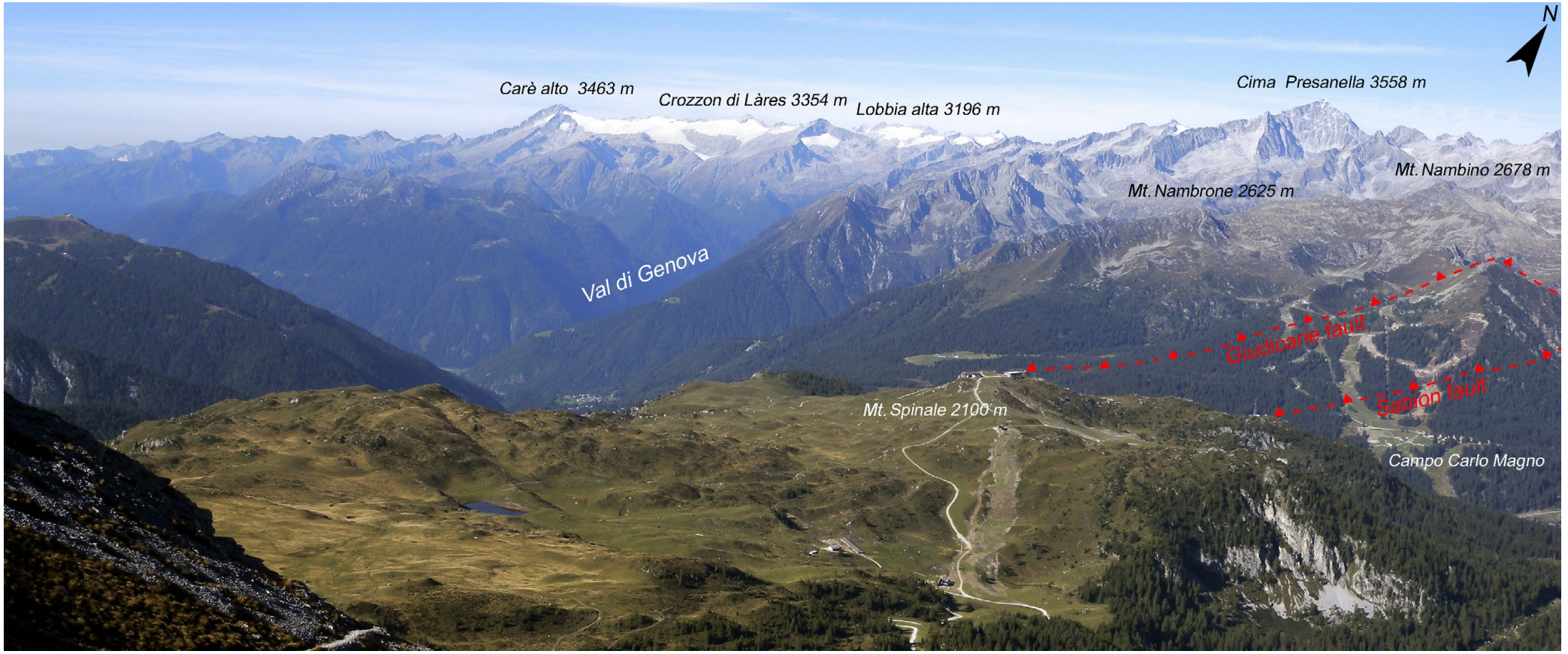

Fig. 55 - View to the SW: Carè Alto (Adamello Massif), Cima Presanella, M.te Nambino-M.te Nambrone high, Passo Campo Carlo Magno.

A major NNE-trending fault is present along the Nambrone Valley, where it separates the Mt. Nambrone-Mt. Nambino topographic high from the tonalites of the Cima Presanella Massif.
The Giudicarie and Sabion faults can be interpreted as inherited normal faults connected to the Mesozoic rifting, later reactivated during the Neoalpine phase as transpressive to reverse faults. The footwall of the Giudicarie fault comprises Permian to Paleogene sedimentary rocks overlying Permian magmatic rocks.
Along the northern branch of the Giudicarie fault (not shown in Fig. 57) the Tonale nappe of the Austroalpine basement thrusts over the Southalpine basement and its sedimentary cover (Martin et al., 1991; Prosser, 1998; Martin et al., 2009).

DOI: 10.3301/GFT.2018.01

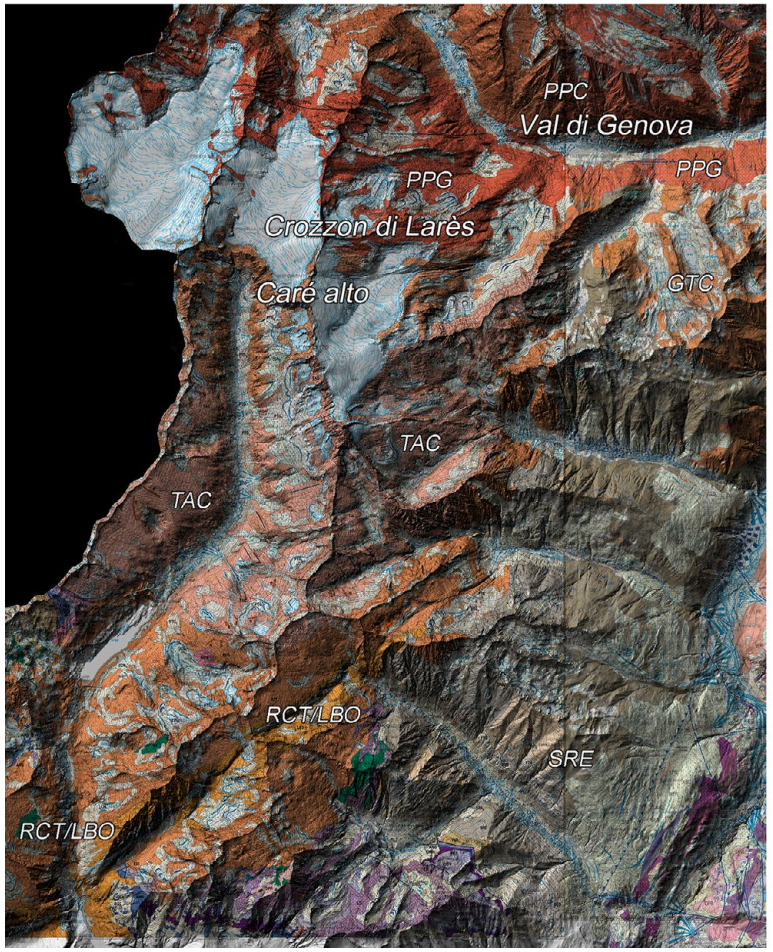

PPC — *Tonalite Presanella Centrale, coarse grained, bt-amph rich, with femic bands and concentration, Oligocene*

PPG — *Tonalite Avio - Val di Genova, fine grained, bt-rich, foliated, Upper Eocene - Oligocene*

TAC — *Tonalite Adamello Centrale, coarse grained, bt-amph rich, with magmatic foliation, femic enclaves, sometimes porphyric, Upper Eocene*

GTC — *Granodiorite-Trondhjemite Corno Alto - Sostino, coarse grained , bt-amph poor with porphyric plagioclase, Eocene*

RCT/LBO — *Tonalite Re di Castello - Leucotonalite Lago Boazzo, fine to mid grained, bt-amph rich, locally folliated, mid Eocene*

SRE — *Rendena micaschists and paragneiss with contact metamorphism, Pre - Permian*

Fig. 56 - Geological map of the Carè Alto to Val Rendena area.

Looking northwards, we can observe the mountain ranges on the left side of the Sole Valley, where the Southern Austroalpine Units crop out. In more detail, we can see the highest peaks of the Cevedale Massif, separated from the Cima Vegaia ridge by the Peio Valley. The Cevedale Massif is made up of garnet-staurolite micaschists (OMI) with intercalated orthogneiss and amphibolite in the lower part, whereas chlorite-sericite schists (OME) occur in the upper part.
In front of us, behind the Sole Valley, the Cima Vegaia ridge is visible. It is made up of kyanite-garnet gneiss with intercalated orthogneiss, serpentinite, metagabbro of the SW Ulten unit (TUG), belonging to the Tonale

DOI: 10.3301/GFT.2018.01

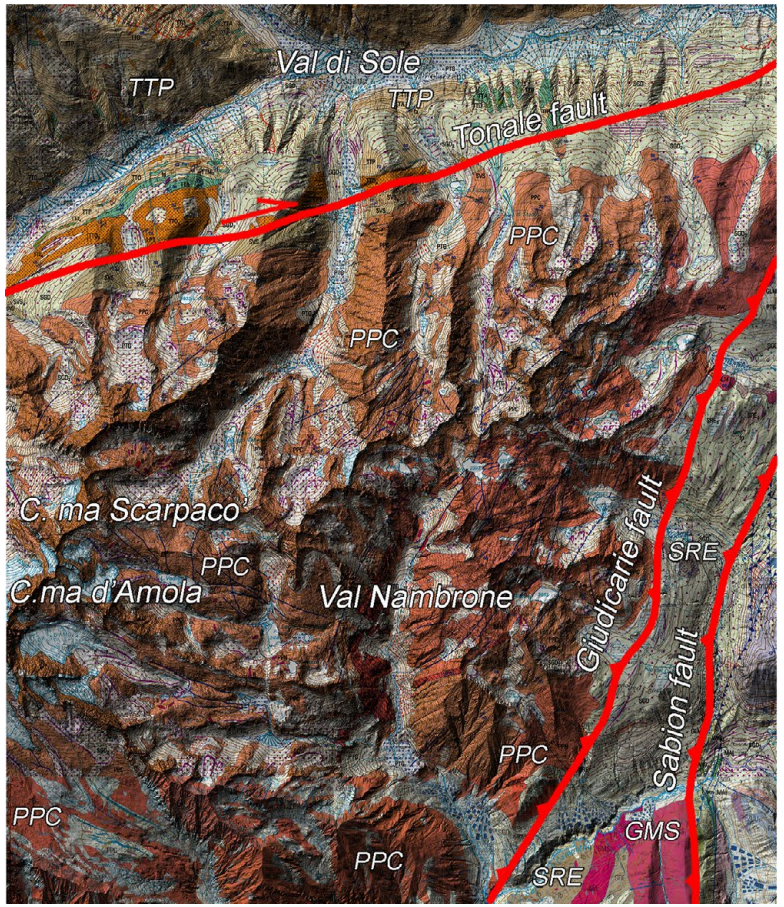

PPC — *Tonalite Presanella Centrale, coarse grained, bt-amph rich, with femic bands and concentration, Oligocene*

PPG — *Tonalite Avio - Val di Genova, fine grained, bt-rich, foliated, Upper Eocene - Oligocene*

TTP — *Tonale unit, gt - sill - + Kfeld paragneiss, with intercalation orthogneiss, amphibolite, marble, serpentinite*

SRE — *Rendena micaschists and paragneiss with contact metamorphism, Pre - Permian*

GMS — *Granodiorite Dos del Sabion - Granite of Madonna di Campiglio, coarse grained locally with gt, white mica, Permian.*

Fig. 57 - Geological map of the northern Presanella massif, from Val Meledrio to Val di Sole.

nappe. Along the right side of the Sole Valley, the Tonale fault separates the Tonale unit from the Southalpine basement (Val di Sole schists, SVS), intruded by the Northern Presanella pluton (Brack et al., 2008 and references therein).

The Tonale fault is the central segment of the Periadriatic Lineament. This fault consists of a ductile shear zone, up to 0.7 km in thickness, whose mylonites record a continuous dextral strike-slip movement during the emplacement and cooling of the Oligocene Presanella pluton. Mylonites of the Tonale fault derive from both the Southalpine schists and quartzites and the Tonale gneisses. In particular, in the Austroalpine rocks mylonites are mainly localized within a thin belt of augengneisses (Stavel gneisses; Trener, 1906; Martin et al., 1991), which

DOI: 10.3301/GFT.2018.01

may represent an upper Palaeozoic granite intruded in the Tonale gneisses. After the post-intrusive cooling, deformation continued in brittle conditions, producing a few hundred metres thick cataclastic-ultracataclastic belt (Martin et al., 1991) overprinting the previous greenschist facies mylonites.
The northern boundary of the Tonale nappe is represented by the Peio normal fault (Martin et al., 1991; Martin et al., 2009). This SE-dipping fault separates the Tonale nappe, in the hanging-wall, from the Peio unit of the Ortler-Campo nappe (staurolite-garnet schists, OMI-OME; Dal Piaz et al., 2007) at the footwall. The Peio unit consists of paragneiss, micaschist, quartzite, metabasite and marble intruded by Ordovician, Permian and Oligocene magmatic bodies (Martin and Montresor, 2008; Martin et al., 2009).
The mylonites of the Peio fault formed during the Late Cretaceous Ducan-Ela phase (Froitzheim et al., 1994). This ductile shear zone was later reactivated by contractional deformation during the Cenozoic (Martin et al., 1991; Martin et al., 2016). This event was responsible for localized thrusting along the Peio and produced a large-scale antiform affecting the Ortler-Campo nappe and the Peio mylonites. This structure is cut across by dykes of Oligocene age (32-30 Ma; Dal Piaz et al., 1988; Müller, 1998), which post-date folding.

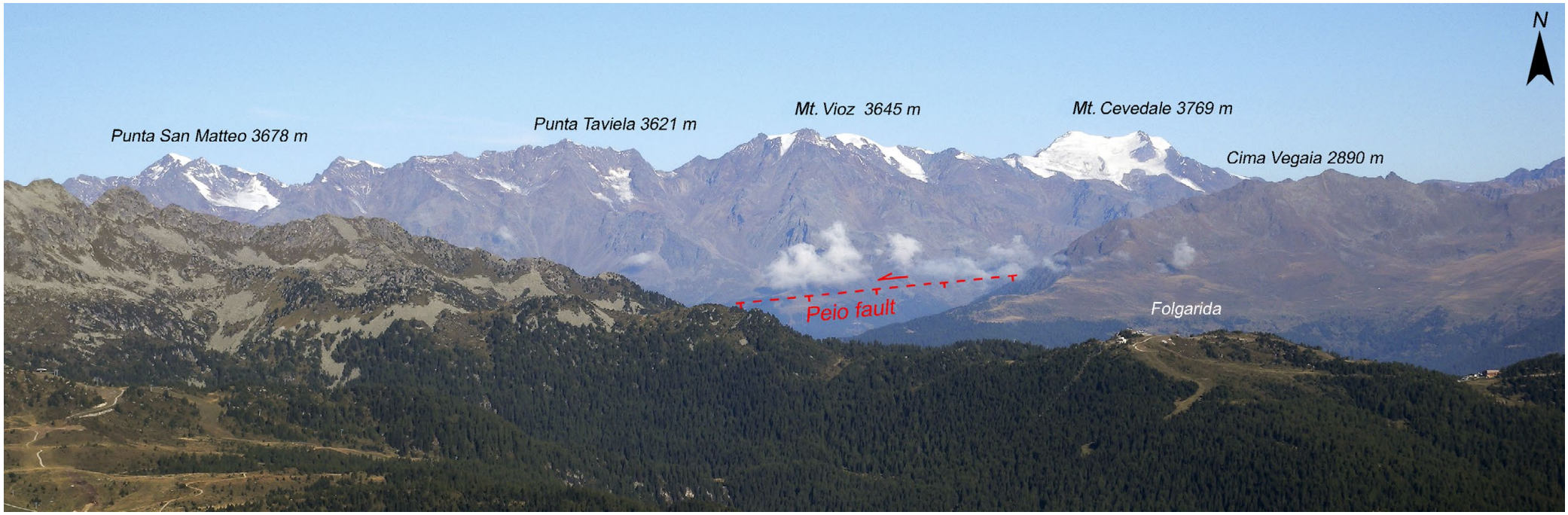

Fig. 58 - View northwards of the Cevedale Massif, Val di Peio (close to the fault), and Cima Vegaia.

DOI: 10.3301/GFT.2018.01

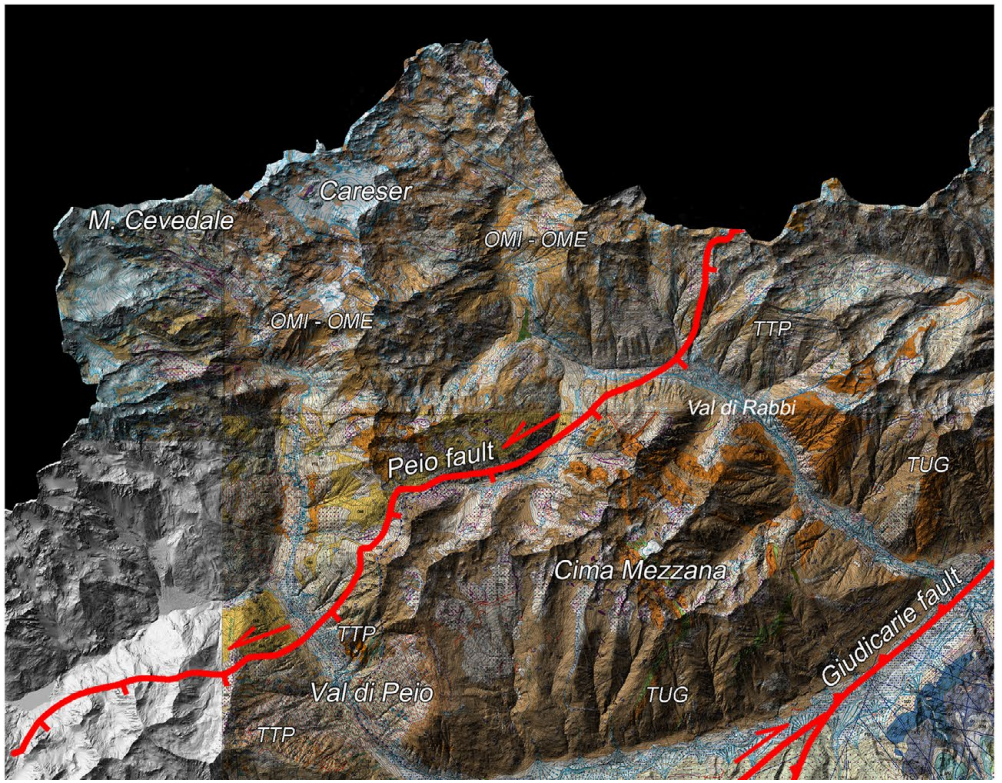

OMI - OME — *Peio unit, gt - st - bt micaschists, mid grained with intercalated orthogneiss, amphibolite, marble, serpentinite*

TTP — *Tonale unit, gt - sill - + Kfeld paragneiss, with intercalation orthogneiss, amphibolite, marble, serpentinite*

TUG — *Ulten unit, gt - ky - bt paragneiss grading to migmatite associated with amphibolite*

Fig. 59 - Geological map of the Austroalpine Ortler-Campo and Tonale, cropping out in the Val di Peio and Val di Sole.

STOP 2.3: The puzzle of the Monte Spinale klippe and its Quaternary evolution

The Monte Spinale is a relief near Madonna di Campiglio, in the western portion of the Brenta Dolomites. The main tectonic structures of this area of the Southalpine chain are a set of N-trending sinistral to transpressive faults, which correspond to inherited normal faults related to the Norian-Early Jurassic continental rifting, later inverted during Miocene post-collisional convergence (Neoalpine events; Fig. 60). South of Monte Spinale, a system of E- and ENE-trending thrusts acting as frontal ramp (Cima Tosa thrust) is also present. Since the Early Miocene, the structures propagated toward SE from the South Giudicarie fault to the Venetian plain, where the Southalpine belt is still experiencing contractional deformation.
The Mesozoic succession of the Brenta Massif and Monte Spinale ridge is formed by a thick pile of peritidal limestones, which include Norian dolostones (Dolomia Principale), with local intraplatform basin limestones

DOI: 10.3301/GFT.2018.01

(Calcare di Zorzino) and Rhaetian (Calcare di Zu) to Lower Jurassic limestones (Calcari Grigi Group), for a total thickness of about 2500 meters.

Two geological features make peculiar the Monte Spinale area: (i) the presence of a deformed body of Quaternary breccias on the top; (ii) the klippe discovered during the last CARG surveys (the project aims to realize the new Geological Map of Italy at 1:50,000 scale) (Fig. 61).

The Monte Spinale is bounded by NNW-SSE and N-S trending faults of regional importance (Fig. 62). The western boundary consists of two nearly parallel faults: (i) the South Giudicarie fault, a major sinistral transpressive fault where the Eocene-Oligocene Adamello-Presanella plutons overthrust the Southalpine crystalline basement; (ii) the Sabion transpressive fault along which the basement, intruded by the Permian Doss del Sabion granodiorite, overthrusts the entire Mesozoic succession (up to the Upper Cretaceous flysch of the Val d'Agola fm.). The eastern boundary is represented by the W-dipping synrift system of the Vedretta dei Camosci normal fault (Figs. 61 and 62).

The top of Monte Spinale ridge (about 2000 m high) is nearly flat and it is formed by nearly flat-lying limestones belonging to Calcare di Zu (Tremalzo mb., locally Grostè mb.) and Monte Zugna fm., which thrust onto the Calcari Grigi Group rocks (Monte Zugna and Loppio Oolitic Limestone fms.). The thrust plane is nearly horizontal in its southern part, whereas it dips eastward in the northern and western Spinale area (Fig. 63). The structure is bounded by the Sabion

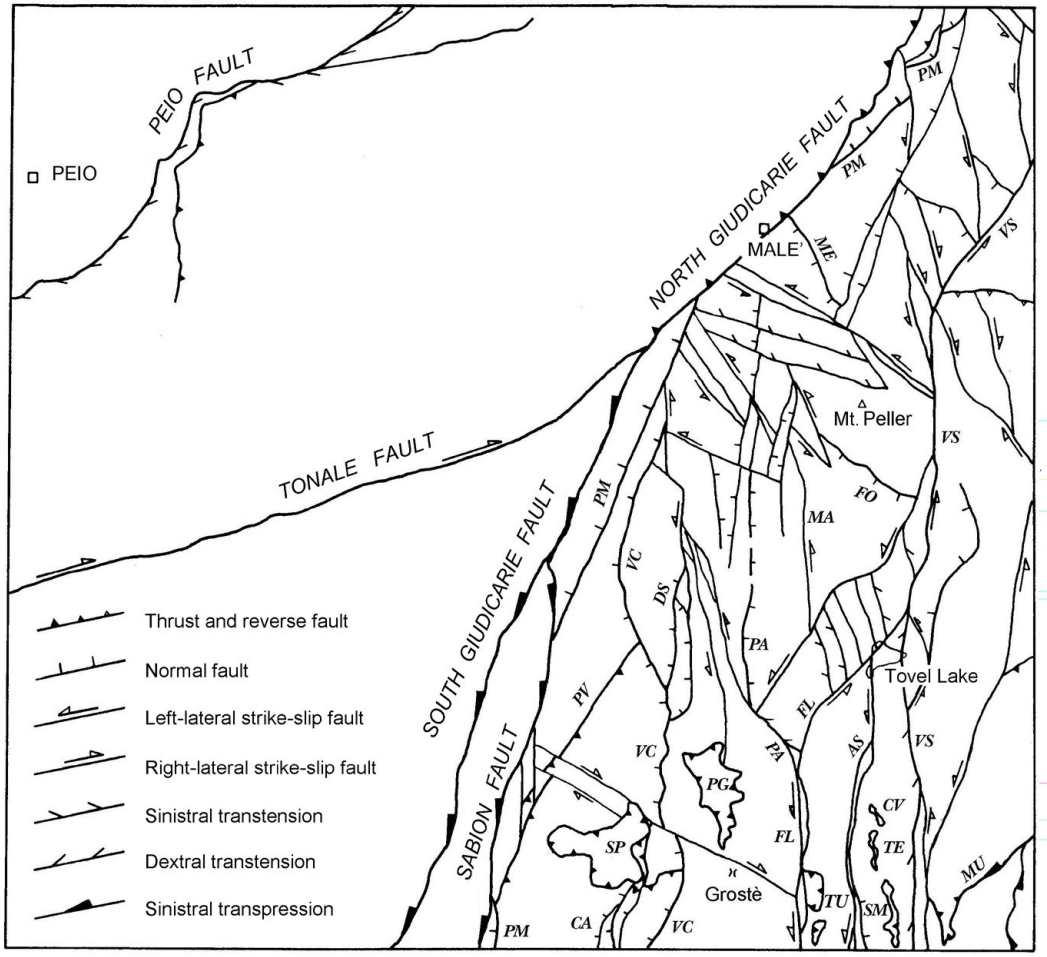

Fig. 60 - Tectonic scheme of the northern Brenta Dolomites. PG: Pietra Grande klippe; PM: Pala dei Mughi line; PV: Pozza Vecchia reverse fault; SP: Spinale klippe; VC: Vedretta dei Camosci fault (modified from Dal Piaz et al., 2007; courtesy of the Geological Survey of the Autonomous Province of Trento).

DOI: 10.3301/GFT.2018.01

and Vedretta dei Camosci lines. The erosion isolated the thrust hanging-wall as a klippe in the Monte Spinale ridge. The southward-dipping thrust ramp, marked by fault breccias, is partly eroded but still outcrops in the southeastern side of Monte Spinale. This observation indicates that the klippe is the relict of a north-verging thrust sheet and that the Vedretta dei Camosci fault system acted as transfer fault, dissecting the thrust ramp.

Klippe structures are common in the Northern Brenta Dolomites (i.e., Pietra Grande, Turrion, and Campa Massif klippen), all interpreted as back-verging intercutaneous décollements along the Calcare di Zu, within the hanging-wall of the Cima Tosa - Passo Clamer south-verging thrusts (Castellarin et al., 1993; Dal Piaz et al., 2007). Similarly, the Monte Spinale klippe is interpreted as a north-verging thrust sheet due to the presence of the Vallon blind thrust ramp, located 10 km southward. The décollement horizon is here represented by black shales and limestones of the Calcare di Zu (Grosté mb.).

The involvement of basement rocks along the Sabion line and the aforementioned klippe near the South Giudicarie fault can be referred to Chattian - Tortonian Neoalpine compressional events (Insubric and Valsugana events; Castellarin et al., 2006). Some previous authors (Schwinner, 1912; Trevisan, 1939) have interpreted the rocks of the klippe as being part of the Monte Spinale breccias (see below).

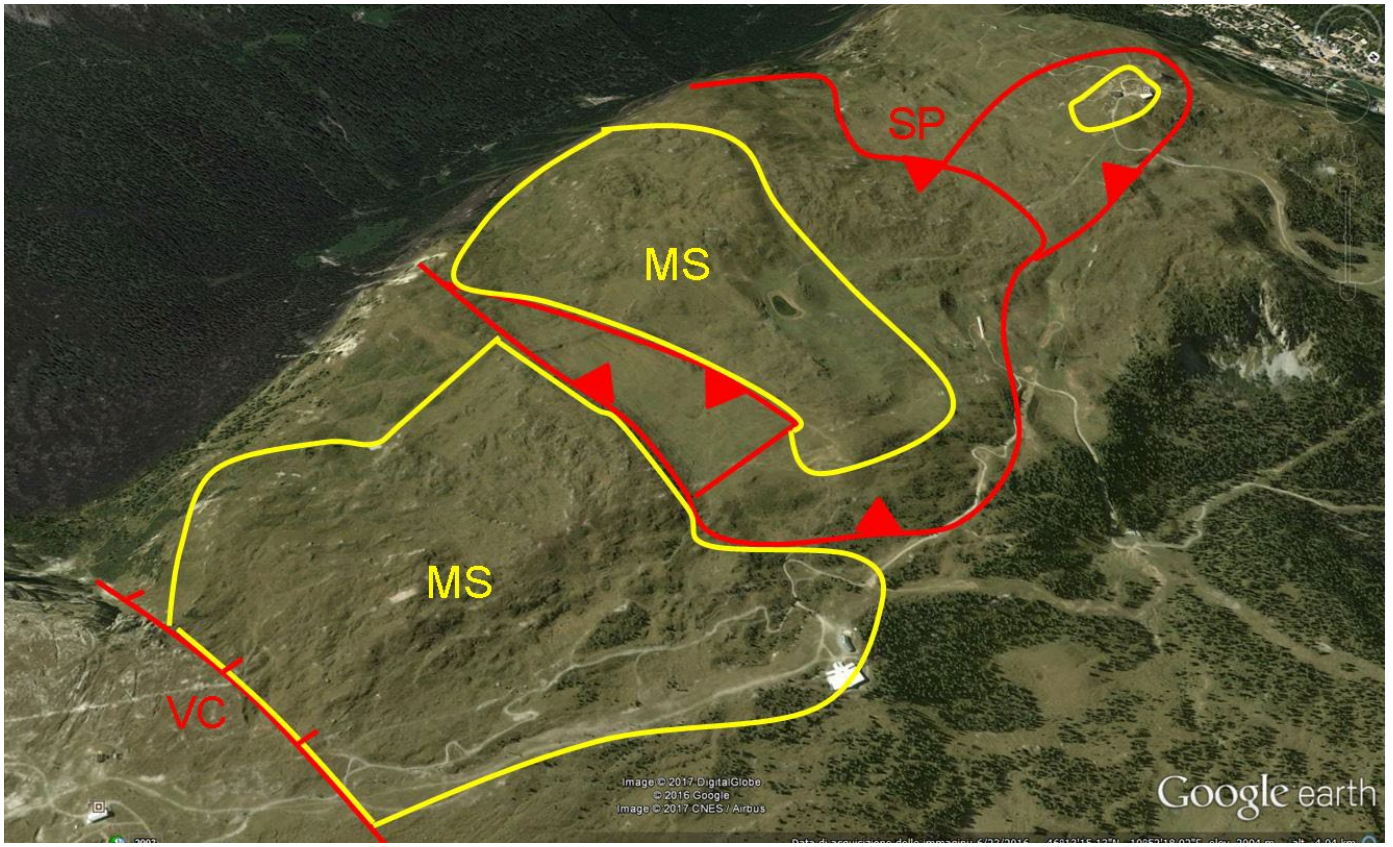

Fig. 61 - Panoramic view and geological scheme of Monte Spinale from Pietra Grande (base map from Google Earth). The Monte Spinale breccias (MS), Spinale klippe (SP) and Vedretta dei Camosci normal fault (VC) are shown.

DOI: 10.3301/GFT.2018.01

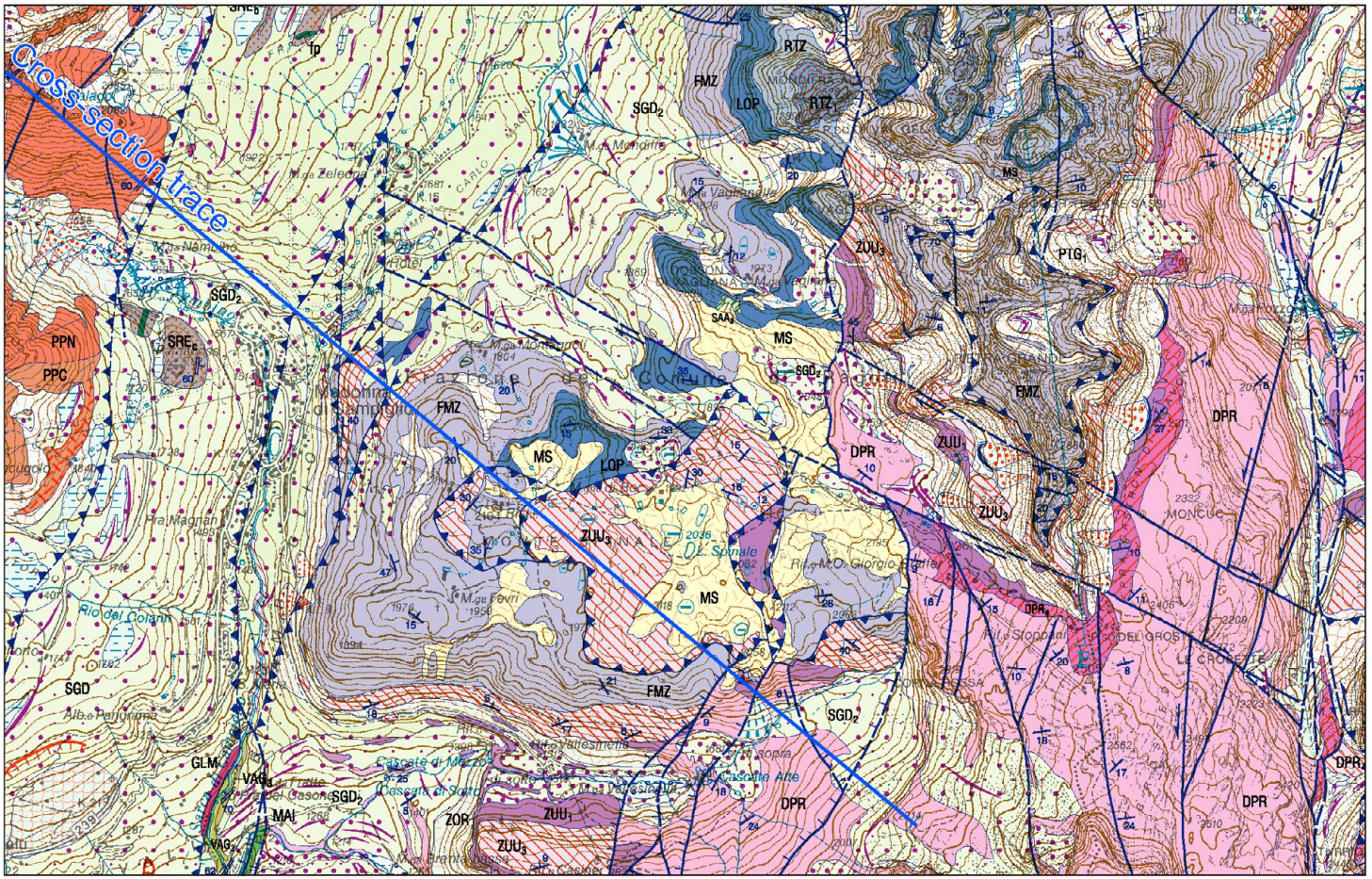

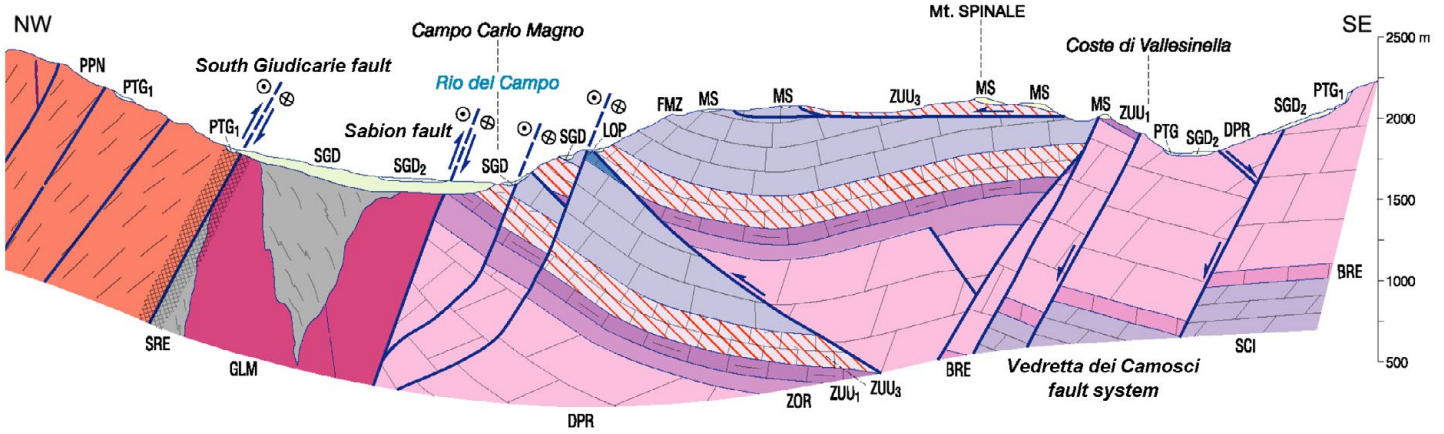

Fig. 62 - Geological map (upper) and cross-section of Monte Spinale (lower). Geological formations: SRE Rendena schists (pre-Permian), GLM Sabion granite (Permian), SCI dolomia dello Sciliar (Ladinian), BRE Breno fm. (Ladinian-Carnian), DPR Dolomia Principale (Carnian-Norian), ZOR Calcare di Zorzino (Norian), ZUU_1 Calcare di Zu Grostè mb. (Rhaetian), ZUU_3 Calcare di Zu Tremalzo mb. (Rhaetian), FMZ Monte Zugna fm. (Sinemurian), LOP Loppio Oolitic Limestone (Sinemurian), RTZ Rotzo fm. (Pliensbachian), MAI Maiolica (Lower Cretaceous), VAG Val d'Agola (Upper Cretaceous), PPN, PPC Presanella pluton (Oligocene), MS Monte Spinale breccias (Plio-Pleistocene); (modified from Dal Piaz et al., 2007; courtesy of the Geological Survey of the Autonomous Province of Trento).

DOI: 10.3301/GFT.2018.01

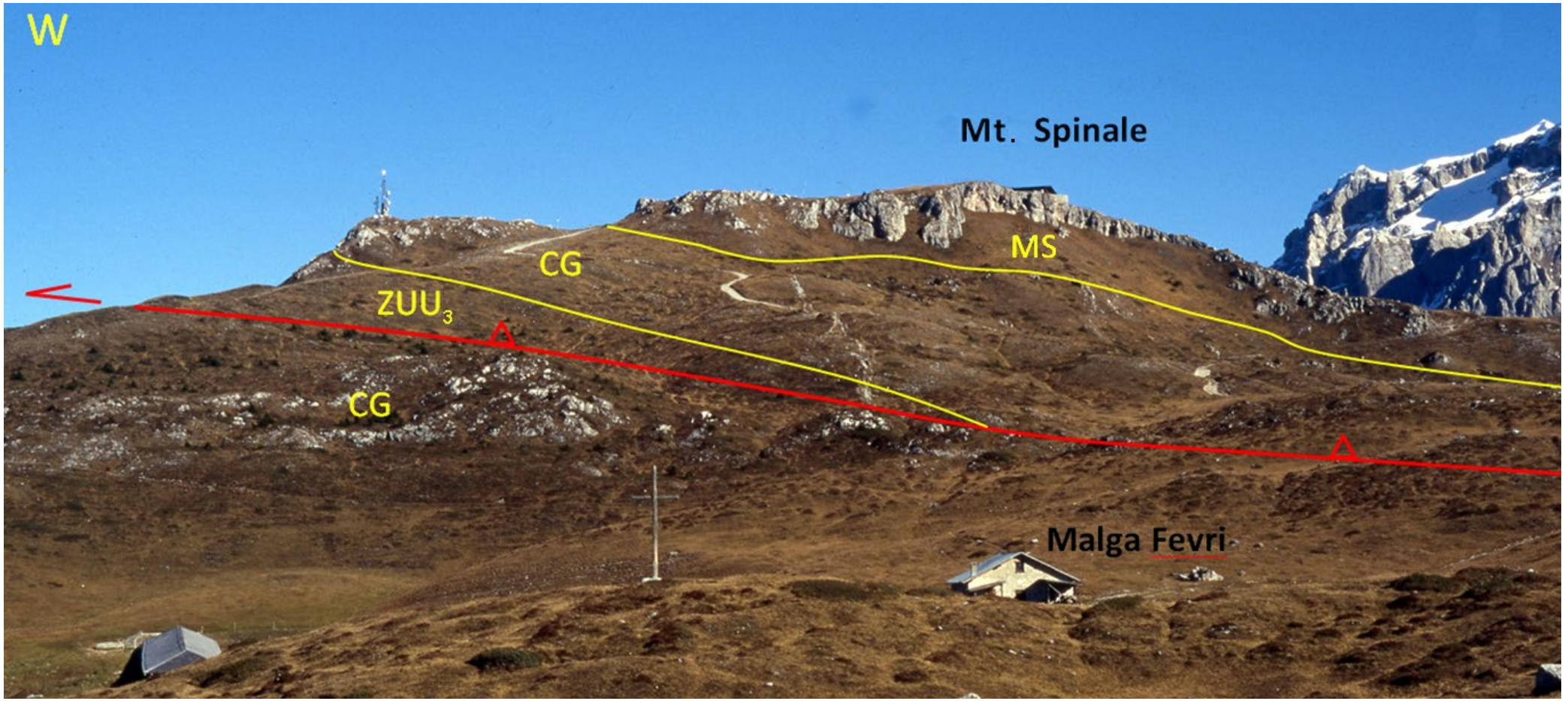

Fig. 63 - The reactivated west-verging thrust at the Monte Spinale top. The Monte Spinale breccias (MS) are east-dipping and similarly deformed.

The Monte Spinale breccias are a body, locally up to 50 m in thickness, of strongly cemented breccias composed of eterometric, angular and subangular fragments (mm to dm, locally up to m in diameter), well bedded and sorted, derived from the erosion of sedimentary rocks cropping out in the surrounding areas: Dolomia Principale, Calcare di Zu, Monte Zugna, and Loppio Oolitic Limestone formations.
Two types of breccias are present. In the eastern area, they consist of eterometric angular fragments (cm to m) hard cemented, without matrix and rich of voids. These breccias are clinostratified, with clinoforms dipping in different directions, and are interpreted as talus deposits deformed by karst sinking.

DOI: 10.3301/GFT.2018.01

In the western area and near the Spinale lake, breccias do not show voids but are characterized by a light brown calcareous abundant matrix, and contain clasts of Scaglia Rossa. These latter probably derive from completely dismantled netpunian dykes, which are still observable in the southwestern sector of the Brenta Massif (Castellarin, 1972; Castellarin et al., 2005a). This breccia is probably related to old debris flow deposits sourcing from the Grostè area. In general, the Monte Spinale breccias cover an erosional surface and are covered by glacial deposits related to the Last Glacial Maximum.
Many interpretations of these breccias were suggested by different authors. Schwinner (1912) correlated them to big rockslides from the Pietra Grande summit, mixed with talus. Wiebols (1938) referred the cropping out rocks to local debris and talus, while Trevisan (1939) to "marocche". We interpret these breccias to old overlapping debris flow and talus deposits coming from the reliefs located to the east (Pietra Grande and Grostè areas).
The age of the Monte Spinale breccias is unknown, but they are supposed to be older than the present-day topography and settled before the valley incision (Vallesinella and Val Meledrio). Assuming an erosional rate of 0.3-0.4 mm/year, we estimate a minimum age of about 2 My, which corresponds to a vertical erosion of 500-600 m along the Monte Spinale slopes.
The breccia covering the top of Monte Spinale is deformed by two tectonic events, a first E-W trending shortening, followed by WNW-directed extension.
The Monte Spinale klippe was reactivated by an E-W trending compression, documented by local indications of westward vergence close to the Monte Spinale summit, where the thrust plane dips eastward. The Monte Spinale breccias are also involved in this deformation, showing an eastward dip parallel to the basal décollement surface of the klippe. The Pozza Vecchia line, a west-verging reverse fault cutting the western Monte Spinale slope, can be referred to the same event. In general, these out-of-sequence structures can be related to the late stages of the so-called Adriatic event of Messinian to Quaternary age (Castellarin et al., 2006).
The more recent tectonic pulse is an extensional event documented by reactivations of the Vedretta dei Camosci fault as a normal fault, and other minor structures in the Monte Spinale breccias. Along this fault, breccias are tilted (dipping toward the west) and dragged in the hanging-wall by fault slip, consistent with a WNW-trending extensional axis.

Stop 2.3.1: Thick palaeosoils (46.2185 °N, 10.8889 °E)

Near Rifugio Graffer, the top of the Dolomia Principale crops out. This formation is about 1300 thick and makes up the backbone of the central Brenta Massif. Here, the peculiar facies of Malga Flavona mb. testifies to a long period of subaerial exposure of the carbonate platform. Three facies are present: (i) thick paleosoil beds

DOI: 10.3301/GFT.2018.01

(Fig. 64a) testifying to this long period of subaerial exposure; (ii) a horizon of white breccias, related to tidal channels (Fig. 64b), with angular fragments of Dolomia Principale stromatolitic layers; (iii) red breccias (Fig. 64c) related to sea rising, leading to the Calcare di Zu deposition. The Norian structural high was bordered by N-S faults related to Mesozoic rifting.

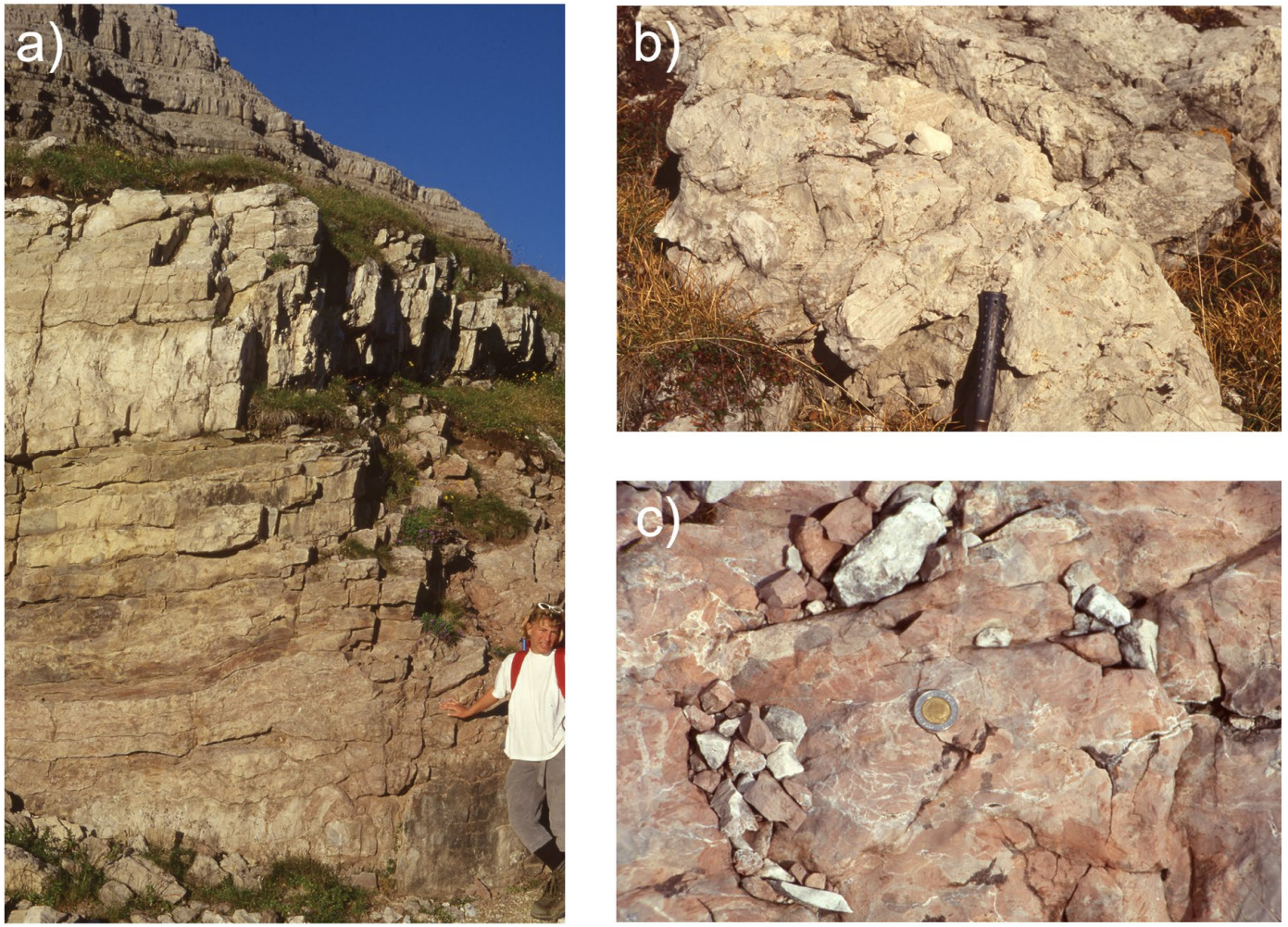

Fig. 64 - Palaeosoils (a) and breccias (b-c) near Rifugio Graffer.

Stop 2.3.2: The dragged Monte Spinale breccias in the Vedretta dei Camosci fault hanging-wall (46.2179 °N, 10.8861 °E)

The well-bedded Spinale breccias in the hanging-wall of the Vedretta dei Camosci normal fault are tilted of about 10-40° (Fig. 65). The fault footwall is made of Dolomia Principale (Fig. 66).
The breccias are strongly cemented with no matrix (Fig. 67). They are related to talus deposits, but they are dipping in different directions and also deformed (probably by karst sinking).

Stop 2.3.3: Scaglia Rossa megablocks in the Monte Spinale breccias (46.2202 °N, 10.8665 °E)

The Lago Spinale lies on a Scaglia Rossa block (Fig. 68) coming from neptunian presently eroded dykes (Fig. 69a). It is supposed that they were originally located in the Grostè Pass area, where breccias include fragments

DOI: 10.3301/GFT.2018.01

of Scaglia Rossa and an abundant light brown matrix related to debris flow deposits can be observed (Fig. 69b).
The W-dipping Monte Spinale breccias (onlapping Calcare di Zu) are clinostratified (Fig. 69c-d) but the reliefs that produced the debris are today totally eroded.

Fig. 65 - The Monte Spinale tilted breccias.

Stop 2.3.4: The Monte Spinale thrust (46.2240 °N, 10.8753 °E)

The Monte Spinale thrust is an intercutaneous wedge related to the Vallon blind structure (Fig. 70). This décollement surface developed within the black shales of the Calcare di Zu and is outlined by cataclastic fault rocks. The klippe, which is north-verging and shows recent reactivation with westward vergence, involves the Spinale breccias which at the Monte Spinale summit are fractured and tectonized (Fig. 71).

DOI: 10.3301/GFT.2018.01

Fig. 66 - The Vedretta dei Camosci normal fault, separating the Dolomia Principale (on the left) from the Monte Spinale breccias (on the right).

Fig. 67 - The typical aspect of the Monte Spinale breccias.

Fig. 68 - The Lago Spinale on Scaglia Rossa.

DOI: 10.3301/GFT.2018.01

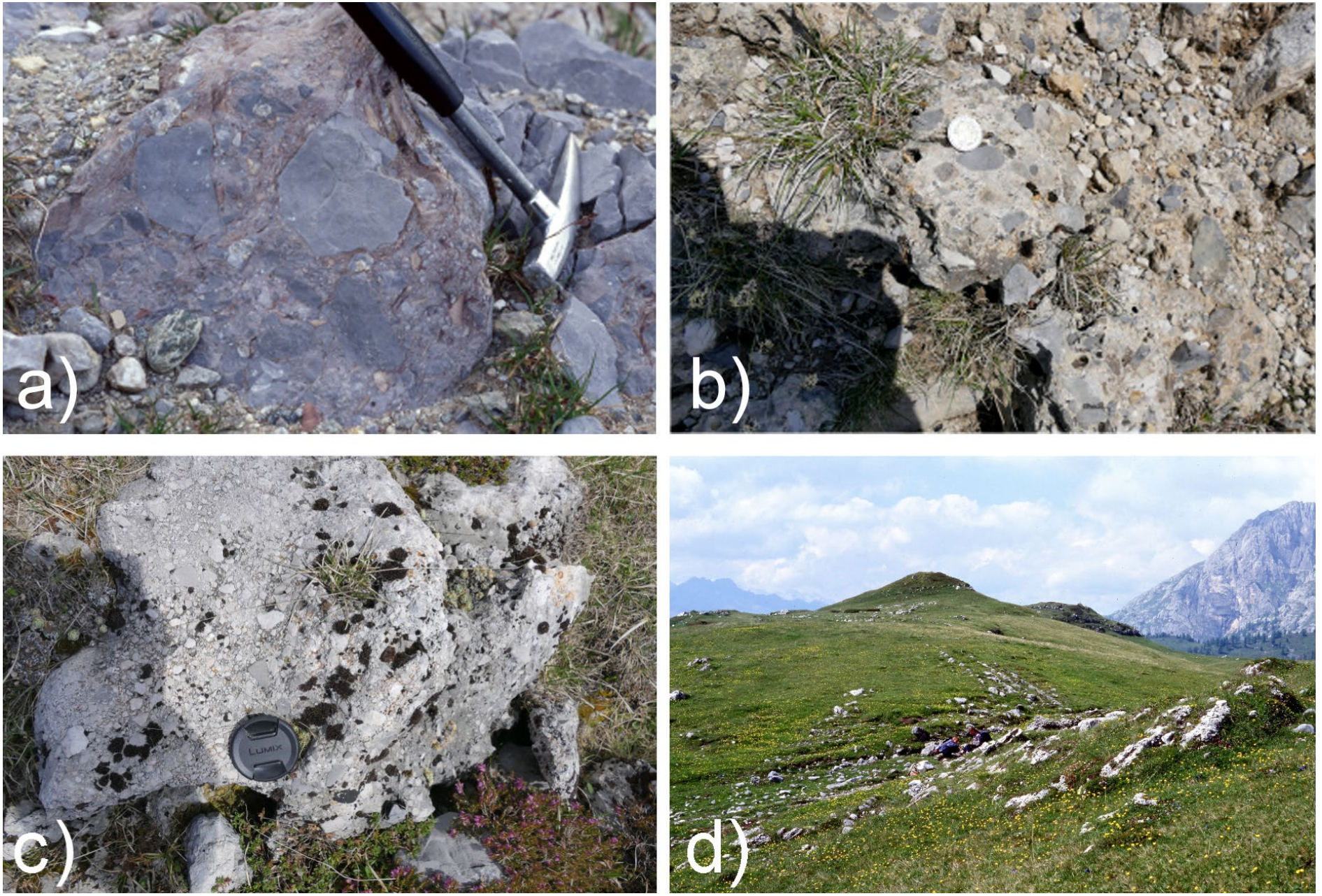

Fig. 69 - Eroded block coming from a neptunian dyke (a) and breccias (b) near Lago Spinale. A typical outcrop of the Monte Spinale breccias (c), which show evident clinostratification (d).

DOI: 10.3301/GFT.2018.01

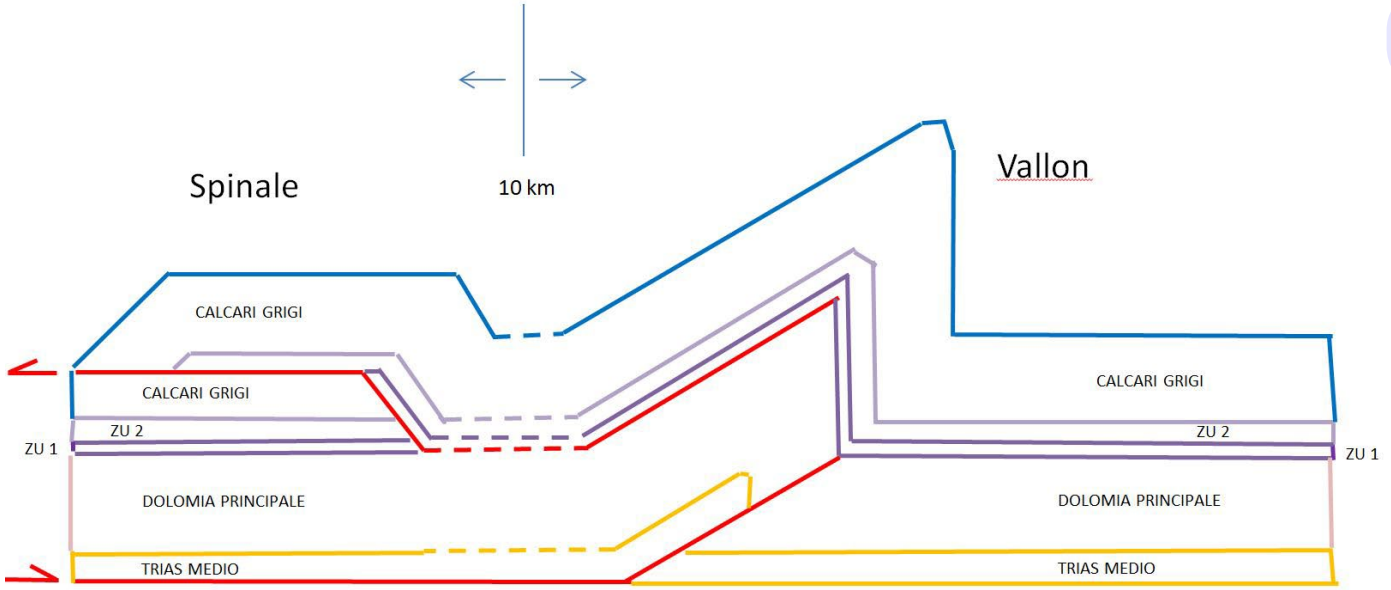

Fig. 70 - Schematic tectonic model of the Monte Spinale thrust.

ACKNOWLEDGEMENTS

The authors gratefully acknowledge the Geological Survey of the Autonomous Province of Trento and all the supporting institutions and participants of the 2017 GIGS Meeting. Thanks are also due to M. Mattei, an anonymous reviewer and to the Editor in Chief A. Zanchi, for their helpful comments and suggestions.

Fig. 71 - Tectonized Monte Spinale breccias near the Monte Spinale summit.

DOI: 10.3301/GFT.2018.01

References

Abele G. (1974) - Bergstürze in den Alpen. In: Ihre Verbreitung, Morphologie und Folgeerscheinungen. Wiss. Alpenvereinshefte, 25, p. 230. Munchen.

Alighieri D. (1314) - Divina Commedia, Inferno, XII, 4-9.

Avanzini M., Piubelli D., Mietto P., Roghi G., Romano R., Masetti D. (2006) - Lower Jurassic (Hettangian-Sinemurian) dinosaurs track megasites, southern Alps, northern Italy. New Mexico Museum Nat. Hist. Sci. Bull., 37, 207-216.

Avanzini M., Bargossi G.M., Borsato A., Selli L. (2010) - Note illustrative della Carta Geologica d'Italia alla scala 1:50.000, Foglio n. 060, Trento, 244 pp.

Barbieri G. and Grandesso P. (2007) - Note illustrative della Carta Geologica d'Italia alla scala 1:50.000, Foglio n. 082, Asiago, 135 pp.

Bassetti M. (1997) - Studio geomorfologico sulle "Marocche" di Dro (Trentino occidentale). Studi Trent. Sci. Nat. Acta Geol., 72, 5-30.

Bini A., Cita M.B, Gaetani M. (1978) - Southern Alpine lakes – hypothesis of an erosional origin related to the Messinian entrenchment. Mar. Geol., 27, 271-288.

Boore D.M., Stewart J.P., Seyhan E., Atkinson G.M. (2014) - NGA-West2 equations for predicting PGA, PGV, and 5% damped PSA for shallow crustal earthquakes. Earthq. Spectra, 30, 1057-1085.

Borgatti L. and Soldati M. (2010) - Landslides as a geomorphological proxy for climate change: a record from the Dolomites (northern Italy). Geomorphology, 120, 56-64.

Brack P., Dal Piaz G.V., Baroni C., Carton A., Nardin M., Pellegrini G.B., Pennacchioni G. (2008) - Note illustrative della Carta Geologica d'Italia alla scala 1:50.000, Foglio n. 058, Monte Adamello, 140 pp.

Burrato P.F., Poli M.E., Vannoli P., Zanferrari A., Basili R., Galadini F. (2008) - Sources of M_w 5+ earthquakes in northeastern Italy and western Slovenia: an updated view based on geological and seismological evidence. Tectonophysics, 453, 157-176.

Caputo R. (1996) - The polyphase tectonics of Eastern Dolomites, Italy. Mem. Sci. Geol. Padova, 48, 93-106.

Castellarin A. (1972) - Evoluzione paleotettonica sinsedimentaria del limite tra "piattaforma veneta" e "bacino lombardo", a Nord di Riva del Garda. Giorn. Geol., 2, 38/1, 11-212.

Castellarin A., Piccioni S., Prosser G., Sanguinetti E., Sartori R., Selli L. (1993) - Mesozoic continental rifting and Neogene inversion along the South Giudicarie Line (Northwest Brenta Dolomites), Mem. Soc. Geol. It., 49, 125-144.

Castellarin A., Dal Piaz G.V., Picotti V., Selli L., Cantelli L., Martin S., Montresor L., Rigatti G., Prosser G., Bollettinari G., Pellegrini G.B., Carton A., Nardin M. (2005a) - Note illustrative della Carta Geologica d'Italia alla scala 1:50.000, Foglio n. 059, Tione di Trento, 159 pp.

Castellarin A., Picotti V., Cantelli L., Claps M., Trombetta L., Selli L., Carton A., Borsato A., Daminato F., Nardin M., Santuliana E., Veronesi L., Bollettinari G. (2005b) - Note illustrative della Carta Geologica d'Italia alla scala 1:50.000, Foglio n. 080, Riva del Garda, 145 pp.

Castellarin A., Vai G.B., Cantelli L. (2006) - The Alpine evolution of the Southern Alps around the Giudicarie faults: a Late Cretaceous to Early Eocene transfer zone. Tectonophysics, 414, 203-223.

Dal Piaz G.V., Del Moro A., Martin S., Venturelli G. (1988) - Post-collisional magmatism in the Ortler-Cevedale Massif (Northern Italy). Jahrb. Geol. Bundesanstalt, 131, 533-551.

DOI: 10.3301/GFT.2018.01

Dal Piaz G.V., Castellarin A., Martin S., Selli L., Carton A., Pellegrini G.B., Casolari E., Daminato F., Montresor L., Picotti V., Prosser G., Santuliana E., Cantelli L. (2007) - Note illustrative della Carta Geologica d'Italia alla scala 1:50.000, Foglio n. 042, Malé, 143 pp.

DISS Working Group (2018) - Database of Individual Seismogenic Sources (DISS), Version 3.2.1: A compilation of potential sources for earthquakes larger than M 5.5 in Italy and surrounding areas. http://diss.rm.ingv.it/diss/, Istituto Nazionale di Geofisica e Vulcanologia; DOI:10.6092/INGV.IT-DISS3.2.1.

Doglioni C. and Bosellini A. (1987) - Eoalpine and mesoalpine tectonics in the Southern Alps. Geol. Rundsch., 76, 735-754.

Felber M., Veronese L., Cocco S., Frei W., Nardin M., Oppizzi P., Santuliana E., Violanti D. (1998) - Indagini sismiche e geognostiche nelle valli del Trentino meridionale (Val d'Adige, Valsugana, Valle del Sarca, Valle del Chiese), Italia. Studi Trent. Sci. Nat. Acta Geol., 75, 3-52.

Fondriest M., Smith S.A.F., Di Toro G., Zampieri D., Mittempergher S. (2012) - Fault Zone Structure and Seismic Slip Localization in Dolostones, an example from the Southern Alps, Italy. J. Struct. Geol., 45, 52-67.

Franceschi M., Massironi M., Franceschi P., Picotti V. (2014a) - Spatial analysis of thickness variability applied to an Early Jurassic Carbonate Platform in the central Southern Alps (Italy): a tool to unravel synsedimentary faulting. Terra Nova, 26, 239-246.

Franceschi M., Dal Corso J., Posenato R., Roghi G., Masetti D., Jenkyns H.C. (2014b) - Early Pliensbachian (Early Jurassic) C-isotope perturbation and the diffusion of the Lithiotis Fauna: insights from the western Tethys. Palaeogeogr., Palaeoclim., Palaeoecol., 410, 255-263.

Frisia S., Borsato A., Richards D.A., Miorandi R., Davanzo S. (2005) - Variazioni climatiche ed eventi sismici negli ultimi 4500 anni nel Trentino meridionale da una stalagmite della Cogola Grande di Giazzera. Studi Trent. Sci. Nat. Acta Geol., 82, 205-223.

Froitzheim N., Schmid S.M., Conti P. (1994) - Repeated change from crustal shortening to orogen-parallel extension in the Austroalpine units of Graubünden. Eclogae geol. Helv., 87, 559-612.

Galadini F., Poli M.E., Zanferrari A. (2005) - Seismogenic sources potentially responsible for earthquakes with M>6 in the Eastern Southern Alps (Thiene-Udine sector, NE Italy). Geophys. J. Int., 161, 739-762.

Gudmundsson A. (2004) - Effects of Young's modulus on fault displacement. C. R. Geoscience, 336, 85-92.

Guidoboni E. and Comastri A. (2005) - Catalogue of Earthquakes and Tsunamis in the Mediterranean Area from the 11th to the 15th Century. Istituto Nazionale di Geofisica e Vulcanologia, Storia Geofisica Ambiente, Bologna, Italy.

Guidoboni E., Ferrari G., Mariotti D., Comastri A., Tarabusi G., Valensise G. (2007) - CFTI4Med, Catalogue of Strong Earthquakes in Italy (461 B.C.-1997) and Mediterranean Area (760 B.C.-1500). Istituto Nazionale di Geofisica e Vulcanologia, Storia Geofisica Ambiente, Bologna, Italy. Available at: http://storing.ingv.it/ cfti4med/.

Guo D., He C., Xu C., Hamada M. (2015) - Analysis of the relations between slope failure distribution and seismic ground motion during the 2008 Wenchuan earthquake. Soil Dyn. Earthq. Eng., 72, 99-107.

Heap M.J., Faulkner D.R., Meredith P.G., Vinciguerra S. (2010) - Elastic moduli evolution and accompanying stress changes with increasing crack damage: implication for stress changes around fault zones and volcanoes during deformation. Geophys. J. Int., 183, 225-236.

DOI: 10.3301/GFT.2018.01

Hungr O., Evans S.G., Bovis M.J., Hutchinson J.N. (2001) - A review of the classification of landslides of the flow type. Environ. Eng. Geosci., 7, 221-238.

Ivy-Ochs S., Martin S., Campedel P., Hippe K., Vockenhuber C., Carugati G., Rigo M., Pasqual D., Viganò A. (2017a) - Geomorphology and age of large rock avalanches in Trentino (Italy): Castelpietra. In: Mikoš M., Vilímek V., Yin Y., Sassa K. (Eds.) Advancing Culture of Living with Landslides. WLF 2017. Springer, Cham, 347-353.

Ivy-Ochs S., Martin S., Campedel P., Hippe K., Alfimov V., Vockenhuber C., Andreotti E., Carugati G., Pasqual D., Rigo M., Viganò A. (2017b) - Geomorphology and age of the Marocche di Dro rock avalanches (Trentino, Italy). Quat. Sci. Rev., 169, 188-205.

Kissling E., Schmid S.M., Lippitsch R., Ansorge J., Fügenschuh B. (2006) - Lithosphere structure and tectonic evolution of the Alpine arc: new evidence from high-resolution teleseismic tomography. In: Gee D.G. and Stephenson R.A. (Eds.) European lithosphere dynamics. Geol. Soc., London, Memoirs 32, 129-145.

Maerten L. and Maerten F. (2006) - Chronologic modelling of faulted and fractured reservoirs using geomechanically based restoration: Technique and industry applications. AAPG Bulletin, 90(8), 1201-1226.

Martin S. and Montresor L. (2008) - Note Illustrative della Carta Geologica della Provincia di Trento alla scala 1:25.000, Tavola n. 042 IV, Peio, 77 pp.

Martin S., Prosser G., Santini L. (1991) - Alpine deformation along the Periadriatic lineament in the Italian Eastern Alps. Ann. Tecton., 5, 118-140.

Martin S., Zattin M., Del Moro A., Macera P. (1996) - Chronologic constraints for the evolution of the Giudicarie belt (Eastern Alps, NE Italy). Ann. Tecton., 10, 60-79.

Martin S., Bigazzi G., Zattin M., Viola G., Balestrieri M.L. (1998) - Neogenic kinematics of the Giudicarie Fault (Central-Eastern Alps, Italy): new apatite fission-track data. Terra Nova, 10, 217-221.

Martin S., Montresor L., Mair V., Pellegrini G.B., Avanzini M., Fellin G., Gambillara R., Tumiati S., Santuliana E., Monopoli B., Gaspari D., Sapigni M. (2009) - Note illustrative della Carta Geologica d'Italia alla scala 1:50.000, Foglio n. 025, Rabbi, 187 pp.

Martin S., Campedel P., Ivy-Ochs S., Viganò A., Alfimov V., Vockenhuber C., Andreotti E., Carugati G., Pasqual D., Rigo M. (2014) - Lavini di Marco (Trentino, Italy): ^{36}Cl exposure dating of a polyphase rock avalanche. Quat. Geochron., 19, 106-116.

Martin S., Godard G., Laurenzi M.A., Viganò A. (2016) - Pseudotachylytes of the Tonale nappe (Italian Alps): petrogenesis, ^{40}Ar-^{39}Ar geochronology and tectonic implications. It. J. Geosci., 135, 217-235.

Martinelli M., Franceschi M., Massironi M., Rizzi A., Salvetti G., Zampieri D. (2017) - An extensional syn-sedimentary structure in the Early Jurassic Trento Platform (Southern Alps, Italy) as analogue of potential hydrocarbon reservoirs developing in rifting-affected carbonate platforms. Mar. Petrol. Geol., 79, 360-371.

Masetti D., Fantoni R., Romano R., Sartorio D., Trevisani E. (2012) - Tectonostratigraphic evolution of the Jurassic extensional basins of the eastern and southern Alps and Adriatic foreland based on an integrated study of surface and subsurface data. Am. Ass. Petrol. Geol. Bull., 96, 2065-2089.

McClay K.R. (1990) - Extensional fault systems in sedimentary basins: A review of analogue model studies. Mar. Petrol. Geol., 7, 206-233.

DOI: 10.3301/GFT.2018.01

Müller W. (1998) - Isotope dating of deformation using microsampling techniques: the evolution of the Periadriatic fault system (Alps). ETH Diss., Zürich, 135 pp.

Orombelli G. and Sauro U. (1988) - I Lavini di Marco: un gruppo di frane oloceniche nel contesto morfotettonico dell'alta val Lagarina (Trentino). Suppl. Geogr. Fis. Dinam. Quat. 1, 107-116.

Passchier C.W. and Platt J.P. (2017) - Shear zone junctions: of zippers and freeways. J. Struct. Geol., 95, 188-202.

Picotti V., Prosser G., Castellarin A. (1995) - Structures and kinematics of the Giudicarie - Val Trompia fold and thrust belt (Central Southern Alps, Northern Italy). Mem. Sci. Geol., 47, 95-109.

Pola M., Ricciato A., Fantoni R., Fabbri P., Zampieri D. (2014) - Architecture of the western margin of the North Adriatic foreland: the Schio-Vicenza fault system. Ital. J. Geosci., 133, 223-234.

Prager C., Zangerl C., Patzelt G., Brandner R. (2008) - Age distribution of fossil landslides in the Tyrol (Austria) and its surrounding areas. Nat. Hazards Earth Syst. Sci., 8, 377-407.

Prager C., Ivy-Ochs S., Ostermann M., Synal H.A., Patzelt G. (2009) - Geology and radiometric ^{14}C-, ^{36}Cl- and Th-/U- dating of the Fernpass rockslide (Tyrol, Austria). Geomorphology, 103, 93-103.

Prosser G. (1992) - Analisi strutturale e cinematica lungo la Linea delle Giudicarie nord tra la Val di Sole e la Val di Non (Trentino Occidentale). Studi Trent. Sci. Nat., 67, 87-115.

Prosser G. (1998) - Strike-slip movements and thrusting along a transpressive fault zone: the Giudicarie line (Insubric line, Northern Italy). Tectonics, 17, 921-937.

Rossato S., Monegato G., Mozzi P., Cucato M., Gaudioso B., Miola A. (2013) - Late Quaternary glaciations and connections to the piedmont plain in the prealpine environment: The middle and lower Astico Valley (NE Italy). Quat. Int., 288, 8-24.

Rovida A., Locati M., Camassi R., Lolli B., Gasperini P. (2016) - CPTI15, the 2015 Version of the Parametric Catalogue of Italian Earthquakes. Istituto Nazionale di Geofisica e Vulcanologia, Italy. http://doi.org/10.6092/INGV.IT-CPTI15.

Schwinner R. (1912) - Der Monte Spinale bei Campiglio und andere Bergstürze in den Südalpen. Mittteil. der Geol. Ges. Wien, 5, 128-197.

Selli L. (1998) - Il Lineamento della Valsugana fra Trento e Cima d'Asta: cinematica neogenica ed eredità strutturali Permo-Mesozoiche nel quadro evolutivo del Sudalpino orientale (NE-Italia). Mem. Soc. Geol. It., 53, 503-541.

Slejko D., Carulli G.B., Nicolich R., Rebez A., Zanferrari A., Cavallin A., Doglioni C., Carraro F., Castaldini D., Iliceto V., Semenza E., Zanolla C. (1989) - Seismotectonics of the Eastern Southern-Alps: a review. Boll. Geofis. Teor. Appl., 31, 109-136.

Trener G.B. (1906) - Geologische Aufnahme in nördlichen Abhang der Presanellagruppe. Jahrb. K.K. Geol. Reich., 56, 405-496.

Trener G.B. (1924) - Gli impianti idroelettrici della citta di Trento, II. Geologia delle Marocche, 25-33 con carta geologica 1:25.000. Studi Trentini Sci. Nat., 34, 319-340.

Trevisan L. (1939) - Il Gruppo di Brenta (Trentino Occidentale). Mem. Ist. Geol. Univ. Padova, 13, 1-128.

Viganò A., Bressan G., Ranalli G., Martin S. (2008) - Focal mechanism inversion in the Giudicarie-Lessini seismotectonic region (Southern Alps, Italy): insights on tectonic stress and strain. Tectonophysics, 460, 106-115.

Viganò A., Tumiati S., Recchia S., Martin S., Marelli M., Rigon R. (2011) - Carbonate pseudotachylytes: evidence for seismic faulting along carbonate faults. Terra Nova, 23, 187-194.

DOI: 10.3301/GFT.2018.01

Viganò A., Scafidi D., Martin S., Spallarossa D. (2013a) - Structure and properties of the Adriatic crust in the central-eastern Southern Alps (Italy) from local earthquake tomography. Terra Nova, 25, 504-512.

Viganò A., Tumiati S., Martin S., Rigo M. (2013b) - The Pietra Grande thrust (Brenta Dolomites, Italy): looking for co-seismic indicators along a main fault in carbonate sequences. Geophysical Research Abstracts, 15, 5665.

Viganò A., Scafidi D., Ranalli G., Martin S., Della Vedova B., Spallarossa D. (2015) - Earthquake relocations, crustal rheology, and active deformation in the central-eastern Alps (N Italy). Tectonophysics, 661, 81-98.

Wiebols J. (1938) - Geologie der Brentagruppe. Jahrb. Geol. B.-A., 88, 261-350.

Winterer E.L. and Bosellini A. (1981) - Subsidence and Sedimentation on a Jurassic Passive Continental Margin, Southern Alps, Italy. Am. Ass. Petrol. Geol. Bull., 65, 394-421.

Zampieri D. and Massironi M. (2007) - Evolution of a poly-deformed relay zone between fault segments in the eastern Southern Alps, Italy. In: Cunningham D. and Mann P. (Eds.) Tectonics of Strike-slip Restraining and Releasing Bends. Geol. Soc., London, Special Publication 290, 351-366.

Zampieri D. and Adami S. (2013) - Influence of the geological structure on a rockslide in northeastern Italy. It. J. Eng. Geol. Environ., 6, 507-512.

Zampieri D., Massironi M., Sedea R., Sparacino V. (2003) - Strike-slip contractional stepovers in the Southern Alps (northeastern Italy). Eclogae geol. Helv., 96, 115-123.

DOI: 10.3301/GFT.2018.01